UNIVERSIDAD MICHOACANA DE SAN NICOLÁS DE HIDALGO

DIVISIÓN DE ESTUDIOS DE POSGRADO DE LA FACULTAD DE INGENIERÍA ELÉCTRICA

Voltage Security Boundary-Constrained Optimal Power Flow

TESIS

Que para obtener el Grado de:

DOCTOR EN CIENCIAS EN INGENIERÍA ELÉCTRICA

Presenta:

Víctor Javier Gutiérrez Martínez

ASESOR:
Dr. Claudio Rubén Fuerte Esquivel

CO-ASESOR:
Dr. Claudio A. Cañizares

Morelia Michoacán **Septiembre 2011**

DIVISION POSGRADO

Voltage Security Boundary-Constrained Optimal Power Flow

B Y :
Víctor Javier Gutiérrez Martínez

to obtain the degree of Doctor in Science in Electrical Engineering
in the Universidad Michoacana de San Nicolás de Hidalgo
División de Estudios de Posgrado
Facultad de Ingeniería Eléctrica

A D V I S O R :
Dr. Claudio Rubén Fuerte Esquivel
C O - A D V I S O R :
Dr. Claudio A. Cañizares

September 2011

Abstract

This work presents a new approach to model stability and security constraints in Optimal Power Flow (OPF) problems based on an Artificial Neural Network (ANN) representation of the system security boundary (SB). The novelty of this proposal is that a closed form, differentiable function derived from the system SB is used to represent security constraints in an OPF model. The procedure involves two main steps: First, an ANN representation of the SB is obtained based on Back-Propagation Neural Network (BPNN) training. Second, a differentiable mapping function extracted from the BPNN is used to directly incorporate this function as a constraint in the OPF model. This approach ensures that the operating points resulting from the OPF solution process are within a feasible and secure region, whose limits are better represented using the proposed technique compared to typical security-constrained OPF models. When an insecure operative scenario is identified, the proposed approach uses as a corrective action load shedding, taking advantage of properly knowing the shape of the SB; yielding to determine in an optimal fashion the total amount of load to be curtailed, in such a way that the system returns to the feasible and secure region, taking into account the inherent cost of the load shedding.

The effectiveness and feasibility of the proposed approach is demonstrated through the implementation as well as the testing and comparison using the IEEE 2-area and 118-bus benchmark systems of an optimal dispatch technique that guarantees system security in the context of competitive electricity markets.

Furthermore, in order to demonstrate that the problem in determining the SB becomes a multi-dimensional issue when different system parameters are varied, two types of SBs are presented: the resulting SB when the loading directions are varied maintaining fixed generator's dispatch directions at prespecified values, and the resulting SB when the dispatch directions of generators are varied maintaining fixed loading directions.

Acknowledgments

I would like to express my deepest gratitude to my advisor, Ph.D. Claudio Fuerte, whose invaluable assistance, support, and guidance have considerably improved my graduate experience. Thanks for the confidence and opportunity to be one of his doctoral students, as well as your unconditional friendship.

I must also acknowledge my co-advisor Ph.D. Claudio A. Cañizares for his technical assistance and great hospitality during my stay at Waterloo. I must give him a very special acknowledgment for accepting me as a visiting student at the ECE Department of the University of Waterloo. I wish to express my gratitude for sharing his time, knowledge and experience with me.

My acknowledgment is also due to the members of the doctoral committee, for the support they provided to improve the level of this thesis report. Their valuable suggestions were very helpful to finish this thesis.

A great acknowledgment to the Consejo Nacional de Ciencia y Tecnología and the Universidad Michoacana de San Nicolás de Hidalgo for providing the financial and academic means to develop this thesis.

There are no words to express my love to my wife Mayra Edith. Thank you for your dedication, patience, love, and confidence in me. I really appreciate the great effort you made in accompany me in the fun and great adventure in Canada. Also, I apologize to my little children Juan Javier and Pamela Sofia for the time we did not play together. However, I hope some day this may help as a small example to overcome and achieve their goals. I love you with all my heart.

My parents deserve special mention for their constant support and guidance to reach my goals. Thank you father for teaching me how a man must support and care for his family, I am sure you are with God in heaven, because you always were a fair and good man; I wish someday I will ever be at least half of what you were. Mother I appreciate your countless prayers for me and my family. I am proud to be your son. God bless you.

Dedication

To my father

Javier Gutierrez Franco.†

To my wife Mayra Edith,
my son Juan Javier, and my daughter Pamela Sofia.

To my mother Maria Socorro.

To Juan Servin Trejo.

To my aunts Juana and Tina†.

Contents

List of Figures

List of Tables

List of Publications

1. V. J. Gutierrez-Martinez, and C. R. Fuerte-Esquivel, "Power flow formulation as a nonlinear programming problem," *International Journal on Power System Optimization (IJPSO)*, vol. 1, no. 1, January-June 2009. ISSN: 0975-458X.

2. V. J. Gutierrez-Martinez, C. A. Cañizares, C. R. Fuerte-Esquivel, A. Pizano-Martinez, and X. Gu, "Neural-network security-boundary constrained optimal power flow", IEEE Trans. on Power Systems, vol. 26, no. 1, pp. 63-72, February 2011. ISSN: 0885-8950.

3. R. Ramírez-Betancour, V. J. Gutierrez-Martinez, C. R. Fuerte-Esquivel, "Static simulation of voltage instability considering effects of governor characteristics and voltage and frequency dependence of loads," in *North American Power Symposium (NAPS) 2010*, pp. 1 - 7, 26-28 Sept. 2010.

4. C. Battistelli, C. A. Cañizares, M. Chehreghani, V. J. Gutierrez-Martinez, and C. R. Fuerte-Esquivel, "Practical security-boundary-constrained dispatch models for electricity markets," accepted at the *17th Power Systems Computation Conference,* August 22-26 2011, Stockholm, Sweden.

5. V. J. Gutierrez-Martinez, C. R. Fuerte-Esquivel, and N. Solis-Ramos, "Analysis of static voltage collapse in a real subtransmission power system," in preparation.

List of Terms

ANN	Artificial Neural Network
AVR	Automatic Voltage Regulator
BPNN	Back-Propagation Neural Network
CM	Continuation Method
DAE	Differential-Algebraic Equations
EP	Equilibrium Point
HB	Hopf Bifurcation
LIB	Limit Induced Bifurcation
MSV	Minimum Singular Value
NR	Nonlinear Regression
ODEs	Ordinary Differential Equations
OPF	Optimal Power Flow
SB	Security Boundary
SBC-OPF	Security-Boundary Constrained OPF
SC-OPF	Security-Constrained OPF
SNB	Saddle Node Bifurcation
SSC-OPF	Small-Perturbation Stability-Constrained OPF
VSC-OPF	Voltage-Stability-Constrained OPF

Chapter 1

Introduction

1.1 Research Motivation

Because of the highly stressed operating conditions faced by electric power systems, insecure and dangerous operation scenarios have been frequently present as limits of system stability are reached [Hines et al., 2008]. This is due to transmission utilization is increasing in sudden and unpredictable directions, and competition together with other regulatory requirements make new transmission facility construction more difficult. All these limits and restrictions jeopardize system security and reliability, and have led to concerns on the part of system operators regarding the secure operation of power networks, particularly in the new competitive electricity market environment [U.S.-Canada Power System Outage Task Force, 2004].

Among these limits, the most important are the thermal equipment limits, generation capability limits, voltage stability, oscillatory stability and transient stability limits. Consequently, system operators are demanding tools that allow them to make fast and effective decisions, in order to prevent power systems from being operated close to these limits [Avalos, 2008]. Therefore, the proper knowledge of the shape of the region delimited by these constraints allow for taking better corrective and preventive actions for the cases when the system is operating beyond or approaching the boundary of this region. This stability/security region is defined as a set of load demands and power generations (in the controlled parameter space) or voltages and their phase angles (in the state variables space) for which the power flow equations and the stability/security constraints are satisfied [Wu and Kumagai, 1982], [Kaye and Wu, 1982]. In this context, it is important to identify between security and stability regions is important: when the limits mentioned are taken into account and no contingencies are considered, the resulting region is called *stability region*. On the other hand, if at least

an N-1 contingency criterion is considered, i.e. accounting for the worst single contingency in the system, the resulting region is called *security region*. In the present work, a security rather than stability region is considered, since it better represents the main operative considerations used in electricity markets.

In the competitive electricity market environment, security assessment can be divided into two levels: classification and boundary determination. Classification involves determining whether the system operating point is secure or insecure under a set of prespecified contingencies. However, classification does not in itself indicate distance from the operating condition to the insecure or secure conditions, whereas boundary determination gives the necessary information to prevent and/or to correct insecure scenarios. A boundary is represented by the aforementioned limits often called constraints, which are imposed on parameters characterizing the set of prespecified contingencies, called critical parameters. Once the boundary is identified, security assessment for any operating point can be carried out. The problem with these limits is that they do not always represent the actual security limits directly associated with the current market and system conditions, given the variability of dispatch because of economic drivers, resulting in some cases in insecure operating conditions and/or inappropriate price signals [Cañizares and Kodsi, 2006], [Ghasemi and Maria, 2008]; thus, the security region delimited by these limits may mask possible insecure scenarios, presenting them as secure and reliable operating points.

Better market and system operating conditions may be attained when system security is better accounted for in typical electric energy auction systems, avoiding the masking effect on undesirable operating points. Thus, research has been carried out to improve the representation of the security region. The inherent issue resides in the fact that this region is highly complex in shape, and as a result, its boundary is highly nonlinear, not allowing to be directly mapped by a smooth nonlinear function.

In the present work, a new approach to better represent the security region is developed. The main goal is to obtain a closed-form differentiable function derived from the system's SB, in order to use it as a constraint in an OPF model to more accurately account for system security in an operating environment. For this purpose, a BPNN is used to map the high nonlinear SB. The BPNN is trained and tested until it reproduces the SB with enough accuracy, then the information is extracted to obtain the aforementioned function.

1.2 Literature Review

As previously mentioned, the SBs must be accounted for in operational planning and real time operations to maximize the power transfers and to take full advantage of transmission facilities. Hence, various approaches have tried to determine and to approximate the security region in order to employ it as a security constraint in OPF models.

The approach of security regions of power systems was first proposed by [Hnyilicza et al., 1975]. In [Fischl et al., 1976] and [DeMaio et al., 1976] methods to identify steady-state security regions were developed. The idea of steady-state security regions was expanded by [Banakar and Galiana, 1981], where a method to construct the so-called "security corridors" is suggested for security assessment; this security region, which was formed by keeping the set of inequality constraints as small as possible, was implicit and was difficult to manage in the power system security analysis and security operation. One of the first approaches that suggested a region-wise approach to power system security analysis was proposed in [Wu and Kumagai, 1982]. This approach characterizes the set of all steady-state secure operating points by using various operating and security constraints. A stability region in the state space in terms of load voltage and load-tap-changer position is computed in [Vu and Liu, 1992] based on the monotonic fall of system voltages; it also shows that when the reactive capability of generators is reached the voltage stability region shrinks in such a way that voltage collapse takes place when the system trajectory falls outside the shrunken region. However, important characteristics of this region are not discussed because of the simple models used to represent the synchronous generator and its controls.

One of the important problems in defining power system security regions is the adequate description of its boundary, in such a way that secure and/or insecure operating scenarios can be readily identified. Therefore, there is a need to develop an analytical description and/or approximation of the boundary; the SB approximation means a sort of interpolation between the boundary points obtained, which can be used as a part of the analytical boundary description, or separately for the purposes of visualization. Hence, the general trend observed in the area of obtaining the corresponding security region consist of determining security boundary points in a specified stress direction, locating the closest (critical) bifurcation point, calculating the critical and sub-critical distances to instability, and finally building the entire security region and its boundaries in the parameter or state space.

In the context of OPF models, the analytical description and/or approximation of the SB usually consists in the use of linear or nonlinear inequality constraints applied to a certain number of critical parameters such as power flows, load levels, voltage magnitudes, etc, in

such a way that if all constraints are satisfied, the analyzed operating point is considered to be inside the security region. One of the first approaches which attempted to include voltage stability/security constraints into a conventional OPF formulation is presented in [Rosehart et al., 1999]; there optimization techniques are applied to voltage collapse studies based on a "Maximum Distance to Voltage Collapse" algorithm that incorporates constraints on the power system current operating conditions. In [Cañizares et al., 2001] the Minimum Singular Value (MSV) of the power flow Jacobian matrix, which is an index to detect proximity to voltage instability [Lof et al., 1992], is used as a security constraint to develop a Voltage-Stability-Constrained OPF (VSC-OPF) restricting the resulting operating points to be within a certain "reasonable" distance from voltage collapse. An enhancement to this approach is presented in [Kodsi and Cañizares, 2007], where oscillatory and voltage instability conditions are used to develop a Small-Perturbation Stability-Constrained OPF (SSC-OPF) based on the inclusion of a "dynamic" MSV stability index. However, in [Cañizares et al., 2001] and [Kodsi and Cañizares, 2007], the proposed stability index is an implicit function of the optimization variables, and hence their derivatives can be only approximated numerically in order to be included in the OPF solution process; these approaches present some implementation and numerical problems due to the MSV-based index being nonlinear. An improved approach is presented in [Avalos et al., 2008], where an equivalent constraint based on a singular value decomposition of the Jacobian power flow is proposed to explicitly represent the MSV constraint in the OPF model. In [Gan et al., 2000], a stability-constrained OPF model is proposed based on a time-domain numerical representation of the dynamic equations which are included as constraints in the OPF process. A somewhat similar approach is used in [Bruno et al., 2002] to develop a time-domain dispatch algorithm that considers contingencies.

An alternative approach to including security constraints in an OPF model is to introduce a differentiable function representing the SB as a constraint in the model. In [Jayasekara and Annakkage, 2006] the transient stability boundary is approximated by a polynomial obtained from an interpolation procedure and a nonlinear transformation applied to the system state variables, representing in a more accurate way the complex shape of the SB. A similar conceptual idea is proposed in this thesis to include security constraints in an OPF model, based on a differentiable function extracted from an ANN which represents the stability/security boundary.

Extensive research has been carried out on the application of ANNs to properly represent power system stability/security margins. The idea behind the techniques based on ANNs is to select a set of critical parameters such as power flows, loads, and generator limits, and

then train an ANN on a set of simulation data to estimate the security margin. The advantages of the ANN models include their ability to accommodate nonlinearities and their very fast performance in real time. For example, in [Aggoune et al., 1991], an approach based on an ANN to assess power system stability based on training samples from off-line stability studies is presented. In [Eduards et al., 1996], state-variable values are computed for a given set of contingencies, and these are then used as inputs to an ANN to predict a transient stability margin. Similarly, making use of nomograms, the system SB is characterized in [McCalley et al., 1997] by means of critical system parameters randomly generated to yield an ANN input training set; the ANN is then trained and tested to obtain a SB representation. A BPNN is applied in [Sahari et al., 2003] to predict voltage instabilities using as inputs both system load information and a voltage stability index; based on these inputs, the BPNN predicts new voltage stability index values for different operating scenarios. In [Gu and Cañizares, 2007], a representation of the system stability boundary based on a trained BPNN is proposed for predicting the available transfer capability of a system for any given dispatch. Finally, in [Miranda et al., 1995] an ANN is used to evaluate the sensitivities of a stability index based on a transient energy function method with respect to the generator's power outputs for multiple contingencies, and these sensitivities are then introduced in the objective function of an OPF to indirectly account for system security in the dispatch process; this method approximately accounts for system security in the OPF process, as opposed to directly representing these security margins as constraints in the OPF model, as proposed in the present work.

When the load in a power system significantly exceeds generation, the system can survive only if enough loads are disconnected from the system. Conventional methods for system load shedding do not effectively calculate the correct amount of load to be shed [Hirodontis et al., 2009], since there is no insight about the operating point with respect to the boundary of the security region. As a consequence, deciding which curtailment direction to follow in order to ensure the secure operation of the power system is not simple. Hence, with a more accurate SB representation the optimal amount of load to be curtailed can be properly determined, as shown in the present work.

1.3 Objectives

The objectives of the present work can be summarized as follows:

- To analyze different types of equilibrium points, and the way they lose stability by

using bifurcation theory.

- To establish the SB determination procedure once the power system model is defined as a set of DAE. This procedure will be based on the determination of a critical load matrix obtained for each generation pattern considered.
- To numerically determine the SB by using continuation-based methods, OPF-based methods, and eigenvalue analysis, in order to obtain two main types of SBs such as loading directions-based and dispatch directions-based SBs.
- By using BPNN and Nonlinear Regression (NR) to approximate the SB, and to test these two approaches on two IEEE benchmark systems such as the two-area and the 118-bus system.
- To include the smooth-nonlinear differentiable function resulting from the trained BPNN into an OPF, in order to consider this function as a security constraint. Hence, the so-called Security-Boundary Constrained OPF (SBC-OPF) will be able to ensure that the resulting optimal point is also secure.
- Finally, the proposed approach will be tested by using the same two IEEE benchmark systems mentioned above.

1.4 Main Contribution

The current work proposes a novel approach based on BPNNs to obtain explicit differentiable functions of the system stability/security boundaries. This allows the introduction of the boundaries characterized by BPNNs as constraints in OPF models. In order to achieve this goal, SBs as defined in [Sauer and Pai, 1988] are constructed, and then BPNNs are trained and tested to accurately represent these boundaries. From these BPNNs, explicit, differentiable functions of the OPF variables are obtained, which are then introduced as constraints in an OPF model. A SBC-OPF model for optimal dispatch in the context of competitive electricity markets is proposed, illustrated and tested using a pair of IEEE test systems.

1.5 Thesis Outline

The thesis is organized into five chapters as follows:

In this Chapter the research motivation, the literature review about the power system's SB characterization, and the use of ANN to consider security constraints into OPF models are presented. Furthermore, the objectives and main contribution of the present work are highlighted. Finally, the thesis outline is presented.

In Chapter 2 the power system models considered in the present work are described. By using bifurcation theory, the dynamics related to the resulting set of differential algebraic equations are analyzed from the point of view of critical points. Then, the SB determination procedure is explained in detail, describing the numerical methods employed to obtain the corresponding critical points. Two kinds of SBs are presented: the corresponding SB when the generator's dispatch directions are kept fixed at prespecified values while varying the loading directions, and the SB when the loading directions are kept fixed at prespecified values while varying the generator's dispatch directions. Conclusions about the multidimensional complexity of the SB are drawn.

The approximation of the SB by using BPNNs is presented in Chapter 3. The selected BPNN architecture and the training and tested procedures are discussed in detail. Based on the basic neuron structure, the smooth nonlinear differentiable function is obtained from the resulting trained BPNN. By using two IEEE benchmark systems, comparisons between the proposed approach and a NR technique are shown in order to demonstrate that BPNNs are suitable tools to map complex SBs.

In Chapter 4, some relevant security-constrained OPF (SC-OPF) auction models are presented and discussed, and the proposed SBC-OPF model is described. Furthermore, discussions and comparisons based on the results obtained from the implementation and application of the SBC-OPF model to the IEEE 2-area and IEEE 118-bus benchmark systems are presented, demonstrating the feasibility and benefits of the proposed BPNN-SB and SBC-OPF.

Finally, the main results, contributions, and papers resulting from this work are summarized and highlighted in Chapter 5.

Chapter 2

Theoretical Concepts

2.1 Introduction

In this Chapter models of the main devices embedded in the power system are presented, resulting in a set of differential-algebraic equations. It is shown how by using the implicit function theorem the stability of an EP of the DAE system, for a given value of system parameters, is obtained by analyzing the eigenvalues of the resulting state matrix. Using this concept and bifurcation theory, the way in which the DAE system experiences bifurcations like a simple ODE system is analyzed.

Once critical points have been qualitatively characterized using bifurcation theory, the concept of stability and security boundaries are presented, and the procedure to obtain these boundaries is proposed.

Finally, by using numerical methods for SB determination, the loading directions-based SB and the dispatch directions-based SB are obtained for the IEEE 118-bus benchmark system, in order to show the complexity of the security surfaces and the high-nonlinearity of the corresponding SBs.

2.2 Power System Mathematical Representation

Generally speaking, an electric power system can be divided into the following:

1. A transmission network which interconnects the system buses to transmit the energy from the generation stations to consumers.

2. The connected equipment such as generators, transformers, loads, and mechanical

and/or electronically controlled devices. The loads are connected through the system at a variety of voltage levels, whereas the control devices are embedded in the system in order to guarantee the instantaneous power balance between generators and loads, avoiding or correcting undesirable operating system conditions.

Since the power system dynamics interact at widely-varying time constants, the mathematical representation of the dynamics associated with the transmission network and the connected equipment can be quite different and is expressed in different frames of reference. In this context, as shown in 2.1, conversion equations linking these different models are typically needed, in such a way that generators, electronically controlled devices, composite load models, the AC network, and other equipment, are modeled under the same frame of reference. However, the inherent multiple time scales existing in the dynamics of a power system also crates the possibility of obtaining reduced order models relevant to a particular time scale. This implies that the power system's mathematical model directly depends on the phenomenon under analysis [Sauer and Pai, 1988], i.e. the level of modeling detail will depend on the time frame of the dynamic phenomena [Kundur et al., 2004].

In the present work the dynamic phenomenon under study has a quasi-stationary nature, i.e. the dynamics of the system occur in a few minutes interval, which implies that slow system dynamics must be properly represented by the resulting power system model, while the fast-time varying dynamics are not represented at all and are characterized by their equilibrium conditions. This time-scale decomposition is represented in Fig. 2.2, where x_f is a state vector representing fast-time varying dynamics; x_s is a state vector representing slow-time varying dynamics; y is a state vector representing transmission network dynamics, which are expected to change instantaneously with variations of the equipment or load states; $p \subseteq (\rho \cup \lambda)$ is a system parameter vector; ρ is a vector of controllable parameters, such as generator terminal voltage magnitude settings; and λ is a vector of non-controllable parameters, such as active load and reactive power levels, which change continuously.

Based on the above explanation, the considered models contain two divisions:

1. Models related to the transmission level, which basically consist of the power flow equations. These equations are algebraic because the internal dynamics of the network are sufficiently fast as to be considered instantaneous: they have no effect on problems related to the power flow. These algebraic equations can be written in vectorial form as

$$0 = g(x_f, x_s, y, p) \tag{2.1}$$

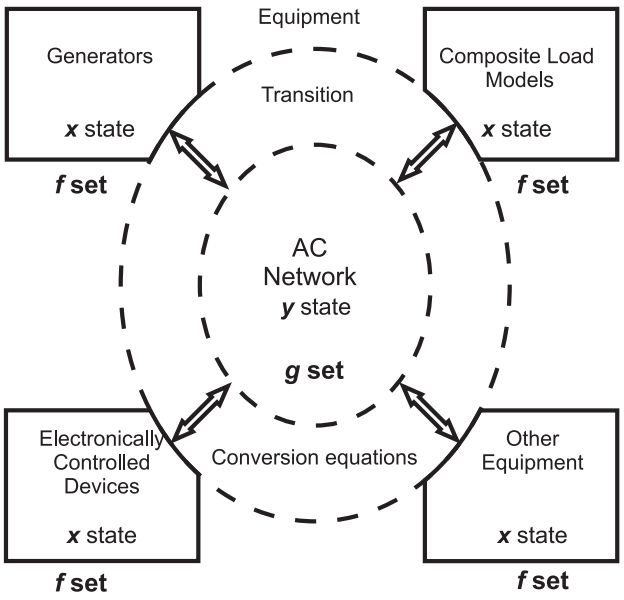

Figure 2.1: Structure of the power system modeling.

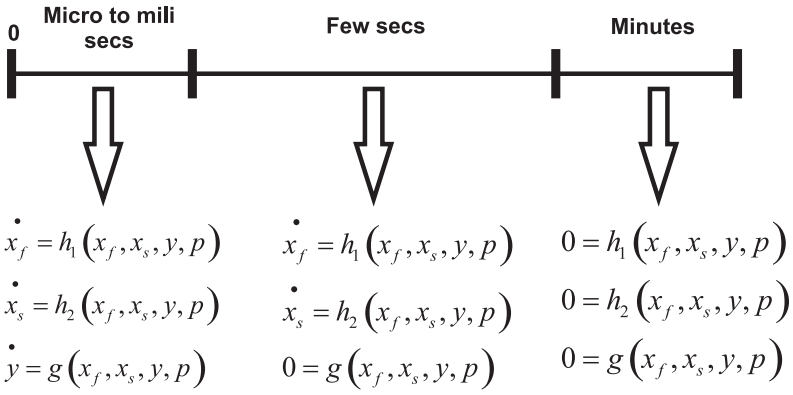

Figure 2.2: Power system model time-scale decomposition.

where g represents the set of algebraic equations. Since the existing coupling of the electromechanical power flow at the generator end and the power consumption at the load end are expressed in terms of the apparent power, considering the coupling equations as power balance equations becomes necessary.

2. Models related to system equipment whose dynamic behavior is slower, and as a consequence, have a direct influence on the total dynamics of the system. Thus, differential equations are needed to describe the behavior of equipment such as generators, composite loads, etc. These differential equations can be written as

$$\dot{x_f} = h_1 (x_f, x_s, y, p) \tag{2.2}$$

$$\dot{x_s} = h_2 (x_f, x_s, y, p) \tag{2.3}$$

where $h_1$and $h_2$represent the set of differential equations associated with fast- and slow-time varying dynamics, respectively. Equations 2.2 and 2.3 are commonly expressed as

$$\dot{x} = h (x, y, p) \tag{2.4}$$

where $x = \begin{bmatrix} x_f & x_s \end{bmatrix}^T$ represents the full system dynamics.

Hence, the full power system model may be represented by the following set of parameter-dependent Differential-Algebraic Equations (DAE) as

$$\begin{aligned} \dot{x} &= h (x, y, p) \\ 0 &= g (x, y, p) \end{aligned} \tag{2.5}$$

The specific models of each component of the power system are formulated in the following subsections. Common power system notation is used.

2.2.1 The Synchronous Machine Model

The dynamics of synchronous machines have been extensively studied and are well understood [Sauer and Pai, 1988]. The two-axis model describing the synchronous machine dynamics, when stator transients are ignored, can be given as [Sauer and Pai, 1988], [Sauer and Pai, 1990]:

$$\dot{\delta}_i = (\omega_i - \omega_m) \omega_0 \quad i = 1, \cdots, m-1 \tag{2.6}$$

$$\omega_i = M_i^{-1}\left[P_{mi} - D_i\left(\omega_i - \omega_m\right) - \left(E_{qi}^{'} - X_{di}^{'} I_{di}\right) I_{qi} - \left(E_{di}^{'} - X_{qi}^{'} I_{qi}\right) I_{di}\right] \quad i = 1, \cdots, m \tag{2.7}$$

$$\dot{E_{qi}^{'}} = T_{d0i}^{-1}\left[E_{fdi} - E_{qi}^{'} - \left(X_{di} - X_{di}^{'}\right) I_{di}\right] \quad i = 1, \cdots, m \tag{2.8}$$

$$\dot{E_{di}^{'}} = T_{q0i}^{-1}\left[-E_{di}^{'} - \left(X_{qi} - X_{qi}^{'}\right) I_{qi}\right] \quad i = 1, \cdots, m \tag{2.9}$$

where m is the number of system generators and the m^{th} generator is chosen as the system angle reference; ω_m is the system frequency; P_{mi} is the machine input mechanical power; ω_i is the i^{th} machine frequency (generator angular speed); ω_0 is the system rated frequency; I_{di} and I_{qi} are direct axis and quadrature axis currents, respectively; $E_{di}^{'}$ and $E_{qi}^{'}$ are transient d axis and q axis electromechanical forces, respectively; T_{d0i} and T_{q0i} are d axis and q axis open circuit time constants, respectively; X_{di} and X_{qi} are synchronous d axis and q axis reactances; $X_{di}^{'}$ and $X_{qi}^{'}$ are d axis and q axis transient reactances; M_i is inertia constant; and D_i is the damping constant of the machine. Interface voltage equations are given as follows:

$$E_{qi}^{'} = V_i cos\left(\delta_i - \theta_i\right) + R_{si} I_{qi} + X_{di}^{'} I_{di} \quad i = 1, \cdots, m \tag{2.10}$$

$$E_{di}^{'} = V_i sin\left(\delta_i - \theta_i\right) + R_{si} I_{di} + X_{qi}^{'} I_{qi} \quad i = 1, \cdots, m \tag{2.11}$$

where V_i and θ_i are bus phasor voltage and angle, respectively; and R_{si} is armature resistance of the machine.

It is important to mention that the results obtained in the present work apply to any version of generator models, from the two axes model with damper windings, through the classical model with constant voltage behind a transient reactance.

2.2.2 Excitation Control System

Typical excitation controls with their models are presented in [IEEE Committee Report, 1981]. It is common to use a simplification of the IEEE type DC-1 excitation control system shown in Fig. 2.3 when the problem of voltage stability is analyzed. This excitation control system is linear, unless hard limits are reached [IEEE Committee Report, 1981].

Thus, this simplified model version is employed in the present work, and its corresponding model is as follows:

$$\dot{E_{fdi}^{'}} = T_{ei}^{-1}\left[V_{ri} - S_{ei}\left(E_{fdi}\right) E_{fdi}\right] \quad i = 1, \cdots, m \tag{2.12}$$

$$\dot{V_{ri}} = T_{ai}^{-1}\left[-V_{ri} + K_{ai}\left(V_{refi} - V_i - R_{fi}\right)\right] \quad i = 1, \cdots, m \tag{2.13}$$

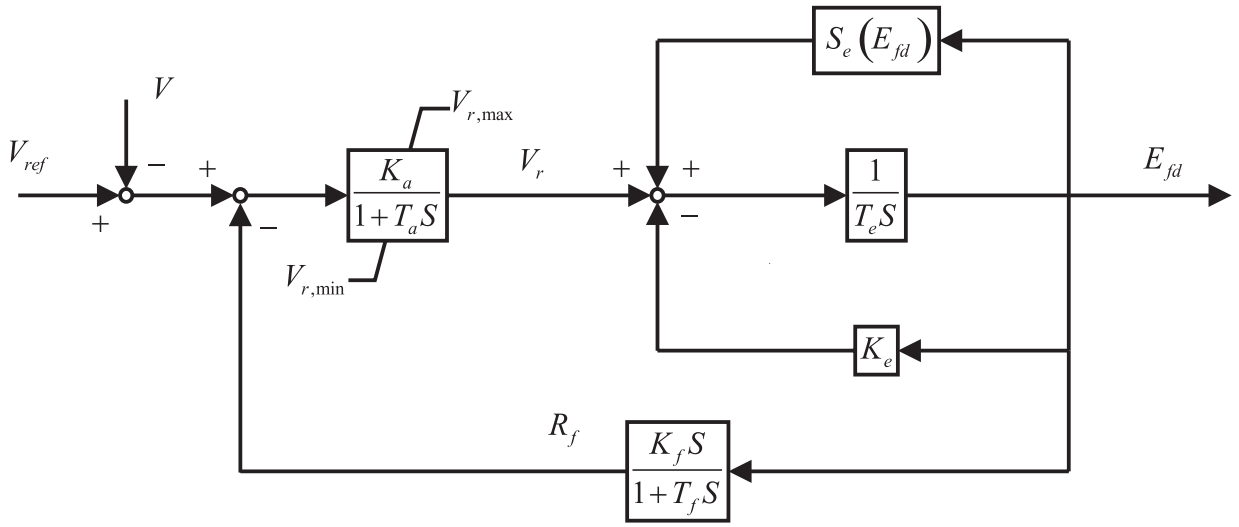

Figure 2.3: IEEE-type DC-1 excitation control system.

$$\dot{R_{fi}} = T_{fi}^{-1}\left[-R_{fi} - \left(K_{ei} + S_{ei}\left(E_{fdi}\right)\right)K_{fi}E_{fdi}/T_{ei} + K_{fi}V_{ri}/T_{ei}\right] \quad i = 1, \cdots, m \tag{2.14}$$

where V_{refi} is the reference voltage of the Automatic Voltage Regulator (AVR); V_{ri} and R_{fi} are the outputs of the AVR and exciter soft feedback; E_{fdi} is the voltage applied to the generator field windings; T_{ai}, T_{ei} and T_{fi} are the AVR, exciter and feedback time constants; K_{ai}, K_{ei} and K_{fi} are gains of the AVR, exciter and feedback loop; $V_{ri,min}$ and $V_{ri,max}$ are the lower and upper limits of V_{ri}.

2.2.3 Prime-mover and Speed Governor

Fig. 2.4 shows the block diagram for a simplified prime-mover and speed governor. The following two differential equations describe the dynamics when no limits in the steam valve or water gate are reached:

$$\dot{P}_{mi} = T_{chi}^{-1}\left(\mu_i - P_{mi}\right) \quad i = 1, \cdots, m \tag{2.15}$$

$$\dot{\mu_i} = T_{gi}^{-1}\left[P_{gsi} - \left(\omega_i - \omega_{ref}\right)/R_i - \mu_i\right] \quad i = 1, \cdots, m \tag{2.16}$$

where P_{gsi} is the designated real power generation; P_{mi} is the mechanical power of the prime-mover; μ_i is the steam valve or water gate opening; R_i is the governor regulation constant representing its inherent speed-droop characteristic; ω_{ref} (=1.0) is the governor reference speed; and T_{chi} and T_{gi} are the time constants related to the prime-mover and speed governor, respectively.

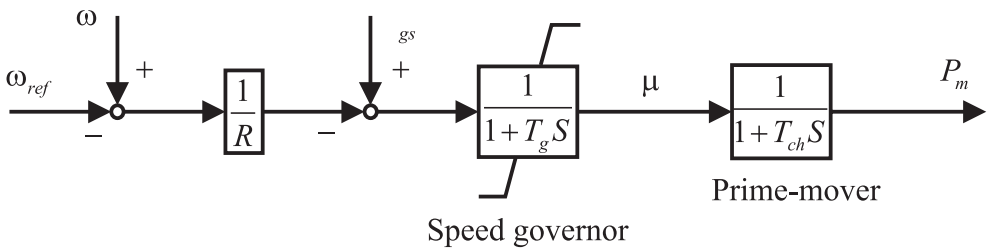

Figure 2.4: Simplified speed governor and prime-mover.

2.2.4 Loads

Modeling the composite load is still a relatively unsolved problem in power system studies. All results presented in this work are applicable to any mathematically smooth load model. However, in order to focus the analysis on the security regions rather than the load model, and without loss of generality, the load model used may be written as

$$S_d = P_d + Q_d \tag{2.17}$$

where

$$\begin{aligned} P_d &= \lambda P_{d_0} \\ Q_d &= \lambda Q_{d_0} \end{aligned} \tag{2.18}$$

where P_{d_0} and Q_{d_0} represent the active and reactive base case load at each system node, respectively. The non-controllable parameter λ represents the load increases which drives the system to insecure operative scenarios from the voltage stability viewpoint.

2.2.5 Network Power Equations

The transmission system model consists of the typical power flow equations describing the relations between the bus-injected active and reactive power flows, and the bus phasor voltage magnitude and phase. In this context, a satisfactory circuit representation of the transmission lines is possible assuming that they have moderate length and that the system is operating within the quasi-stationary phasor range. Thereby, a satisfactory approximation is defined by introducing R-, L-, and C-based parameters on approximate π circuits [Illic and Zaborszky, 2000]. On the other hand, conventional transformers may typically be modeled by an equivalent T circuit, consisting of an ideal transformer together with elements which represent the imperfections of the real transformer [Gomez-Exposito et al., 2009]. On-

Load Tap Changer and Phase-Shifter Transformers are not covered in the present work; however, their models could be readily included.

The power flow mismatch equations may be derived by considering the components' models described above and are given by the following:

$$\begin{aligned} P_{si} - \lambda P_{d_{0i}} - P_{inyi} &= 0 \\ Q_{si} - \lambda Q_{d_{0i}} - Q_{inyi} &= 0 \end{aligned} \qquad i = 1, \cdots, n \tag{2.19}$$

where

$$\begin{aligned} P_{inyi} &= \sum_{k=1}^{n} V_i V_k Y_{ik} cos\left(\theta_i - \theta_k - \varphi_{ik}\right) \\ Q_{inyi} &= \sum_{k=1}^{n} V_i V_k Y_{ik} sin\left(\theta_i - \theta_k - \varphi_{ik}\right) \end{aligned} \qquad i = 1, \cdots, n \tag{2.20}$$

and

$$\begin{aligned} P_{si} &= I_{di} V_i sin\left(\delta_i - \theta_i\right) + I_{qi} V_i cos\left(\delta_i - \theta_i\right) \\ Q_{si} &= I_{di} V_i cos\left(\delta_i - \theta_i\right) - I_{qi} V_i sin\left(\delta_i - \theta_i\right) \end{aligned} \tag{2.21}$$

where n is the number of system buses; P_{si} and Q_{si} are the generator output powers, which are primarily determined by the inherent characteristics of the speed governors and AVRs; and P_{inyi} and Q_{inyi} are the powers injected into the network at bus i.

2.3 Bifurcation Theory

Recall that a dynamical system is one whose states evolve with time (t), and this evolution is governed by a set of rules that specifies the values of the state variables for continuous values of t. The set of rules describing the dynamical system behavior are expressed in the form of differential equations, and the analysis of the system stability can be executed in a qualitative fashion, avoiding the extensive computational effort of numerically integrating the set of dynamic equations when its parameters are varying.

As mentioned earlier, an electric power system is generally represented by an implicit mixed set of parameter-dependent DAEs (2.5), such that variations of any parameter in the system may result in a complex behavior which could lead to system instability. Hence, this behavior must be systematically studied by means of the calculation of the steady-state solutions. In this context, the asymptotic behavior of a dynamical system, as $t \to \infty$, is called steady-state or equilibrium solution of the system, and the corresponding steady-state solution may be either a static solution or a dynamic solution, i.e. the solution can be either constant or time varying. The time-constant solutions are often called fixed points or

stationary solutions, whereas the time-varying solutions are simply called dynamic solutions [Nayfeh and Balachandran, 2004]. Even though these static and dynamic solutions indicate that the system has reached an equilibrium on its state variables, to understand their stability, further analyses are required. There is a theorem which relates the stability in the sense of Lyapunov and the asymptotic stability and may be used to determine the stability of the equilibrium solutions as follows [Nayfeh and Balachandran, 2004]: Assume a dynamical system described by the following system of Ordinary Differential Equations (ODEs)

$$\dot{x} = h\left(x, p\right) \tag{2.22}$$

which is fairly similar to Equation 2.4. Consider that the equilibrium solutions of Equation 2.22 for some given value p_0 of p are (x_0, p_0). Furthermore, assume that there exists an at least once differentiable scalar function $V\left(x, p\right)$ defined in a neighborhood of these equilibrium solutions such that $V\left(x_0, p_0\right) = 0$ and $V\left(x, p\right) > 0$ if $(x, p) \neq (x_0, p_0)$. The derivative of V along the solution trajectories of Equation 2.22 is $\dot{V} = \nabla V \cdot h = \nabla V^T h$. Hence, if $\dot{V} \leq 0$ in the chosen neighborhood of (x_0, p_0) the equilibrium solution is stable; if $\dot{V} < 0$ in the chosen neighborhood of (x_0, p_0) the equilibrium solution is asymptotically stable. However, the use of this theorem presents the disadvantage of having no general methods for determining the function $V\left(x, p\right)$, called Lyapunov function, and as a consequence finding such a function for power system models may be difficult. An alternative approach to determine the stability of equilibrium solutions is discussed next.

For a fixed value of p, the Equilibrium Points (EPs) of the dynamic model are given by

$$0 = h\left(x, p\right) \tag{2.23}$$

To determine the stability of these equilibrium solutions a small disturbance ϵ is considered, obtaining

$$x\left(t\right) = x_0 + \epsilon\left(t\right) \tag{2.24}$$

Substituting Equation 2.24 in Equation 2.22 yields

$$\dot{\epsilon} = h\left(x_0 + \epsilon, p\right) \tag{2.25}$$

Thus the fixed point x_0 has been transformed into the fixed point $\epsilon = 0$. Assuming that h is at least twice differentiable, Equation 2.25 can be expanded in a Taylor series about x_0 as

$$\dot{\epsilon} = h(x_0, p_0) + D_x h(x_0, p_0)\,\epsilon + O\left(\|\epsilon\|^2\right) \tag{2.26}$$

where D_x is the derivative operator w.r.t. x, and $O\left(\|\epsilon\|^2\right)$ represents higher order terms. Retaining only linear terms in the disturbance leads to

$$\dot{\epsilon} \approx D_x h(x_0, p_0) = J\epsilon \tag{2.27}$$

where J is the matrix of first partial derivatives called the Jacobian matrix. As can be proven, the eigenvalues of this matrix provide information about the local stability of the fixed point x_0 as follows [Nayfeh and Balachandran, 2004]: The solution of Equation 2.27 that passes through the initial condition $\epsilon_0 \in R^n$ at time $t_0 \in R$ can be expressed as

$$\epsilon(t) = e^{(t-t_0)J}\epsilon_0 \tag{2.28}$$

where

$$e^{(t-t_0)J} = \sum_{j=0}^{\infty} \frac{(t-t_0)^j}{j!} J^j \tag{2.29}$$

If the eigenvalues λ_i of the matrix J are distinct, then there exists a matrix P such that $P^{-1}JP = D$, in such a way that

$$D = \begin{bmatrix} \lambda_1 & 0 & \cdots & 0 \\ 0 & \lambda_2 & \cdots & 0 \\ \vdots & \vdots & \ddots & \vdots \\ 0 & 0 & \cdots & \lambda_n \end{bmatrix} \tag{2.30}$$

Introducing the transformation $\epsilon = Pv$ in Equation 2.27 results in

$$P\dot{v} = JPv \tag{2.31}$$

or

$$\dot{v} = Dv \tag{2.32}$$

Hence a solution of Equation 2.32 can be expressed as

$$v = e^{(t-t_0)D} v_0 \tag{2.33}$$

where $v_0 = v(t_0) = P^{-1}\epsilon_0$. In terms of ϵ, this solution becomes

$$\epsilon(t) = Pe^{(t-t_0)D}P^{-1}\epsilon_0 \tag{2.34}$$

The matrix $e^{(t-t_0)D}$ is a diagonal matrix with entries $e^{(t-t_0)\lambda_i}$. Hence, the eigenvalues of J are also known as the characteristic exponents associated with h at (x_0, p_0).

A slight modification must be considered in the above-mentioned procedure when the eigenvalues of J are not distinct. If this is the case, then there exists a matrix P such that $P^{-1}JP = J_c$ has a Jordan canonical form with off-diagonal entries as

$$J_c = \begin{bmatrix} J_1 & \phi & \cdots & \phi \\ \phi & J_2 & \cdots & \phi \\ \vdots & \vdots & \ddots & \vdots \\ \phi & \phi & \cdots & J_k \end{bmatrix} \tag{2.35}$$

where ϕ represents a matrix with zero entries and

$$J_m = \begin{bmatrix} \lambda_m & 1 & 0 & \cdots & 0 \\ 0 & \lambda_m & 1 & \cdots & 0 \\ 0 & 0 & \lambda_m & \ddots & \vdots \\ 0 & 0 & 0 & \cdots & \lambda_m \end{bmatrix} \tag{2.36}$$

where $m = 1, 2, \cdots, k$.

Hence the same procedure may be applied considering J_c instead of D.

Based on the analysis described above, the associated response of Equation 2.22 is qualitatively described by the characteristic exponents associated with Equation 2.27 and can be used to determine the stability of the EPs as follows [Seydel, 2010], [Nayfeh and Balachandran, 2004]: When all of the eigenvalues of J have nonzero real parts, the corresponding EP is called hyperbolic equilibrium solution, irrespective of the values of the imaginary parts; otherwise it is called non-hyperbolic equilibrium solution. The word hyperbolic is due to the fact that solution trajectories near a hyperbolic equilibrium point lay on pieces of hyperbolas centered in that point with respect to a suitable coordinate system, i.e. a solution point is hyperbolic if all sufficiently small perturbations on the equilibrium points of the corresponding set of differential equations close to that equilibrium point have similar behavior [Glendinning, 1994].

If all of the eigenvalues of J have negative real parts, then all of the components of the

disturbance ϵ decay in time, and hence x approaches the equilibrium solution x_0 of Equation 2.22 as $t \to \infty$; therefore, the solution x_0 is asymptotically stable. On the other hand, if one or more of the eigenvalues have positive real parts, some of the components of ϵ grow in time, and x moves away from the equilibrium solution x_0 as t increases; thus, the solution x_0 is said to be unstable in this case. As a result, for these type of equilibrium solutions the local nonlinear dynamics near $x = x_0$ are qualitatively similar to the linear dynamics near $\epsilon = 0$, and a qualitative change in the local nonlinear dynamics can be detected by examining the associated linear dynamics, as per the Hartman-Grobman Theorem [Nayfeh and Balachandran, 2004].

A non-hyperbolic equilibrium solution is unstable if one or more of the eigenvalues of J have positive real parts. If some of the eigenvalues have negative real parts while the rest have zero real parts, the equilibrium solution $x = x_0$ is said to be neutrally or marginally stable. For these type of equilibrium solutions the Hartman-Grobman Theorem loses validity, i.e. the linearization of the nonlinear dynamical system fails. An alternative may then be to take high-order terms of the Taylor series expansion of Equation 2.26 in order to address this issue.

Since eigenvalues are a useful tool for analyzing the stability of EPs, the manner in which these lose stability is of interest. To do so, recall the concept of bifurcation, which refers to a qualitative change in the features of a dynamical system, such as the number and type of solutions, under the slow variation of one or more system parameters. When this change is analyzed in the neighborhood of an EP, it is referred to as a local bifurcation [Nayfeh and Balachandran, 2004]. Bifurcations are represented in a space formed by the state variables and the varied parameters, called state-control space, or more commonly bifurcation space. Therefore, starting with values of system parameters corresponding to a stable equilibrium solution, and then varying them slowly, the equilibrium solutions of Equation 2.22 can lose stability, typically through one of the following bifurcations:

a) Saddle-node bifurcation (SNB)

These types of co-dimension 1 (i.e. when only a single parameter is varied), static generic bifurcations occur when two equilibrium points, typically one stable and one unstable in practice, merge and disappear as the parameter slowly changes, as illustrated in the PV curve of Fig. 2.5. Mathematically, assume that for $p = p^c$ Equation 2.22 satisfies the following at an equilibrium point (x^c, p^c) [Seydel, 2010]:
1) $\frac{\partial h(x^c,p^c)}{\partial x}$ has $n-1$ eigenvalues with negative real part and a simple eigenvalue 0 with right eigenvector v and left eigenvector w.

2) $w^T \left(\left(\frac{\partial h}{\partial p} \right) (x^c, p^c) \right) \neq 0$.

3) $w^T \left(\frac{\partial^2 h}{\partial x^2} \mid_{(x^c,p^c)} (v, v) \right) \neq 0$.

Then, there is a smooth curve of equilibria passing through (x^c, p^c), tangent to $\Re^n \times p^c$. Depending on the signs in 2) and 3), there are no equilibrium points near (x^c, p^c) when $p <$ or $> p^c$, and two hyperbolic equilibrium points exist, one stable and one unstable, when $p <$ or $> p^c$.

In power systems, SNBs are associated with voltage collapse [IEEE/PES Tech. Rep., 2002].

b) Limit-induced bifurcation (LIB)

These types of co-dimension 1 generic bifurcations in power systems were first studied in detail in [Dobson and Lu, 1992], and are typically encountered in these systems since as the load increases, reactive power demand generally increases as well, and thus reactive power limits of generators or other voltage regulating devices are reached. These bifurcations result in reduced voltage stability margins [Avalos et al., 2009], and in some cases the operating point "disappears" in a LIB causing a voltage collapse, as illustrated in Fig. 2.6, where Q_{Smax} represents the reactive power limit supplied by the generator and V_0 represents the generator's voltage set point. LIBs occur at the equilibrium point (x^c, p^c) where the eigen-system of the matrix J undergoes a discrete change due to x reaching a limit condition, which changes the structure of Equation 2.22 and hence the associated Jacobian, which is nonsingular [Venkatasubramanian et al., 1995].

c) Hopf bifurcation (HB)

The type of bifurcation that connects equilibria with periodic motions is an HB; it is the bifurcation of a static EP into a dynamic EP of the model defined by Equation 2.22 as shown in Fig. 2.7, and it is responsible for power system oscillatory behaviors. In this case, the Jacobian matrix J has a pair of purely imaginary eigenvalues while all of its other eigenvalues have nonzero real parts. Mathematically, the following conditions define an HB at the equilibrium point (x^c, p^c) [Seydel, 2010]:

1) $f(x^c, p^c) = 0$.

2) The Jacobian $\frac{\partial f(x,p)}{\partial x} \mid_{(x^c,p^c)}$ has a simple pair of purely imaginary eigenvalues $\mu = 0 \pm i\beta$ and all other eigenvalues have negative real parts.

3) $\frac{d(Re(\mu(p)))}{dp} \mid_{p^c} \neq 0$.

If these three conditions are satisfied, there is a birth or death of limit cycles at the point (x^c, p^c) depending on the sign of equation defined in 3).

The main reason to consider only these three types of bifurcations resides in the fact that in power systems HBs, SNBs and LIBs are generic and can be basically characterized by the oscillatory, and the local merging and disappearance of the power flow solutions as certain system parameters, particularly system demand, slowly change [IEEE/PES Tech. Rep., 2002].

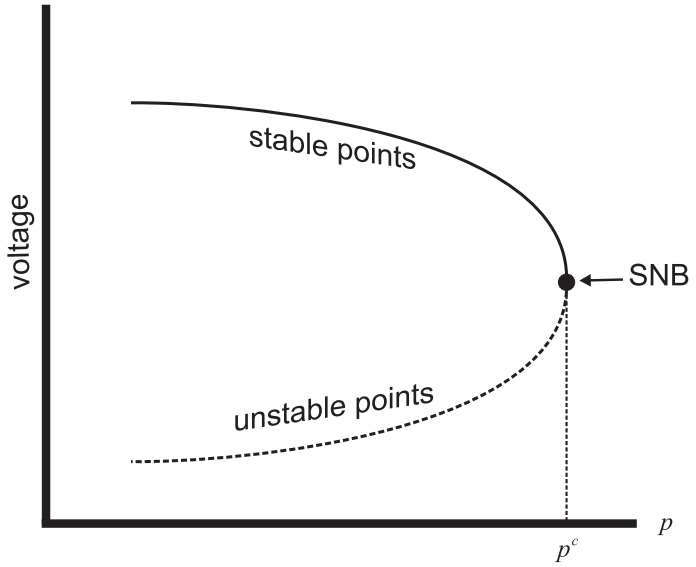

Figure 2.5: SNB in a PV curve.

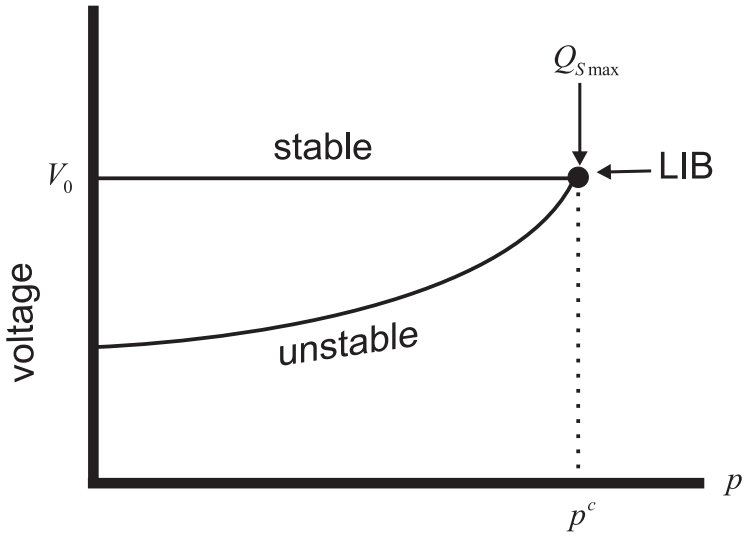

Figure 2.6: LIB in a PV curve.

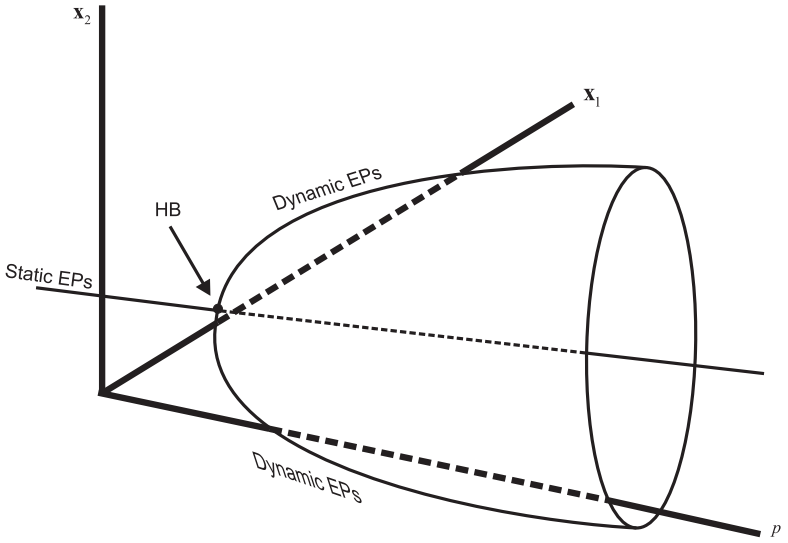

Figure 2.7: Bifurcation of static EPs into HBs.

2.4 Differential Algebraic Equations Equivalent System and Equilibrium Points

Systems in the form of Equations 2.5 are "theoretically problematic," because the set of algebraic equations may have singular points where it cannot be solved for the dependent algebraic variables y, and consequently at these points the response of the system cannot be defined [Van Cutsem and Vournas, 2008]. These differential-algebraic systems are analyzed establishing conditions under which systems equivalent to Equations 2.5 and comprised solely of differential equations can be derived. These equivalent systems have the same dynamic and algebraic properties as the full model. Hence, based on Schur's Theorem [Seydel, 2010] and the Implicit Function Theorem, there exists a locally unique, smooth function F of the form

$$\dot{x} = F(x, p) \tag{2.37}$$

from which the algebraic variables have been eliminated. Since F can be defined and is smooth at all points where g_y is nonsingular, from the existence theorem there is a unique solution of the DAE system (2.5) for all these points. The domain of F in state space for a given value of the parameter p is bounded by the points satisfying the singularity condition of g_y. Hence, EPs of dynamical system models such as those resulting from the electric power systems (Equations 2.5) can be obtained when they satisfy the equations:

$$\begin{aligned} 0 &= h\left(x, y, p\right) \\ 0 &= g\left(x, y, p\right) \end{aligned} \tag{2.38}$$

The stability of these EPs can be determined by linearizing Equations 2.38 around the equilibrium:

$$\begin{bmatrix} \triangle\dot{x} \\ 0 \end{bmatrix} = J \begin{bmatrix} \triangle x \\ \triangle y \end{bmatrix} \tag{2.39}$$

where J is the unreduced Jacobian of the resulting equivalent DAE system

$$J = \begin{bmatrix} h_x & h_y \\ g_x & g_y \end{bmatrix} \tag{2.40}$$

Assuming g_y is nonsingular $\triangle y$ can be eliminated from Equation 2.39

$$\triangle\dot{x} = \left[h_x - h_y g_y^{-1} g_x\right] \triangle x \tag{2.41}$$

The state matrix of the linearized system is

$$A = H_x = \left[h_x - h_y g_y^{-1} g_x\right] \tag{2.42}$$

which is the Schur complement of the Jacobian's algebraic equation g_y in the unreduced Jacobian J.

The stability of an EP of the DAE system (2.5) for a given value of p is obtained by analyzing the eigenvalues of the state matrix A [Hill and Mareels, 1990]. As p varies, the DAE may experience bifurcations like a simple ODE system, as presented in the previous Section. Therefore, as system inputs (demand and generation) vary or unexpected equipment contingencies occur, the basic problem of whether the system could sustain its operation under the new condition arises. In electric power system studies this problem is known as the small-signal stability problem [Kundur et al., 2004].

2.5 Stability/Security Boundaries

The concept of security regions is very useful in conceptualizing and, under certain conditions, in explicitly characterizing the multidimensional boundaries where power networks may operate in a secure fashion in terms of controllable parameters. The security boundaries

are crucial in defining any type of power interchange and the corresponding capability of power networks.

The region in the parameter space in which the power network satisfies all steady-state and transient operational requirements under both the existing network topology and a set of contingency-degraded network topologies is called Security Region [Venkatasubramanian et al., 1995] and [Venkatasubramanian et al., 1995-1]; it is important to recall that when no contingencies are considered a stability, rather than security, region is obtained. To find the boundary of this region, even for a simple system, normally requires a sequence of simulations that repeatedly vary the generation patterns and load levels until meeting all security constraints becomes impossible. This procedure and the numerical tools used to obtain the set of points determining and characterizing the SB are described in this Section. Furthermore, two types of SB are described: the SB resulting when the loading directions are varied considering prespecified dispatch patterns, and the resulting SB when the dispatch patterns are varied considering prespecified loading levels reflecting the practical fact of the inelasticity of loads.

2.6 SB Determination Procedure

Recalling that the main goal of the present research work is to provide a closed-form differentiable function which represents the highly nonlinear SB, the procedure to obtain such a boundary must be established. The SB is constructed by loading the power system until the stability limits are reached for the most critical single contingency (N-1 contingency criterion), considering multiple and realistic generator dispatch patterns; these dispatch patterns are also called dispatch directions due to the fact that each dispatch pattern defines a trajectory in which generators will increase their generating power.

In order to obtain the SB, the power system model defined by Equations 2.5 may be written as follows [Sauer and Pai, 1988]:

$$\begin{aligned} \dot{x} &= h\left(x, y, \rho, \lambda\right) \\ 0 &= g\left(x, y, \rho, \lambda\right) \end{aligned} \tag{2.43}$$

where ρ and λ change continuously, moving the system from one EP to another. As it was previously mentioned, the region in the parameter space where all the operating points can be reached without causing instability is called a feasible region [Venkatasubramanian et al., 1995], and [Venkatasubramanian et al., 1995-1]. Since at the boundary of this region,

the system EPs change their stability characteristics, the feasible region and the associated boundary can be constructed based on stability analyses of the EPs associated with the differential-algebraic Equations 2.43 representing the power system.

In the operation of power systems, the system loads and generators vary throughout the operating horizon. For a given generation dispatch pattern, each specific pattern or "direction" of load changes (load increases are typically more relevant from a security standpoint than load reductions) drives the system to unstable conditions when the operating point reaches the feasibility boundary. Therefore, a SB can be constructed through voltage, angle and frequency stability studies for various loading changes and considering an N-1 contingency criterion.

As a first step to compute this boundary, let $\lambda_i = \begin{bmatrix} \lambda_{i1} & \lambda_{i2} & \cdots & \lambda_{iN} \end{bmatrix}^T$ be an i^{th} particular set of load increase rates for the N loads in (2.43), so that

$$\begin{aligned} \lambda_{i1} &= \alpha d_{i1} \\ \lambda_{i2} &= \alpha d_{i2} \\ &\cdots \\ \lambda_{iN} &= \alpha d_{iN} \end{aligned} \tag{2.44}$$

where $\alpha \geq 0$ is a scalar value typically referred to as the loading factor, and d_{ij}, $j = 1, 2, \cdots, N$, represents the loading increase "direction" for load j in the i^{th} particular set of load increase rates, with the following conditions:

$$0 \leq d_{ij} \leq 1 \ \ \forall j \tag{2.45}$$

$$\sum_{j=1}^{N} d_{ij} = 1 \tag{2.46}$$

Thus, considering Equations 2.18 and assuming a constant power factor, the load may be defined as

$$\begin{aligned} P_{d_{ij}} &= \lambda_{ij} P_{d_{j0}} = \alpha d_{ij} P_{d_{j0}} \\ Q_{d_{ij}} &= \lambda_{ij} Q_{d_{j0}} = \alpha d_{ij} Q_{d_{j0}} \end{aligned} \tag{2.47}$$

where $P_{d_{j0}}$ and $Q_{d_{j0}}$ are the "base" active and reactive powers demanded at the j^{th} load bus.

Once the loading direction vector $d_i = \begin{bmatrix} d_{i1} & d_{i2} & \cdots & d_{iN} \end{bmatrix}^T$ is defined, the system load can be increased until an EP on the SB is reached by increasing the loading factor α; this boundary can then be associated with "critical" λ_{ij}^c values. To obtain a discrete representation of the SB, the N system loads can be varied in M different sets of load directions for given

generation dispatch criteria. The SB can then be represented in the λ-parameter space. Computationally, this boundary may be represented by means of a critical load matrix as follows:

$$M_\lambda = \left[\begin{array}{cccc} c_1 & c_2 & \cdots & c_N \end{array} \right] = \left[\begin{array}{cccc} \lambda_{11}^c & \lambda_{12}^c & \cdots & \lambda_{1N}^c \\ \lambda_{21}^c & \lambda_{22}^c & \cdots & \lambda_{2N}^c \\ \vdots & \vdots & \ddots & \vdots \\ \lambda_{M1}^c & \lambda_{M2}^c & \cdots & \lambda_{MN}^c \end{array} \right] \tag{2.48}$$

Observe that for each generation pattern considered, a similar matrix can be obtained.

The loading directions should cover the whole range $0 \leq d_{ij} \leq 1$ to attain a complete boundary and should have an even distribution. To attain this even distribution in a multi-dimensional d-parameter space, the interval [0 1] on each axis is divided into M points: $i = 1, 2, \ldots, M$, where M is selected so that a reasonable density is achieved. Thus, all the possible combinations of the points that satisfy Equation 2.46 can be employed to obtain the boundary points required to train the BPNN.

2.7 SB Numerical Determination

For a given generation dispatch, the critical λ_{ij}^c values that define the SB for the system model (2.43) are computed using continuation power flows, eigenvalue analyses and transient stability studies considering an N-1 contingency criterion, as described in some detail in [Gu and Cañizares, 2007]. These critical points obtained along different loading directions for different generation patterns that make up the SB constitute the training and testing set of the BPNN.

It is important to mention that for each contingency and dispatch scenario a unique stability limit, which is a point of the stability boundary, can be obtained. The SB is then made up of the stability limit points obtained for each system dispatch and its corresponding "worst" contingency scenario: the contingency that yields the smallest loading margin associated with the system stability limit for the given dispatch, as per the N-1 contingency criterion. Again, observe that if no contingencies are considered, a stability boundary rather than a SB is obtained. In the following sections, the different studies considered to obtain the points defining the SB are presented. Furthermore, the two types of SBs which may be obtained based on these studies are discussed: the loading-directions-based SB and the dispatch-directions-based SB.

2.7.1 Continuation-based Methods

The power system physical constraints impose a maximum loadability limit, which is the amount of power that the system is able to supply. Near this loadability maximum, the stability analysis is restricted by the resulting ill-conditioning of the Jacobian matrix when conventional numerical methods to determine the equilibrium point are used. Hence, as the electric power systems are operated closer to their stability limits, computational tools must be numerically robust in order to allow the proper stability assessment. Among the numerical methods commonly used to achieve this numerical robustness are the Continuation Methods (CM) [Ritcher and Decarlo, 1983]; these methods are used as branch tracing or path following and have the particularity of maintaining the Jacobian matrix well-conditioned allowing the computation of complete solution trajectories. The CM allows the tracing of complete PV curves in order to properly assess the power system voltage stability. In this context, the basic idea behind the branch tracing procedure consists of carrying out small successive increments in a system's parameter called the continuation parameter; often this parameter is the system load and is called the loadability parameter. For each load increment, the power system EP will move to a different point, until the desired part of the solution trajectory is determined [Van Cutsem and Vournas, 2008]. The commonly used method to determine the set of points defining such a solution trajectory is the predictor-corrector based CM.

Several computational tools considering this method have been developed and successfully applied to analyze the voltage collapse phenomenon, in such a way that preventive or corrective actions may be assessed in order to increase the voltage stability margins [Cañizares and Alvarado, 1993], [Fluek, 1996], and [Zhu, 2001]. In the present work, this method is used to obtain the SNB and LIB points for each loading direction, considering particular generator's dispatch patterns, so that the resulting set of SNB points make up a subset of the training points used to map the SB, as explained in Chapter 3.

2.7.2 OPF-based Methods

When using the CM to obtain a critical value λ_{ij}^{c} corresponding to a loading direction, several continuation parameter increments must be carried out in order to obtain a SNB or LIB point. Hence, in order to obtain the set of critical points defining the SB, a procedure of this type must be performed for each loading direction, resulting in a time-consuming procedure. However, this computational burden can be reduced as shown in [Avalos et al., 2009] by using an optimization-based approach to identify and analyze SNBs and LIBs of a power system model. In this case, the solution points procured from an optimization model, which is based

on complementarity constraints used to properly represent generators' voltage controls, correspond to SNB or LIB points associated with a loadability direction, avoiding the procedure of successive increments in the continuation parameter.

This approach is based on the application of optimization methods to compute the maximum loadability points, which are directly associated with SNBs and LIBs. The optimization model used may be represented as [Avalos et al., 2009]:

$$\max_{\delta,V,V_s,Q_S} \quad \lambda \tag{2.49}$$

$$s.t. \quad F_{PF}\left(\delta, V, V_s, P_s, Q_s, P_d, Q_d, \lambda\right) = 0 \tag{2.50}$$

$$(Q_{s_k} - Q_{s_{k_{min}}}) V_{a_k} = 0 \ \ \forall k \in G \tag{2.51}$$

$$(Q_{s_k} - Q_{s_{k_{max}}}) V_{b_k} = 0 \ \ \forall k \in G \tag{2.52}$$

$$V_{s_k} = V_{s_{k_o}} + V_{a_k} - V_{b_k} \ \ \forall k \in G \tag{2.53}$$

$$Q_{s_{k_{min}}} \leq Q_{s_k} \leq Q_{s_{k_{max}}} \ \ \forall k \in G \tag{2.54}$$

$$V_{a_k}, V_{b_k} \geq 0 \ \ \forall k \in G \tag{2.55}$$

where G represents the number of system generators; V and δ correspond to the bus voltage phasor components; V_{s_k} is the k^{th} generator voltage; $V_{s_{k_o}}$ is the k^{th} generator voltage regulator set point, i.e. the generator terminal voltage level if the generated reactive power Q_s is within limits; P_s and P_d are the supply and demand power levels in MW, respectively, that cannot exceed their maximum values; $F_{PF}\left(\cdot\right)$ stands for the power flow equations of the system; Q_s and Q_d are the generated and demanded reactive powers in MVars, respectively; the constraints defined by Equations 2.51-2.55 associated with the auxiliary variables V_a and V_b are used to model the actuation limits associated with the generator voltage regulators. As formally demonstrated in [Avalos et al., 2009] a solution to the model (2.49)-(2.55) corresponds to either SNB or LIB points by establishing that the transversality conditions of the corresponding bifurcations are met, based on the optimality conditions of the optimal solution. As a consequence, this model obtains the SNB and LIB points based on powerful optimization solvers, resulting in a more computationally efficient method.

2.7.3 Eigenvalue Analysis

The eigenvalue analysis presented in Section 2.3 also identifies the type of EP associated with HBs, which make up the complementary subset of points defining the SB, which will be the training set of the proposed BPNN. The procedure is based on the CM and consists of detecting the HB at each step of the CM by obtaining the eigenvalues of the resulting Jacobian matrix J; when an HB is detected, it is saved as a critical point, and the CM procedure is interrupted. This procedure is repeated for each loading direction until the full segment of the SB has been determined.

2.7.4 Loading directions-based SB

Since load increases are typically more relevant from a security standpoint, the SB resulting when the loading directions are varied and considering prespecified generator's dispatch patterns is presented in this Section by using a realistic IEEE benchmark system, such as the 118-bus system. This system is composed of 53 generators and 91 loads. The system data and generator bid data are shown in Appendix C.

The system is divided in two operational areas, in such a way that the corresponding SB represents a specific transfer limit between these areas: Area 1 with 45 loads, and Area 2 contains 46 loads. The system SB for an Area 1 - Area 2 interchange is obtained using, for the sake of simplicity and without the loss of generality, voltage stability criteria only, i.e. the boundary is basically composed of SNBs and LIBs [Milano, 2005], [UWPFLOW], with the assumption that a Line 39-40 trip stands for the worst contingency. A total of 631 loading directions are considered to get an even distribution of points, and a generation dispatch pattern based on the base generator powers is used. The loading directions are presented in Appendix D for the case or two groups. The resulting SB is shown in Fig. 2.8.

It is important to recall that each point at the SB represents an equilibrium point at which a bifurcation occurs, and this point is obtained considering a prespecified generator's dispatch pattern. Clearly if an operative point is located outside the region bounded by the set of bifurcation points, the power system no longer fulfills the security requirements for proper operation.

2.7.5 Dispatch directions-based SB

In this section, another type of SB is presented, obtained when the generator's dispatch direction are varied considering pre-specified loading increase rates. For this purpose the

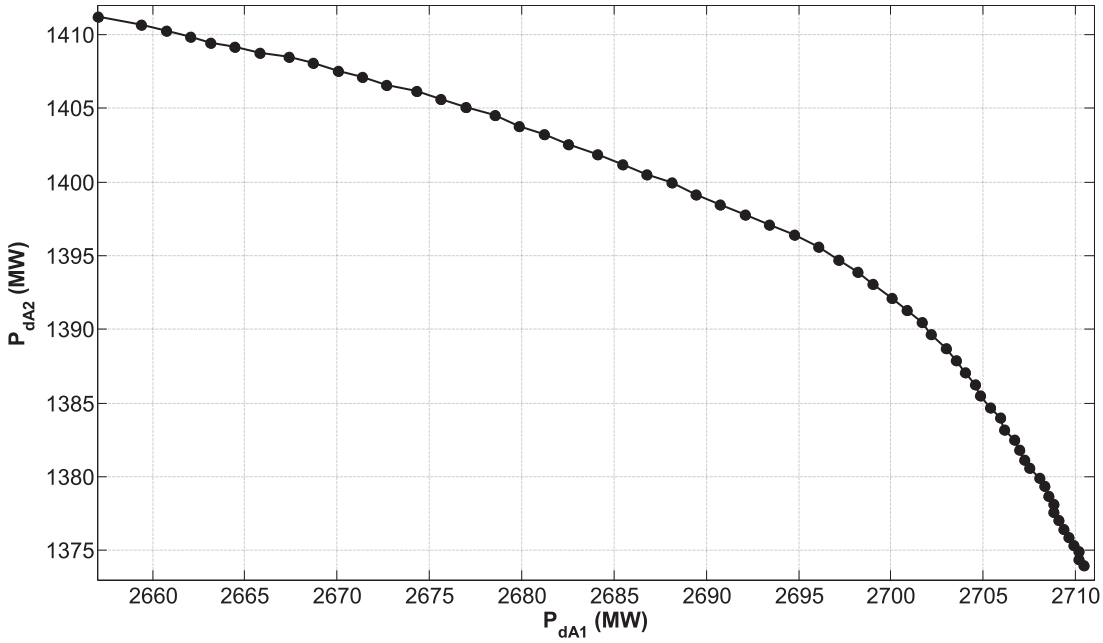

Figure 2.8: SB for the IEEE 118-bus benchmark system considering two loading areas.

same IEEE 118-bus benchmark system used in the previous Section is considered assuming the same line trip as the worst contingency. Two loading groups containing 45 and 46 loads are defined; a fixed value of 0.5 for the loading direction is arbitrarily selected for each loading group without loss of generality. In order to vary the dispatch directions, two generator groups are considered containing 27 generators each, and 21 dispatch directions are selected for the reason explained in the previous Section. As in the previous case, only LIB and SNB points are considered when the SB is obtained. The SB is shown in Fig. 2.9, where P_{G_A} and P_{G_B} represent the generated active power for each area in MW.

For further insight into the complexity of the security region, generators and loads of the system under study are split into three groups each. The loading groups contain 31, 31, and 29 loads each, and the generation groups contain 18 generators each. A fixed value of 0.33 for the loading direction is arbitrarily selected for each loading group, and 631 dispatch directions are selected, as shown in Appendix D. Once more, only LIB and SNB points are considered to obtain the SB, which is shown in Fig. 2.10, where P_{G_A}, P_{G_B}, and P_{G_C} represent the total generated active power for each group.

Thus, the SB must be obtained by taking into account a specific criteria only, depending on the context under analysis: if it is desired to evaluate the system security based on a voltage stability approach, load increments must be implemented in order to obtain the corresponding SB. On the other hand, a specific "base point" may be relocated into its

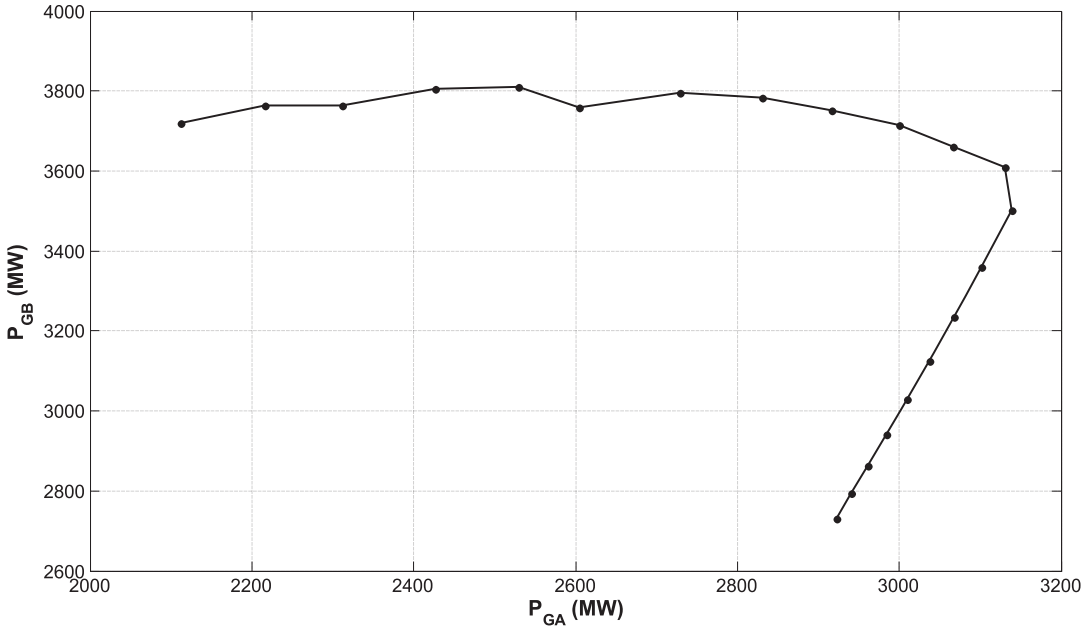

Figure 2.9: SB for the IEEE 118-bus benchmark system considering two dispatch areas.

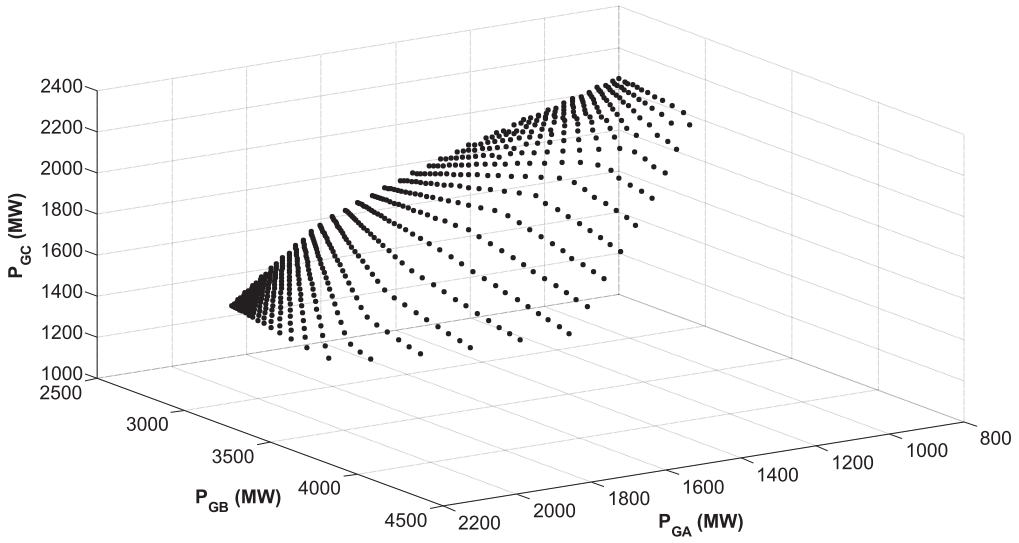

Figure 2.10: SB for the IEEE 118-bus benchmark system considering three dispatch areas.

corresponding SB by means of varying the generator's dispatch patterns, obtaining its SB varying the generator's dispatch directions. In the present work, the SBs are obtained by varying the loading directions assuming pre-specified generator's dispatch patterns. This assumption is reasonably because currently the electric power systems are highly stressed due to the load increments resulting from the demand increase and the rare construction of new generation units and transmission corridors.

2.8 Conclusions

In this Chapter the power system mathematical representation has been reviewed, showing that due to power system dynamics interact at widely-varying time constants, conversion equations are needed. Also, it is reviewed the main concepts of bifurcation theory, which allow to qualitatively describe the stability of solution points of the resulting power system model. Furthermore, based on the implicit function theorem it is shown how the power system model expressed by a set of differential-algebraic equations can be analyzed as a set of ODEs.

It is introduced the concept of stability and security boundaries and it is established the SB determination procedure, which is based on a proposed critical load matrix. By using the techniques applied for this procedure, two types of SB are obtained for the IEEE 118-bus benchmark system: the loading directions-based SB and the dispatch directions-based SB, emphasizing their complex topology.

Chapter 3

Approximations of the Security Boundary

3.1 Introduction

The SB gives the system operator very important information regarding the stability and/or security of the current power system operating point. Thus, all this information must be taken into account by the computational tools used in electricity markets in order to generate adequate market signals to properly address the security-constrained unit commitment, ancillary services auction, and transmission pricing. This information can be used to take preventive and corrective actions when insecure operating points are identified. However, exacting this information could be a challenge because the high nonlinear characteristics of the SB, which as previously shown is very complex.

The goal of the present Chapter is to describe a new methodology to obtain an explicit smooth-nonlinear-differentiable function reproducing the SB with adequate precision, in order to be included as a security constraint in a SC-OPF model in a straightforward way. The approach for it is based on the SB approximation which is implemented with two different mapping tools: BPNN and NR. ANNs have good mapping characteristics, as well as a large degree of freedom that is basically model-independent, which make them easily modifiable in order to map complex multidimensional surfaces resulting from systems containing several generation and loading areas. NR is only capable of mapping low-dimensional surfaces.

3.2 BPNN-based SB

ANNs are mathematical models that try to mimic the brain's neural networks. The brain can be considered a large-scale system that has many neural cells called neurons. Neurons are continuously processing and transmitting information to each other. Massive parallel information processing, learning functions and the self-organizing capabilities are among the main features of a human brain. By analogy, as shown in Fig 3.1, ANNs are formally defined by three elements: a set (layer) of information processing units (neurons), a specific topology of weighted interconnections among the neurons, and a learning algorithm that updates the connection weights. As shown in Figs. 3.1 and 3.2, four basic elements of the neuronal model can be identified [Haykin, 1999]:

1. A set of connecting links, each characterized by a weight w_{ji}^{k}.
2. An adder $\sum$ for summing the input signals, weighted by the respective link of the neuron.
3. An activation function f_i for mapping and producing the output of the neuron.
4. An externally applied bias b_i which has the effect of increasing or lowering the net input of the activation function.

The resulting mathematical expression of a neuron i may be written as

$$Output_i = f_i\left(input_i w_{ji}^{k} + b_i\right) = f_i\left(n_i\right) \tag{3.1}$$

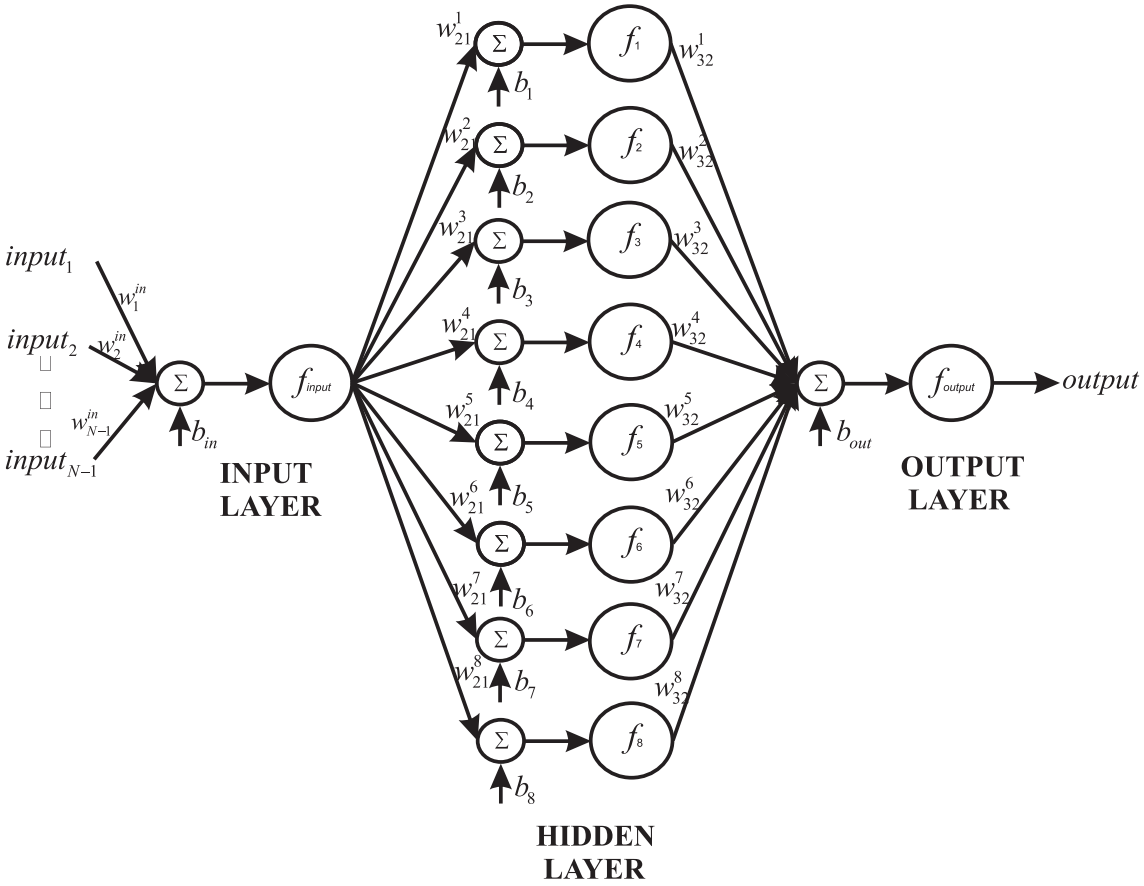

Figure 3.1: BPNN architecture.

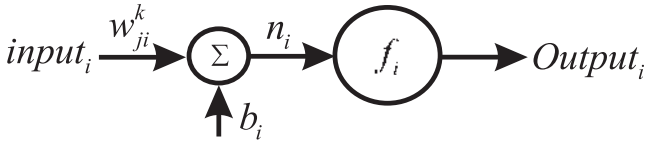

Figure 3.2: Single neuron structure.

There are several activation functions that can be used such as threshold (e.g. piecewise-linear, sigmoid, etc.), and their application will depend on the particular ANN behavior desired [Haykin, 1999].

The goal of ANN applications is to find a model that represents the observations of a system's input/output behavior. An ANN learns through the process of extracting enough information from a training set to form a mapping function that accurately describes the system at all points of interest. These networks can be trained for function approximation, pattern association, or pattern classification.

The training process requires a set of samples of proper network behavior. During training, all network parameters are iteratively adjusted based on a learning rule to minimize a network performance function, which is a measure of how well the network represents the training samples. The learning rule is the procedure by which an ANN modifies its parameters to perform some particular task, and it is referred to as a training algorithm.

When training the ANN, there are several learning rules that can be used such as back-propagation. [Haykin, 1999], and all are based on the way in which the network weights are adjusted along the gradient of the performance function. Properly trained BPNN have been demonstrated to give reasonable answers when presented with inputs that they have never seen. Typically, a new input leads to an output similar to the output for input vectors used in training that are similar to the input being used. This generalization property makes possible to train a network on a representative set of input/target pairs, without having to train the network on all possible input/output pairs. When BPNNs are used as function approximators, the composed set of activation functions, which directly depends on the BPNN architecture, can be viewed as a function whose parameters have been adjusted to perform the required mapping process.

The universal approximation theorem provides the mathematical justification for the robust approximation of any arbitrary continuous function by a nonlinear input-output mapping using BPNN [Haykin, 1999]. In other words, these networks can approximate any function with arbitrary accuracy as long as enough units (neurons and/or layers) are used in the network. Their accuracy will depend on the complexity of their structure; thus, the more complex the BPNN structure, the better accuracy will be obtained when complex functions are mapped.

The lack of success of a BPNN to solve an approximation problem is not because of the innate capabilities of neural networks, but rather due to one or more of the following conditions [Hornik et al., 1989]:

1. There is an insufficient number of units in the network: Depending on the accuracy of the approximation required to solve a given task, a minimum number of nodes may be required. A specific network architecture is initially selected, and if the desired degree of accuracy is not achieved, additional network neurons and/or layers are added until the desired accuracy is met.

2. There is an inability to learn the proper network parameters: The reasons for this inability may be a lack of the number of training samples, a lack of information "richness" in the training set, an ineffective learning algorithm, and/or numerical complications.

The role of the trained BPNN when used to solve a function approximation problem is to properly represent the function $y = f(x)$ that describes the system at each point x in the required domain. In this context, "to solve" implies meeting a desired error threshold rather than perfect performance. Estimating a target function at all points in the domain of interest is known as generalization: the BPNN is asked to "generalize" its representation of the system in areas "unseen" during training. Generalization is concerned with the ability of a model to represent a function (approximation) and the ability to realize the model using finite data (estimation). The main goal here is to use a BPNN as a function approximator in such a way that all the necessary information in the desired SB could be contained in the trained network. The mapping process for each SB involves the following steps:

1. Obtain the matrix M_λ given by Equation 2.48, which constitutes the training and testing sets for the BPNN.

2. Train and test the BPNN.

3. Obtain an explicit function representation of the BPNN for its inclusion in an OPF model.

The BPNN considered in this work is composed of three layers: input, hidden and output layers, as shown in Figs. 3.1 and 3.2. Each layer contains a number of neurons whose connections increase the BPNN's capability to learn complex relationships. The number of neurons was determined considering a compromise between the bias and the variance errors. As it is shown in Fig. 3.2, every connection between the i^{th} layer and the j^{th} consecutive layer through the k^{th} neuron is weighted by a number w_{ji}^{k}. A neuron adds the incoming inputs $input_i$, which could be the weighted output information from other neurons and passes the net sum through an activation function f_i. The activation function of each neuron transforms the net weighted sum n_i of all incoming input signals into one output signal. Also, each neuron has an additional input, called a bias b_i, which is used in the network to generalize the solution and avoid a zero value for n_i, even when an $input_i$ is zero.

The BPNN architecture used in this work was selected based on the criteria of having the simplest array of neurons, capable to map the security or stability boundary with a reasonable precision. Hence, the BPNN consists of one neuron for both input and output layers and eight neurons for the hidden layer, as shown in Fig. 3.1. The neurons composing the hidden layer have the activation function

$$f_i(n_i) = \left(\frac{2}{1 + e^{-2n_i}}\right) - 1 \tag{3.2}$$

where n_i can be an input state variable or algebraic expression depending if the state variables are coming from the input data or from the output of other neurons. The input and output neurons have a linear activation function with unitary value.

In the majority of BPNN applications, the main handicap resides in the fact that BPNNs are handled as "black boxes". That is, once the network is trained, little can be said about the functional approximation or the functional form between any of the inputs with the output. Thus, in order to obtain a differentiable function from a trained BPNN, the following procedure is proposed: The input-output relationship of the neuron single structure is shown in Equation 3.1. From the input-output relationships between the three layers of the trained BPNN shown in Fig. 3.1, the implicit mapping function that relates the network inputs and output can be obtained.

The output of the input layer of the proposed BPNN represented in Fig. 3.1 is:

$$Output_{in} = f_{input}\left(input_i w_i^{in} + b_{in}\right) \quad \forall i = 1, 2, \cdots, N-1 \tag{3.3}$$

where $N-1$ are the loading points making up the boundary provided as inputs to the BPNN. Since the identity function is the input layer activation function , Equation 3.3 may be written as

$$Output_{in} = input_i w_i^{in} + b_{in} \quad \forall i = 1, 2, \cdots, N-1 \tag{3.4}$$

This output represents the input for each neuron at the hidden layer in such a way that the input-output relationship of each neuron at this layer is

$$Output_k = f_k\left(\left(Output_{in}\right)_k w_{21}^k + b_k\right) w_{32}^k \quad \forall k = 1, 2, \cdots, 8 \tag{3.5}$$

where k is the number of neurons at the hidden layer. Substituting Equation 3.4 into Equation 3.5

$$Output_k = f_k\left(\left(input_i w_i^{in} + b_{in}\right)_k w_{21}^k + b_k\right) w_{32}^k \quad \forall k = 1, 2, \cdots, 8 \tag{3.6}$$

These outputs are the inputs of the output layer, thus the output of the output layer is

$$Output_{out} = f_{output}\left[\sum_{k=1}^{8} f_k\left(\left(input_i w_i^{in} + b_{in}\right)_k w_{21}^k + b_k\right) w_{32}^k + b_{out}\right] \tag{3.7}$$

As the identity function is the output layer activation function, Equation 3.7 may be written as

$$Output_{out} = \sum_{k=1}^{8} f_k \left(\left(input_i w_i^{in} + b_{in} \right)_k w_{21}^k + b_k \right) w_{32}^k + b_{out} \quad \forall i = 1, 2, \cdots, N-1 \tag{3.8}$$

Note that following this procedure the extraction of the function associated with a trained BPNN is possible, regardless of the number of layers and the number of neurons in each layer. Furthermore, any type of activation function may be considered, either a standard-predefined activation function or a user-defined activation function, allowing high flexibility when mapping complex-shaped SBs using the proposed BPNN.

3.3 BPNN Training and Testing

The term training or learning algorithm refers to a systematic procedure for adjusting the weights in the network in order to achieve a desired input/output relationship. In the case of "supervised" learning is based on pairs of input vectors and desired output vectors (u^r, y_d^r), where the superscript r ranges over all pairs used to train the network, and the subscript d stands for "desired" output vector. The network then learns to associate the input vector u^r with the output vector y_d^r; then, for a given set of weights, if the network is presented with an input u^r, it will produce an output y^r which should be identical or very close to y_d^r.

The method used to train the BPNN off-line consists of iteratively adjusting the network weights and biases to minimize the network's performance, which in this work is given by the square error between the network outputs and the target outputs. The gradient of the performance function is used to adjust all the weights and biases using an updating technique known as back-propagation, which adjusts the weights of an ANN in order to reduce the value of the performance criterion. Specifically, the error performance is given by [Chassiakos and Masri, 1996]:

$$E = \frac{1}{2} \sum_{r}^{ne} \sum_{k=1}^{m} \left(y_k^r - y_{kd}^r \right)^2 \tag{3.9}$$

where ne is the number of training patterns, and m is the number of outputs.

Back-propagation adjusts the parameters following a gradient algorithm. The gradient of E with respect to a parameter vector called W, which compares all the weights and parameters of a specific layer, is calculated; the parameters are then adjusted in the direction

of the negative gradient. Since neither the input to nor the reference signals for the hidden layers are known, back-propagation starts at the output level and "propagates" the results backwards to the first layer. The summarized steps of the back-propagation algorithm are as follows [Luzardo-Flores, 1997]:

1. Initialize all the parameters of the net.

2. Propagate forward the input u^r to the successive hidden layers up to the output layer.

3. Adjust the parameters starting at the last layer, and then back-propagate the error through the network up to the first layer, as follows:
   - Adjust the parameters by using:

$$W^{new} = W^{old} - \eta \nabla E \tag{3.10}$$

   where η is the step size called learning rate, and ∇E is the gradient of E with respect to the parameters of the corresponding layer.
   - Once the corresponding parameters of a layer are updated, back-propagate the error to the next layer and update the parameters of that layer. This procedure continues until the first layer is reached.

4. Change the input vector and repeat the procedure from step 2 until all the pairs (u^r, y_d^r) are considered.

5. Repeat from step 2 through step 4 until a limit number of epochs is reached.

In order to train the BPNN to represent the SB, the M critical values of the $N-1$ loading points making up the SB are provided as inputs to the BPNN, i.e., in Fig. 3.1, $input_1 = c_1$, $input_2 = c_2$,...,$input_{N-1} = c_{N-1}$ as per Equation 2.48. The target (output) value that must be satisfied within a given tolerance is given by a chosen N^{th} column of M_λ defined in Equation 2.48, i.e. $Output_{out} = c_N$, so that $c_N = f\,(input)$, where $input = \begin{bmatrix} input_1 & \dots & input_{N-1} \end{bmatrix}$, and $f\,(\cdot)$ stands for the "total" BPNN function (Equation 3.8). Observe that a given point on the boundary is basically defined by:

$$\lambda_{iN}^c \approx f\,(\lambda_{i1}, \lambda_{i2}, \dots, \dots, \lambda_{iN-1}) \approx f\left(\hat{\lambda}_i\right) \tag{3.11}$$

In other words, for $N-1$ known load increase rates defined by the vector $\hat{\lambda}_i$, the SB value λ_{iN}^c of a chosen N^{th} load/generation increase is defined by (3.11).

The boundary points can also be represented in the P_d-parameter or loading space based on (2.44), (2.47) and (3.11), so that a critical loading point on the boundary is given by

$$P^c_{d_{iN}} \approx f\left(P_{d_{i1}}, P_{d_{i2}}, \ldots, P_{d_{iN-1}}\right) \approx f\left(\hat{P}_{d_i}\right) \tag{3.12}$$

Therefore, the equation

$$P^c_{d_N} - f\left(\hat{P}_d\right) = 0 \tag{3.13}$$

defines a hyper-surface in the N-dimensional loading space on which the BPNN-SB is defined (e.g. for 2 loads it is a curve, for 3 loads it is a 2-dimensional surface, etc.).

The BPNN training and validation process used here is based on randomly dividing the input vectors and the target vector in three sets as follows: 60% are used for training; 20% are used to validate the BPNN and to stop training before over-fitting as per the above-mentioned performance function; and the last 20% are used as an independent set to test the BPNN generalization [Demoth et al., 2008]. The time that it takes to train the BPNN is in the range of a few seconds to several minutes, depending on the number of loading or generation areas considered to build the SB. Since this is carried out off-line, obtaining the required BPNN-SBs should not represent a problem in a practical implementation of the proposed methodology.

3.4 BPNN and NR Nonlinear Function

Following an inverse procedure, a symbolic algebraic process can be employed to relate the input/output of the BPNN, considering its architecture and the basic neuron structure, as shown in the previous section. Hence, the mapping function that relates the input-output for the BPNN shown in Fig. 3.1, in terms of load/generation increase rates, is obtained from Equations 2.48, 3.8, and 3.11 as

$$\lambda^c_N = \sum_{k=1}^{8} f_k\left(\left(\hat{\lambda}^T w^{in} + b_{in}\right) w^k_{21} + b_k\right) w_{32} + b_{out} \tag{3.14}$$

where $w^{in} = \begin{bmatrix} w^{in}_1 & w^{in}_2 & \cdots & w^{in}_{N-1} \end{bmatrix}^T$. From Equation 2.44, Equation 3.14 can be rewritten as

$$\alpha^c d_N = \sum_{k=1}^{8} f_k \left(\left(\alpha^c \hat{d}^T w^{in} + b_{in} \right) w_{21}^k + b_k \right) w_{32} + b_{out} \tag{3.15}$$

where α^c represents the critical loading factor. Observe that the system operating point associated with a loading/generating level $\lambda_N > \lambda_N^c$ is located outside the security region.

Based on Equation 2.47, the mapping function (Equation 3.14) can be expressed as

$$P_{d_N}^c = \sum_{k=1}^{8} f_k \left(\left(\hat{P}_d^T w^{in} + b_{in} \right) w_{21}^k + b_k \right) w_{32} + b_{out} \tag{3.16}$$

Similarly, system operating points associated with a loading level $P_{d_N} > P_{d_N}^c$ are located outside the security region. Hence, the mapping functions (Equations 3.14 or 3.15) can be used as security constraints in the OPF formulation, as explained in the next Chapter, to achieve a stable equilibrium point from a voltage collapse viewpoint.

On the other hand, the SB can also be approximated by the following polynomial approximation, as proposed in [Jayasekara and Annakkage, 2006]:

$$\lambda_N^c = A + \sum_{i=1, i \neq N}^{8} \left(B_i \hat{\lambda}_i + \sum_{j=i+1, i \neq N}^{8} C_{ij} \hat{\lambda}_i \hat{\lambda}_j + D_i \hat{\lambda}_i^2 \right) \tag{3.17}$$

A NR approach can be used to obtain the A, B, C and D parameters in Equation 3.17, and a similar procedure used for the validation of the BPNN can be employed to validate the NR; thus, 70% of input and target vectors are used in the fitting process, while the rest are used to validate the NR function performance. A mayor problem in using regression techniques is that for complex relationships, a search for a suitable model can be very difficult, as demonstrated with an example later in the Chapter.

3.5 The Bias/Variance Dilemma

The aforementioned mapping tools introduce a bias error (a measure of how different on average the function estimate is from the target function for each training sample) in the estimation of the SB. This error is always present in any approximation process [Haykin, 1999]. For the case of the BPNNs, this can be minimized by increasing the number of neurons in the hidden layer and/or the number of hidden layers, since as the number of neurons and/or layers increases. The network will interpolate the training data to decrease the bias error. However, increasing the size of a network increases the difficulty of estimating the network

parameters, thus affecting the variance error (a measure of how different on average the function estimate is from its expected value over all training samples), and over-fitting may occur. On the other hand, decreasing the number of neurons in the hidden layer and/or the number of hidden layers minimizes the variance error but increases the bias error and may result in under-fitting. The same "dilemma" occurs in the case of the NR model, where if an approximation procedure is performed, the variance error is reduced while increasing the bias error, whereas if an interpolation procedure is performed, the bias error is forced to zero while increasing the variance error. This is commonly referred to as the bias/variance dilemma.

In the proposed approach a trade-off between the bias and variance errors is considered in order to achieve generalization, which as it was previously mentioned, is the ability of a model to properly estimate a process/system based on a set of input/target pairs without having to repeat the approximation procedure for all possible input/output pairs. Thus, these errors must be minimized even though they depend on each other; the bias error minimization implies the increment of the variance error and viceversa, and hence both cannot be reduced at the same time. As a consequence, to achieve generalization a midpoint between these values resulting in a trade-off between them is useful here.

3.6 Study Cases

The results of the proposed approach to map the SB and their comparison with respect to the results obtained by using the NR approximation are presented in this Section. Two test systems are considered, namely IEEE 2-area and IEEE 118-bus benchmark systems, to prove that the accuracy and reliability of the mapping process using BPNN are sufficient for the application to large-scale power systems.

3.6.1 IEEE 2-area Benchmark System

The slightly modified IEEE 2-area benchmark system shown in Fig. 3.3 consists of two similar areas connected through a relatively weak double-circuit tie line; the added variable capacitor at Bus 8 keeps the bus voltage constant to improve voltage profiles for various loading conditions. The system generators were modeled using detailed sub-transient models including simple excitation systems and speed governors. A power system stabilizer was installed on generator G4 to damp possible low frequency oscillations. There are only two loads in the system at Buses 7 and 9, respectively. The system data [Kundur, 1994], generator

bid data, and active power generation limits are shown in Appendix B.

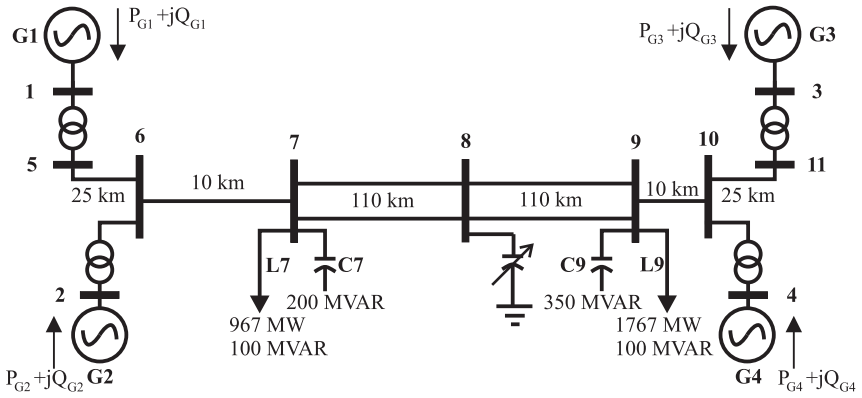

Figure 3.3: IEEE 2-area benchmark system.

A. Two Loads

Following the procedure described in this Chapter, the SB of the system shown in Fig. 3.3 is obtained considering a Line 7-8 trip, based on the 21 different loading directions shown in Appendix D for each load and detailed static and dynamic studies using the tools described in [Milano, 2005] and [UWPFLOW]; the generator dispatch pattern used to obtain the boundary was based on the base generator powers. Hence, the resulting SB is composed of pairs $[\lambda_7^c, \lambda_9^c]$ associated with the loading directions of the loads located at Nodes 7 and 9; these are referred here as training points to better express the inherent training procedure associated with the BPNN. To train the BPNN and to perform the NR, λ_7^c was assumed as the input, and λ_9^c was considered as the target. For the case of the BPNN, it took about 91 secs. on a standard PC to minimize the error between the output and the target to within a 10^{-5} tolerance; and for the case of the NR, it took about 80 secs. to minimize the error to within a 10^{-4} tolerance. It was not possible to obtain a 10^{-5} tolerance by using the NR approach due to its lack of accuracy. Because of the mapped surface's simplicity, good mapping results are obtained, and no significant differences are observed.

The mapping results of the NR and the BPNN are presented in Fig. 3.4.

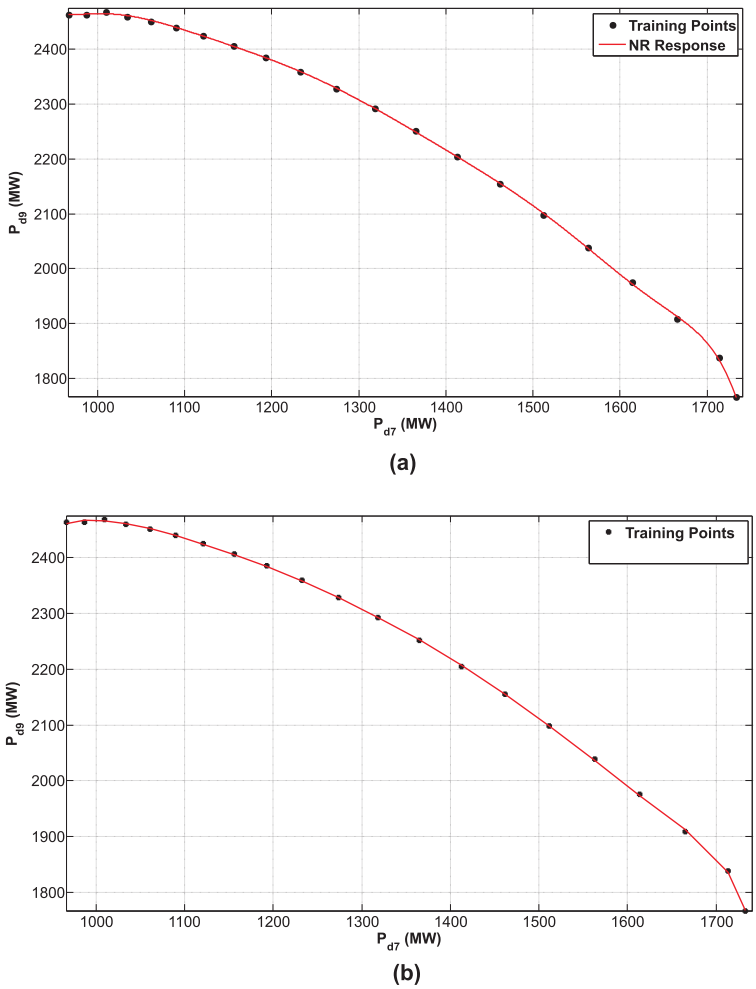

Figure 3.4: Two-load SB mapping for the IEEE 2-area benchmark system (a) using NR and (b) using BPNN.

B. Three Loads

For this case, the system is modified including a load of 800 MW and 50 MVARs at Bus 6. The modified system is shown in Fig. 3.5.

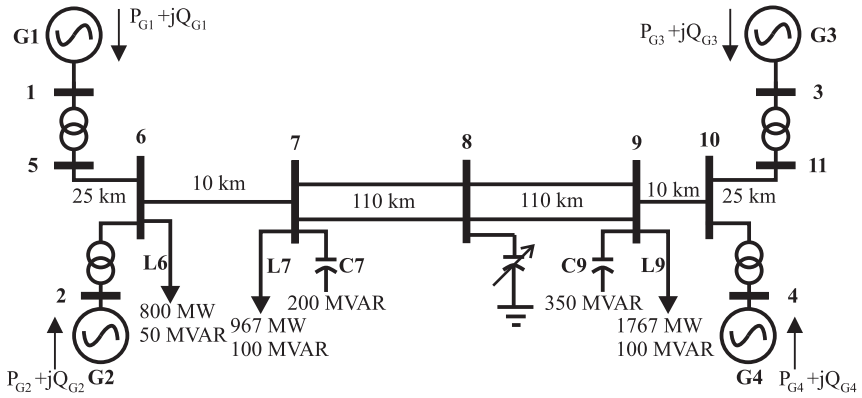

Figure 3.5: IEEE 2-area system including a load at bus 6.

Following the procedure described for the case of two loads, the SB was obtained based on the 631 different loading directions shown in Appendix D for each load, and detailed static and dynamic studies using the tools described in [Milano, 2005] and [UWPFLOW]. The generator's dispatch patterns used to obtain the boundary was based on the base generator powers. As in the previous case, the SB is obtained for a Line 7-8 trip.

The resulting SB is composed of points $[\lambda_7^c, \lambda_9^c, \lambda_6^c]$ associated with the load directions of the loads located at Nodes 7, 9 and 6, respectively, which are also referred as training points. Here, λ_7^c and λ_9^c were assumed to be the inputs to the BPNN and the NR, and λ_6^c was considered as the target. It took about 96 secs. on a standard PC to minimize the error between the output and the target to within a 10^{-5} tolerance for the case of the BPNN. On the other hand, the NR-based mapping procedure is faster than the BPNN-based mapping (it took only about 15 secs.). However, as shown in the resulting SB depicted in Fig. 3.6(a), the NR-based mapping tool does not give appropriate results since the SB presents some discontinuities that, for the case of the BPNN in Fig. 3.6(b), are averaged by the approximation, resulting in a more even surface for obtaining a differentiable nonlinear function in terms of the loading space.

Therefore, if the NR approach is used as SB approximation tool, there will exist regions where the SB is not defined, and there is nothing much to said about the power system's secure operation. The power system would be steering towards insecure operating points having no clue of where the boundary is located, disabling the possibility of taking preventive or corrective actions. The same case occurs for regions unmapped by the NR tool as shown at the bottom part of Fig. [fig:Three-loads-SB-mapping] (a) and (b); also observe how at the right-bottom part there are some points resulting from the NR located outside the SB, which will give false signals regarding the power system's security, i.e. operating points may seem

secure when in reality they are insecure. The opposite cases may be presented: an operative point may be considered as insecure when in reality is secure.

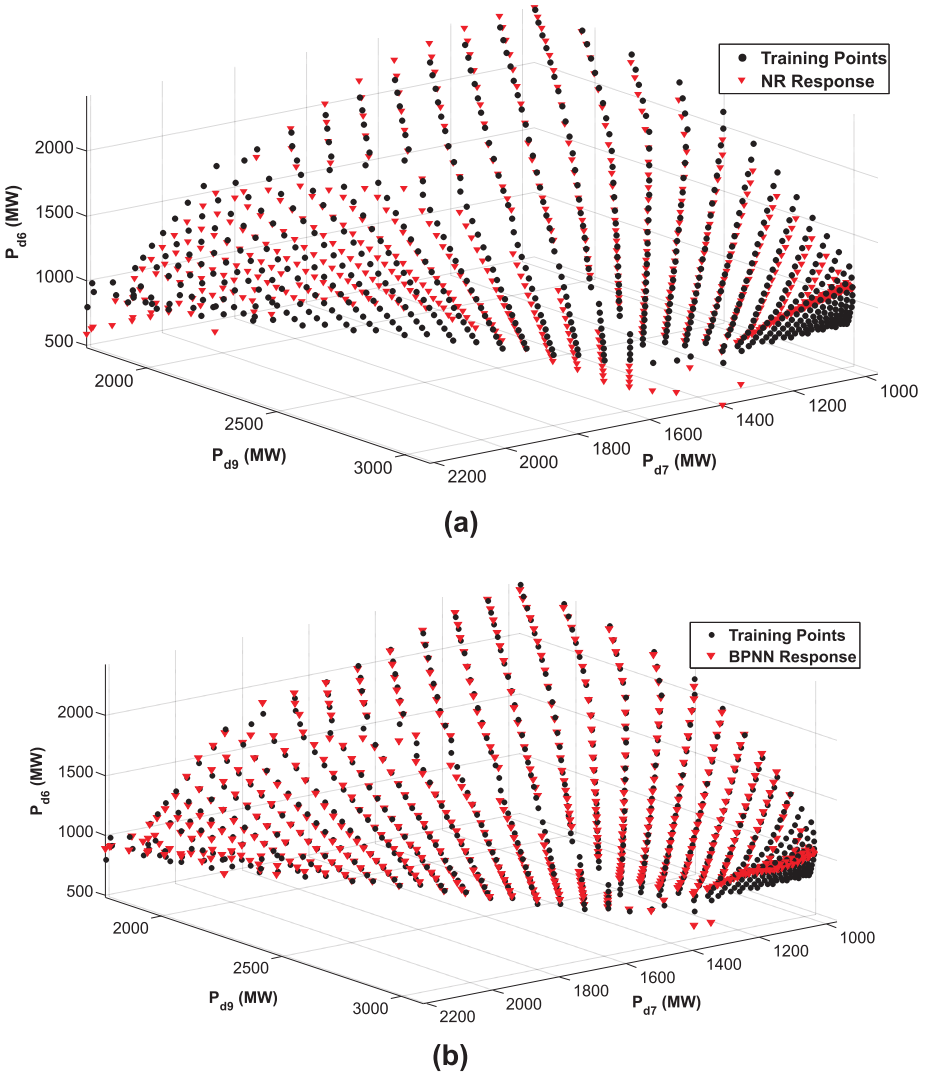

Figure 3.6: Three-load SB mapping for the IEEE 2-area benchmark system (a) using NR and (b) using BPNN.

3.6.2 IEEE 118-bus Benchmark System

In order to test if the proposed approach is capable of handling more complex SBs and to compare its behavior against the NR-based mapping tool, the more realistic IEEE 118-bus Benchmark System presented in Section 2.7.4 is used.

Following standard utility and electricity market practices, the SBs are obtained varying the loading and dispatch directions. For the case when loading directions are varied, the

system was divided into 2, 3, and 4 operational areas as shown in Appendix C, so that the corresponding SBs basically represent transfer limits between these areas. Also, the same 631 loading directions were considered for the reasons explained in Section2.7.4, and a generation dispatch pattern based on the base generator powers was used. Regarding varied dispatch directions, the system is divided into 2 and 3 generating areas as shown in Section 2.7.5, considering 21 and 631 dispatch directions as shown in Appendix D, respectively. The proposed BPNN-SBs were obtained in these cases using the same criteria discussed in Sections 2.7.4 and 2.7.5. A similar training and testing procedure used for the IEEE 2-area system was applied to obtain the required SBs.

Loading Directions

A. Two Areas

The system's SB for an Area 1 - Area 2 interchange and the corresponding NR- and BPNN-based mappings are shown in Fig. 3.7. On a standard PC, approximately 100 secs. were required to minimize the error between the output and the target to within a 10^{-5} tolerance for the case of the BPNN, and 90 secs. for the case of the NR. Similar to the case of the IEEE 2-area benchmark system when two loads are considered, the mapping tools have similar behavior due to the simplicity of the SB. However, for the case of the NR a small deviation in the response on the top left of Fig. 3.7 (a) can be observed.

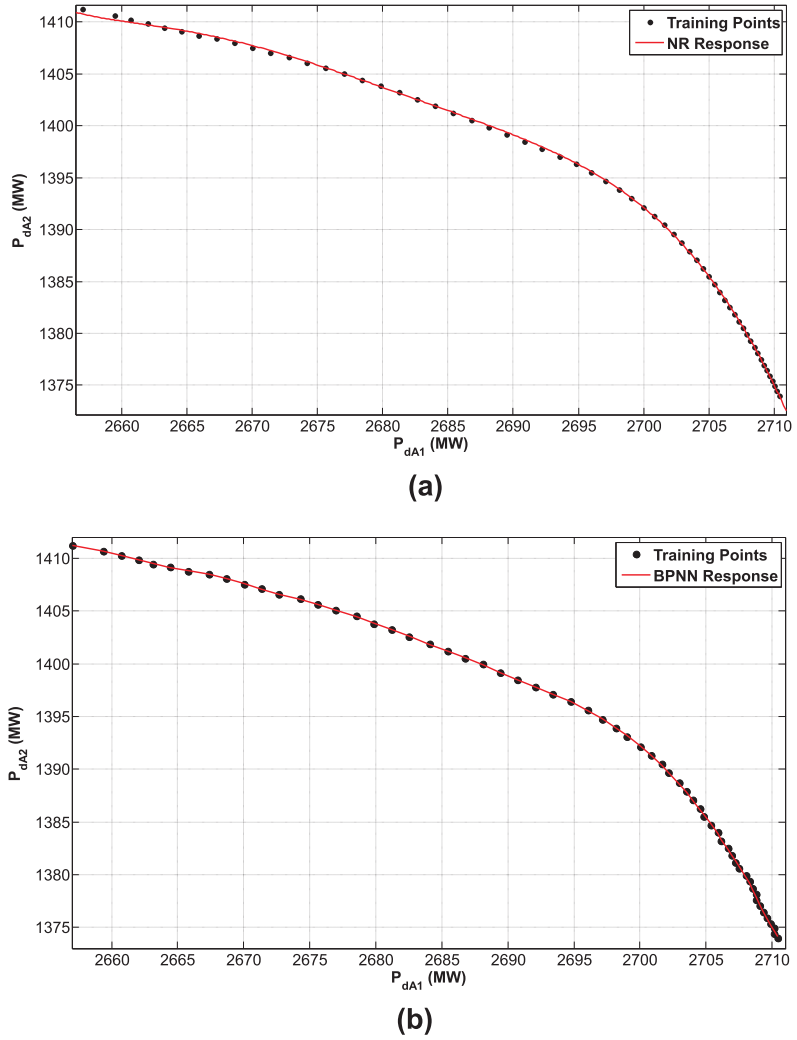

Figure 3.7: SB mapping for the IEEE 118-bus benchmark system considering two loading areas (a) using NR and (b) using BPNN.

B. Three Areas

The system was divided in three operating areas, namely, Area 1 with 31 loads, Area 2 with 31 loads, and Area 3 with 29 loads. The SB mapped by the proposed BPNN and the NR is illustrated in Fig. 3.8 in the P_d-parameter space. It took 156 secs. on a standard PC to train the BPNN and to reduce the error between the output and the target to within a 10^{-5} tolerance. For the case of the NR, it took 150 secs. to minimize this error within a 10^{-3} tolerance.

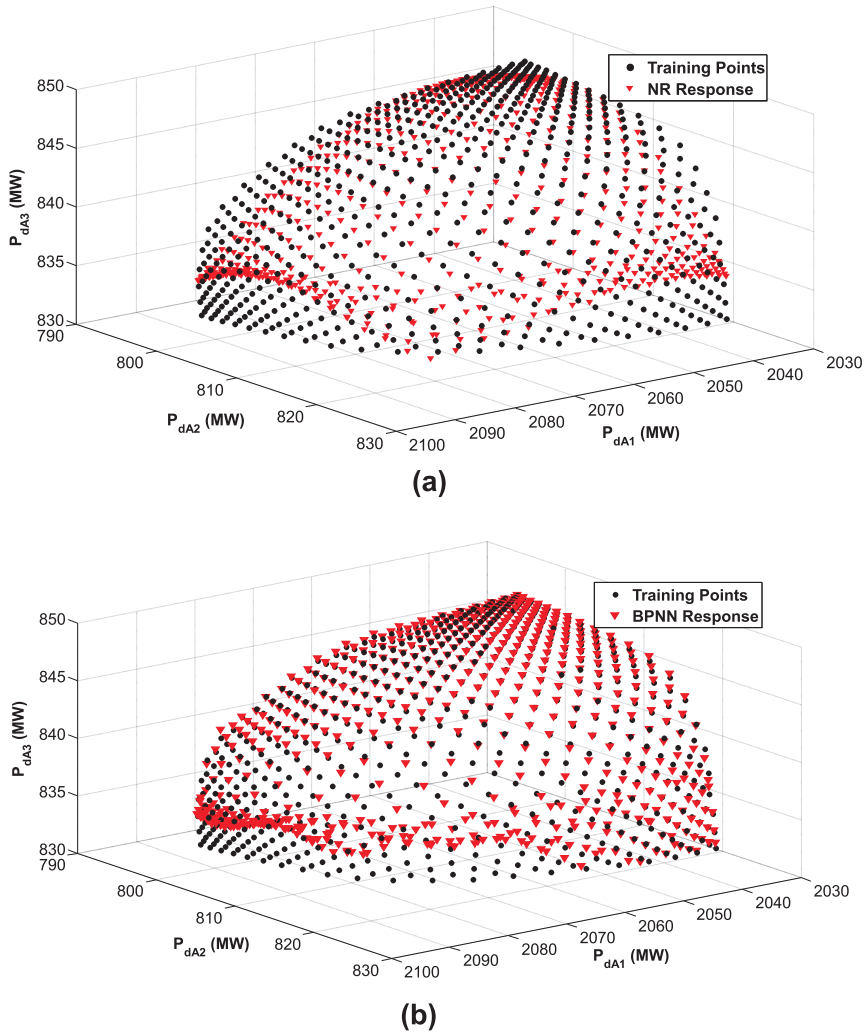

Figure 3.8: SB mapping for the IEEE 118-bus benchmark system considering three loading areas (a) using NR and (b) using BPNN.

From Fig. 3.8 and the error tolerance for each case, it can be seen how the NR does not accurately map the SB. Both mapping tools cannot properly map the bottom of the SB, because it is the region of the SB where more nonlinearities are presented. To overcome this problem the complexity of the BPNN architecture may be increased modifying the number of neurons/layers. However, because the main goal here is to attain the simplest BPNN architecture in order to achieve an "adequate" SB representation, in terms of a smooth-mapped surface which enables the extraction of a differentiable nonlinear function, the development of an "optimal" BPNN which reduces as much as possible the error between the output and the target is not considered here.

C. Four Areas

In this case, the system was divided into the following four areas: Area 1, 2 and 3 with 22 loads each; and Area 4 with 25 loads. The BPNN-SB training took 225 secs., and the NR 180 secs. for tolerances of 10^{-6} and 10^{-4}, respectively. In this case, the flexibility of the BPNN is evident since it is capable of accurately mapping high-dimensional and complex surfaces. Hence, it may be applied to cases where several loads or loading areas are considered.

Dispatch Directions

A. Two Areas

The system is divided in two operating areas as mentioned in Section 2.7.5. The SB mapped by the proposed BPNN and the NR is shown in Fig. 3.9. The NR is unable to map the SB even using a $9th$ degree polynomial, because of the nonlinearity, discontinuities, and few available training points of the SB to be mapped. On the other hand, the proposed BPNN yields the desired results by accurately mapping this more complex SB.

Notice in this figure how it seems not possible to approximate the SB by a single mathematical function, i.e. for each value of P_{GA} correspond two values of P_{GB}, preventing the implementation of the considered approaches. However, observe how in the left part of Fig. 3.9 when the aforementioned it seems to occur the training points are not aligned w.r.t. the x-axis, allowing to using the approximation tools; if it were the case that they were aligned, a little change in the dispatch direction of one of the two training points will be enough to overcome this issue and to produce a deviation between them w.r.t. the x-axis.

B. Three Areas

The system is divided in three operating areas as shown in Section 2.7.5. Several BPNN architectures were tested in order to obtain the simplest one. Because of the complexity of the SB, as shown in Fig. 3.10, it is necessary to use a three-layer ANN containing 25 neurons in the first layer (input layer), 20 neurons in the second layer (hidden layer), both with a sigmoid activation function, and 1 neuron in the third layer (output layer) using a linear activation function. Even when the number of neurons are increased as in this case, the architecture of the BPNN used still can be considered "simple", since it only contains three layers. As illustrated in Fig. 3.10, the NR is unable to successfully map the SB whereas the BPNN shows high accuracy even when complex-shape security regions are presented.

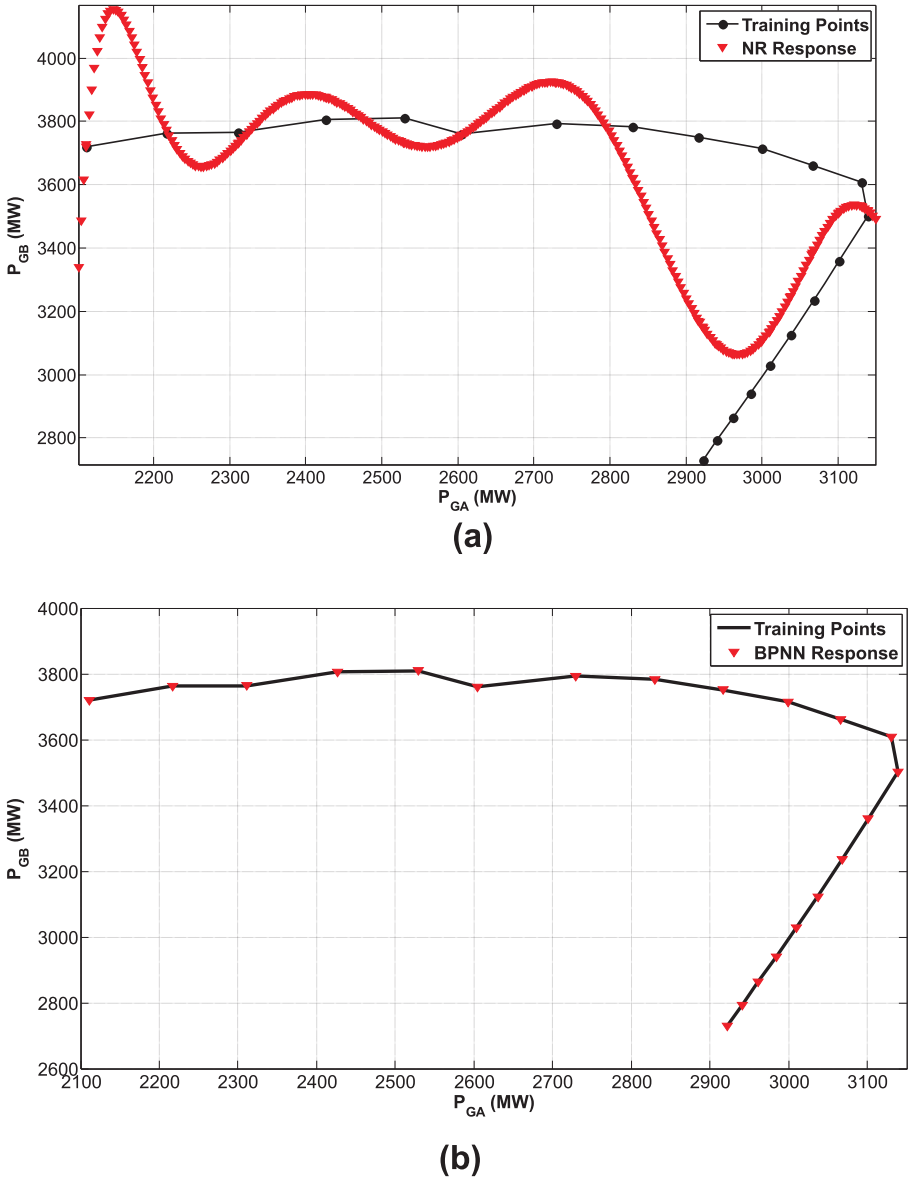

Figure 3.9: SB mapping for the IEEE 118-bus benchmark system considering two dispatch directions (a) using NR and (b) using BPNN.

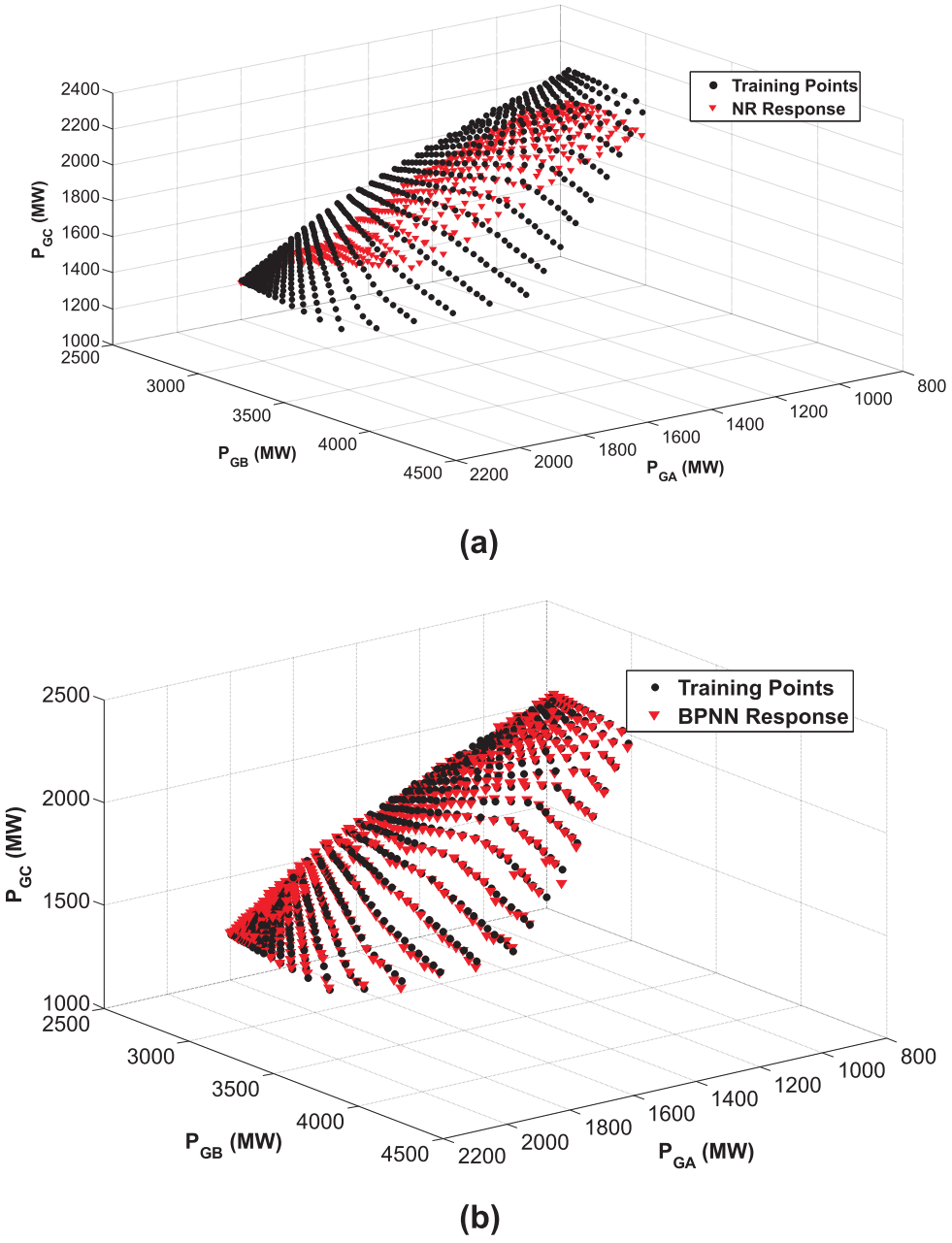

Figure 3.10: SB mapping for the IEEE 118-bus benchmark system considering three dispatch directions (a) using NR and (b) using BPNN.

3.7 Conclusions

The approximations of the SB were presented in this Chapter. Two main approximation tools were considered: the BPNN and the NR.

The role of the trained BPNN when used to solve a function approximation problem is to properly represent the function that describes the system at each point in the required domain. For this case, the SB mapping process consists in obtaining the critical load matrix which constitutes the training and testing sets for the BPNN, training and testing the BPNN, and obtaining the explicit function representation from the BPNN. The BPNN considered in this work is composed of three layers: input, hidden, and output layers; this architecture was selected based on the criteria of having the simplest array of neurons, capable to map the SB with a reasonable precision. Hence, from the trained BPNN a smooth-nonlinear differentiable function was obtained, which may be represented either in the λ-parameter or P_d-parameter space. On the other hand, the SB may also be approximated by polynomial approximation by using NR.

The results of the proposed approach when used to map the SB and their comparison with respect to the results obtained by using the NR were presented. Two test systems were considered, such as the IEEE 2-area and the IEEE 118-bus benchmark systems.

Two cases were presented for the IEEE 2-area benchmark system: two and three loads. In the former no significant differences were obtained due to the simplicity of the SB; however, better tolerances were obtained by using BPNN. In the later case, it was shown how due to the complexity and discontinuity of the SB better mapping results were obtained by using BPNN compared with the results obtained by using NR.

In order to test if the proposed approach is capable of handling more complex SBs and to compare its behavior against the NR-based mapping tool, the more realistic IEEE 118-bus benchmark system was considered. In order to achieve this, two types of SB were presented: the resulting SB obtaining when loading directions are varied, and the SB obtained when the dispatch directions are varied.

For the first case considering two loading areas, no significant differences were observed between the results obtained by using both mapping tools for the same reason as in the 2-area system. When three loading areas were considered, it was shown how the NR it was unable to successfully map the SB; there were unmapped areas and low precision was obtained compared with the better results obtained by using BPNN. When four areas were considered, it was evident the flexibility of the BPNN since it was capable of accurately mapping high-dimensional and complex surfaces.

For the second case where the dispatch directions were varied, two and three operating groups were considered. When two operating groups were considered, the NR was unable to map the SB even by using a 9th degree polynomial, because of the nonlinearity, discontinuities, and few available training points of the SB to be mapped. The proposed BPNN yielded the desired results by accurately mapping this more complex SB. When three operating groups were considered, several BPNN architectures were tested in order to obtain the simplest case because of the complexity of the SB. Again, it was shown how the NR was unable to successfully map the SB whereas the BPNN showed high accuracy even when complex-shape security regions are presented.

Chapter 4

Proposed Security Boundary Constrained-Optimal Power Flow Auction Model

4.1 Introduction

In this Chapter, a discussion of a typical SC-OPF auction model and a novel "dynamic" SC-OPF model are presented. Also, the advantages and disadvantages of both models are discussed. The proposed SBC-OPF auction model is discussed in detail, highlighting the advantages of including a smooth nonlinear differentiable function as an optimization auction security constraint. Furthermore, comparison results between using a BPNN and a NR as tools to map the SB are also presented, showing that the BPNN-based mapping can better represent highly nonlinear multidimensional SB.

4.2 SC-OPF Model

The following is a typical SC-OPF auction model which includes the AC power flow equations as part of the optimization auction constraints to directly account for reactive power and

voltage control and their associated limits [Cañizares and Kodsi, 2006]:

$$\begin{gathered} Min.\ Sb = -\left(C_d^T P_d - C_s^T P_s\right) \\ s.t.\ F_{PF}\left(\delta, V, P_s, Q_s, P_d, Q_d\right) = 0 \\ 0 \leq P_s \leq P_{s_{max}} \\ 0 \leq P_d \leq P_{d_{max}} \\ P_{ij}\left(\delta, V\right) \leq P_{ij_{max}}\ \ \forall i, j, i \neq j \\ I_{ij}\left(\delta, V\right) \leq I_{ij_{max}}\ \ \forall i, j, i \neq j \\ Q_{s_{min}} \leq Q_s \leq Q_{s_{max}} \\ V_{min} \leq V \leq V_{max} \end{gathered} \tag{4.1}$$

where C_s and C_d are vectors of supply and demand bids in \$/MWh, respectively; I_{ij} represents the current in the transmission line ij, so that thermal limits can be directly modeled in the auction process. Finally, $P_{ij_{max}}$ is used to represent transmission system security limits, which are determined off-line by means of stability and contingency studies. It is important to highlight the fact that these security limits do not correspond to the actual system conditions associated with the resulting solutions, since these limits were not necessarily obtained using the operating conditions corresponding to the solution of the OPF-based auction; hence, this model may yield insecure operating conditions and/or inappropriate price signals [Cañizares and Kodsi, 2006], [Ghasemi and Maria, 2008].

4.3 Dynamic SC-OPF Model

A technique that yields a representation of the SB, which accounts for system dynamics, which could be included as an explicit stability function constraint in the OPF model, is proposed in [Jayasekara and Annakkage, 2006]. In this case, the SC-OPF model may be formulated as follows:

$$Min.\ S_b = -\left(C_d^T P_d - C_s^T P_s\right) \tag{4.2}$$

$$s.t.\ F_{PF}\left(\delta, V, Q_s, P_s, P_d, Q_d\right) = 0 \tag{4.3}$$

$$0 \leq P_s \leq P_{s_{max}} \tag{4.4}$$

$$0 \leq P_d \leq P_{d_{max}} \tag{4.5}$$

$$I_{ij}\left(\delta, V\right) \leq I_{ij_{max}}\ \ \forall i, j, i \neq j \tag{4.6}$$

$$Q_{s_{min}} \leq Q_s \leq Q_{s_{max}} \tag{4.7}$$

$$V_{min} \leq V \leq V_{max} \tag{4.8}$$

$$f_{NR_0} - f_{NR}\left(V, \delta\right) \leq 0 \tag{4.9}$$

where the SB is represented by the explicit function $f_{NR}(\cdot)$ in Equation 4.9, and f_{NR_0} is a suitable threshold value. To attain the mapping function $f_{NR}(\cdot)$, the NR fitting technique discussed in Chapter 3 is used. The importance of this approach is that the mapping function can provide a "quick" mapping between an operating point and the corresponding security status, to guarantee that the solution to the OPF problem remains within the SB defined by Equation 4.9. This technique represents an advance in terms of efficiently characterizing the SB with respect to previously proposed SC-OPF methods. Hence, a similar conceptual idea is adopted in this work to develop the proposed BPNN-based SBC-OPF model suitable to obtain stable optimal equilibrium points from a static voltage stability viewpoint.

4.4 Proposed SBC-OPF Model

Given that in practice the majority of system loads are inelastic (price unresponsive) [Bompard, et al., 2000], the OPF model described by Equations 4.2-4.9 can be readily modified to reflect this fact. Thus, the proposed optimization model considers that loads bid on the market only a fraction of their demand which they are willing to curtail if they need to be at a high curtailment price; this better reflects the way markets operate in most jurisdictions. Furthermore, the security constraint (Equation 4.9) can be replaced by the proposed BPNN-SB (Equation 3.14) for each supply pattern considered. Therefore, the following OPF model is proposed:

$$Min.\ S_b = -\left(C_d^T P_d - C_s^T P_s\right) \tag{4.10}$$

$$s.t.\ F_{PF}\left(\delta, V, Q_s, P_s, P_d, Q_d\right) = 0 \tag{4.11}$$

$$0 \leq P_s \leq P_{s_{max}} \tag{4.12}$$

$$Q_{smin} \leq Q_s \leq Q_{smax} \tag{4.13}$$

$$V_{min} \leq V \leq V_{max} \tag{4.14}$$

$$\lambda_N - \sum_{k=1}^{8} f_{k_m}\left(\left(\hat{\lambda}^T w_m^{in} + b_{in_m}\right) w_{21_m}^k + b_{k_m}\right) w_{32_m}^k + b_{out_m} \leq 0\ \ \forall m = 1, \ldots, G \tag{4.15}$$

$$\triangle P_{d_j} \leq 0\ \ \forall j = 1, \ldots, N \tag{4.16}$$

$$\begin{aligned} \triangle P_{d_j} &= \left(\lambda_j - \lambda_{j0}\right) P_{d_{j0}} \\ &= \left(\alpha d_j - \alpha_0 d_{j0}\right) P_{d_{j0}} \end{aligned} \qquad \forall j = 1, \ldots, N \tag{4.17}$$

$$Q_{d_j} = tan\left(\varphi_j\right) P_{d_j}\ \ \forall j = 1, \ldots, N \tag{4.18}$$

$$0 \leq d_j \leq 1\ \ \forall j = 1, \ldots, N \tag{4.19}$$

$$\sum_{j=1}^{N} d_j = 1 \tag{4.20}$$

$$\alpha \geq 0 \tag{4.21}$$

where φ is the power factor angle; m stands for the m^{th} SB obtained for a given generation pattern out of a total of G dispatch patterns; N is the number of loads bidding in the market; C_d represents load curtailment prices; and the load curtailments are represented by $\triangle P_d$, assuming a constant power factor as per Equation 4.18. Observe that constraints represented by Equation 4.16 force $\triangle P_{d_j}$ to be negative or zero for all bidding loads, which, combined with high C_d values, would effectively force the load curtailment to be zero if there is a solution to the problem within the boundaries defined by Equation 4.15. On the other hand, $\triangle P_{d_j}$ becomes nonzero only when there are security violations that cannot be resolved simply with generation dispatch. It is important to highlight the fact that for loads that do not wish to bid in the market $C_{d_j} = \triangle P_{d_j} = 0$. Therefore, this optimization dispatch model properly reflects the basic operating principles of current electricity markets.

This model was solved using two different types of solvers: the Newton-based approach described in [Pizano-Martinez et al., 2007] and [Fuerte-Esquivel et al., 1998], and AMPL [Fourer et al., 2003] with the KNITRO solver [KNITRO]. Both generated the same solutions in all the examples discussed next.

4.5 Study Cases

Numerical results of the proposed method are presented and discussed in this Section. Comparisons between the proposed BPNN-SB mapping approach and the NR proposed in [Jayasekara and Annakkage, 2006] are also presented.

Two sample systems were selected to test and demonstrate the proposed SBC-OPF model, namely, the IEEE 2-area system and the IEEE 118-bus system; the latter shows that the presented approach can be readily applied to realistic power systems. To simplify the presented analyses and explanations of the results, and without loss of generality, the SB was obtained for a "typical" dispatch pattern, i.e. $G = 1$ in Equation 4.15 for both test systems. Furthermore, to test the effect of the security constraint defined by Equation 4.15, all case studies presented are based on load dispatches P_{d_0} that violate the SBs. The corresponding smooth nonlinear differentiable function extracted from the BPNN are found in Appendix A.

4.5.1 IEEE 2-area Benchmark System

The IEEE 2-area benchmark system shown in Fig. 3.3 is used to test the SBC-OPF in order to demonstrate how insecure operating points can be relocated inside the security region using the security constraint defined by Equation 4.15. The two cases presented in Chapter 3 are considered in order to show how the proposed approach can be readily applied to systems containing several loads or loading areas.

4.5.1.1 Two Loads

Following the procedure described in Chapter 3, the resulting stability and SBs are depicted in Fig. 4.1. The latter corresponds to the system stability boundary for a Line 7-8 trip, which is not the worst contingency in this test system since other line trips such as a Line 6-7 trip would yield an unsolvable base power flow; however, this allows to illustrate the application of the proposed dispatch algorithm without loss of generality. Observe the reduced loadability margin when the contingency is considered. Note as well that the boundaries present some discontinuities that are "averaged" by the BPNN approximation, which is a differentiable nonlinear function in the considered loading space.

The values for α, d_{i7}, and d_{i9} shown in Table 4.1 were chosen so that the corresponding P_{d_7} and P_{d_9} values force the system to be outside the SB to test the proposed optimization model, which should yield the most economical dispatch while meeting all security constraints. The

assumed large curtailment bids for the loads were $C_{d_7} = 200\,\$/MW$ and $C_{d_9} = 2200\,\$/MW$, which are, as previously discussed, significantly larger than the generator bids, in the 70 to 90 \$/MWh range, as shown in Appendix B.

Table 4.1: IEEE 2-area system loading scenarios.

Case	α	d_{i7}	d_{i9}	P_{d_7} [MW]	P_{d_9} [MW]
1	0.8	0.4	0.6	1276.44	2615.16
2	0.8	0.5	0.5	1353.80	2473.80
3	0.9	0.6	0.4	1489.18	2403.12
4	0.9	0.7	0.3	1576.21	2244.09
5	1.0	0.8	0.2	1740.60	2120.40

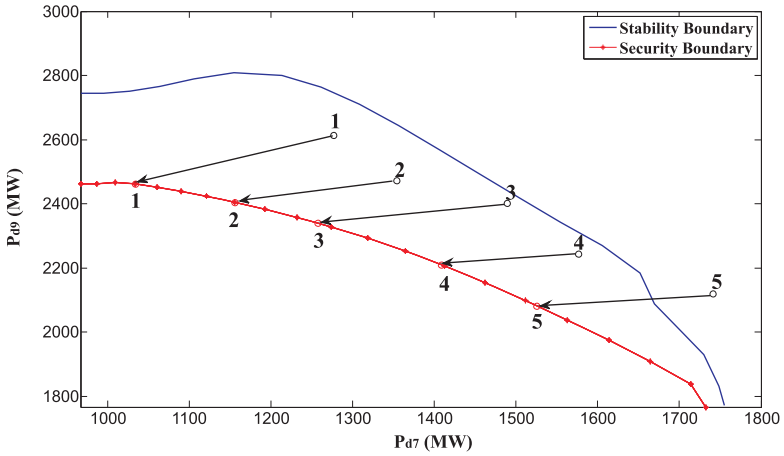

Figure 4.1: Security and stability boundaries for the IEEE 2-area system with two loads.

The load change results obtained by applying the proposed model defined by Equations 4.10-4.20 are shown in Table 4.2. The five initial loading points and five final points with respect to the SB are shown in Fig. 4.1; observe how the loads are minimally curtailed so that the system returns to its SB, curtailing the cheapest load the most, as expected. Thus, in all cases, the cheapest load P_{d_7} is curtailed the most, whereas the most expensive load P_{d_9} is only curtailed in the cases when this is necessary to bring the system within the security limits (Cases 1 and 2), as clearly illustrated with Fig. 4.1.

Table 4.2: IEEE 2-area system load curtailment values.

Case	α	d_{i7}	d_{i9}	ΔP_{d_7} [MW]	ΔP_{d_9} [MW]
1	0.4402	0.1004	0.8996	266.68	148.38
2	0.4402	0.1004	0.8996	344.04	7.02
3	0.5602	0.3574	0.6426	328.56	0.0
4	0.6902	0.6088	0.3912	202.90	0.0
5	0.7436	0.7310	0.2690	247.93	0.0

To test if the proposed approach is successfully curtailing as much as possible the load with the cheaper shedding cost, an interchange in the curtailing bids is carried out considering the same values for α, d_{i7} and d_{i9} shown in Table 4.1. For this case the load at Node 9 is the cheapest load ($C_{d_9} = 200\,\$/MW$), and the load at Node 7 is the most expensive load ($C_{d_7} = 2200\,\$/MW$).

It can be shown from the load change results of Table 4.3 that, as in the previous case, the loads are minimally curtailed so that the system returns to its SB. The cheapest load P_{d_9} is curtailed the most, whereas the most expensive load P_{d_7} is only curtailed in Case 5 because of it is the optimal curtailing scenario. Thus, the proposed SBC-OPF is proved to return the insecure operative points into the security region taking into account economic aspects of the bidding market loads.

Table 4.3: IEEE 2-area system interchanging the load curtailment values.

Case	α	d_{i7}	d_{i9}	ΔP_{d_7} [MW]	ΔP_{d_9} [MW]
1	0.6365	0.5027	0.497	0.0	288.86
2	0.6801	0.5881	0.4119	0.0	211.80
3	0.7422	0.7275	0.2725	0.0	278.78
4	0.7741	0.8139	0.1861	0.0	2.2253
5	0.7918	1.0000	0.0000	7.94	353.40

The proposed BPNN-SB representation (Equation 4.15) is then replaced by the NR polynomial approximation defined by Equation 3.17. The resulting mean square errors for the BPNN and the NR functions are 9.94e-7 and 2.39e-5, respectively, which basically shows that the BPNN approximation fits the boundary better than the NR polynomial approximation. Table 4.4 shows the load changes and the value of the corresponding SB constraint for the BPNN approximation and the NR approximation. Observe that the differences in load curtailments are not significant, but the BPNN security constraint is in general closer to zero

than the NR polynomial one, thus yielding more accurate results at similar computational costs for the solution of the optimization model. Considering that both approximations are based on the same training data, with the BPNN approach requiring a not too costly off-line training process, while the NR approach requires a computationally somewhat cheaper off-line fitting process, the BPNN approximation can be regarded as a better alternative given the more accurate results.

Table 4.4: IEEE 2-area system load curtailment values using BPNN and NR approaches.

	BPNN Approach			NR Approach		
Case	$\triangle P_{d_7}$ [MW]	$\triangle P_{d_9}$ [MW]	Value of eq.(4.15)	$\triangle P_{d_7}$ [MW]	$\triangle P_{d_9}$ [MW]	Value of eq. (3.17)
1	266.68	148.38	-2.2e-5	309.44	148.60	2.3e-5
2	344.04	7.02	-2.2e-5	386.80	7.24	2.3e-5
3	328.56	0.0	-1.8e-5	321.66	0.0	2.2e-5
4	202.90	0.0	1.4e-5	207.12	0.0	-7.4e-5
5	247.93	0.0	3.1e-6	246.75	0.0	-2.6e-5

4.5.1.2 Three Loads

To test if the proposed approach can be applied to systems containing more than two loads or loading areas, the IEEE 2-area benchmark system is modified as shown in Fig. 3.5. The values for α, d_{i6}, d_{i7}, and d_{i9} in Table 4.5 were chosen so that the corresponding P_{d_6}, P_{d_7}, and P_{d_9} values force the system to be outside the SB to test the proposed approach with multi-dimensional SBs. The base load values are depicted in Fig. 4.2. The curtailment bids for the three loads were $C_{d_6} = 20\,\$/MW$, $C_{d_7} = 90\,\$/MW$, and $C_{d_9} = 10\,\$/MW$.

Table 4.5: IEEE 2-area system loading scenarios for three loads.

Case	α	d_{i6}	d_{i7}	d_{i9}	P_{d_6} [MW]	P_{d_7} [MW]	P_{d_9} [MW]
1	2.2	0.7	0.1	0.2	2032	1179.74	2544.48
2	2.2	0.5	0.3	0.2	1680	1605.22	2544.48
3	1.4	0.2	0.1	0.7	1024	1102.38	3498.66

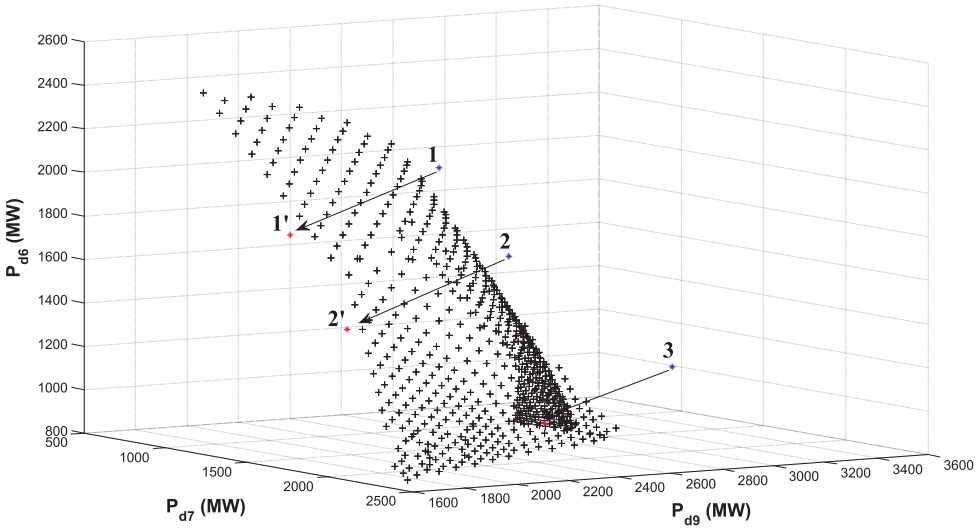

Figure 4.2: 3-D security and stability boundaries for the IEEE 2-area system.

The load change results obtained by applying the proposed model defined by Equations 4.10-4.20 are shown in Table 4.6 and depicted in Fig. 4.2. For the three cases, the cheaper load is curtailed as much as possible in order to return the unstable equilibrium point to the SB. Thus, the proposed approach has prove to be useful in systems with more than two loads or loading areas.

Table 4.6: IEEE 2-area system load curtailment values for three loads.

Case	α	d_{i6}	d_{i7}	d_{i9}	P_{d_6} [MW]	P_{d_7} [MW]	P_{d_9} [MW]
1	1.4957	0.8041	0.1057	0.0903	1762.14	1119.81	2005.53
2	1.4362	0.5112	0.4127	0.076	1387.40	1540.22	1960
3	0.8053	0	0.108	0.892	800	1051.08	3036.28

Similarly to the last example, the polynomial approximation defined by Equation 3.17 has also been employed to obtain the optimal load shedding which assures that the system is operating within the stable region. Table 4.7 shows the load changes and the value of the corresponding SB constraint for the BPNN approximation (Equation 4.15) and the NR approximation (Equation 3.17). As in the previous case, the differences in load curtailments are not significant, but the BPNN security constraint is in general closer to zero than the NR polynomial one.

Table 4.7: IEEE 2-area system load curtailment values for three loads using BPNN and NR approaches.

	BPNN Approach				NR Approach			
Case	$\triangle P_{d_6}$ [MW]	$\triangle P_{d_7}$ [MW]	$\triangle P_{d_9}$ [MW]	Value of eq. (4.15)	$\triangle P_{d_6}$ [MW]	$\triangle P_{d_7}$ [MW]	$\triangle P_{d_9}$ [MW]	Value of eq. (3.17)
1	269.86	59.63	538.95	-1.7e-5	269.80	59.9	537.5	1.0e-5
2	292.6	65	584.48	-1.4e-5	292	65	584.4	2.0e-5
3	224	51.3	462.38	1.8e-5	223	52	462.3	2.1e-5

4.5.2 IEEE 118-bus Benchmark System

To prove the effectiveness of the proposed method with a more realistic system, the IEEE 118-bus benchmark system was used. The system loads are divided into three and four loading groups or areas.

4.5.2.1 Three Areas

The three area loading cases in Table 4.8, which all define operating conditions outside the security region as depicted in Fig. 4.3, were used to test the proposed optimal dispatch model with the following large load curtailment bids per area: $C_{d_{A1}} = 200\,\$/MWh$, $C_{d_{A2}} = 400\,\$/MWh$, and $C_{d_{A3}} = 600\,\$/MWh$. The total area loads were proportionally distributed among the area buses based on their base loading values. The generator bid data are given in Appendix C.

Table 4.8: 118-bus system 3-area loading scenarios.

Case	$P_{d_{A1}}$ [MW]	$P_{d_{A2}}$ [MW]	$P_{d_{A3}}$ [MW]
1	848.64	822.97	2138.85
2	866.944	803.794	2061.444
3	836.16	830.96	2047.185

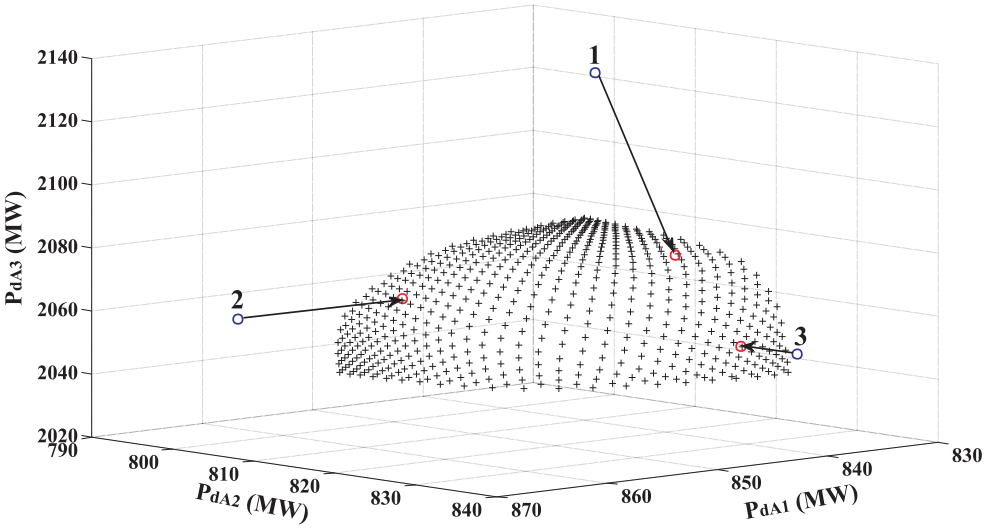

Figure 4.3: SB for the IEEE 118-bus system for three areas.

Table 4.9 shows the total area load changes resulting from the solution of the SBC-OPF dispatch model, which also yields optimal dispatch values for all generators. Observe in Fig. 4.3 how the most expensive Area 3 loads are shed the least, except for Case 1 where this load must also be curtailed for the system to be on the required SB.

Table 4.9: 118-bus system 3-area load curtailment values.

Case	$\triangle P_{d_{A1}}$ [MW]	$\triangle P_{d_{A2}}$ [MW]	$\triangle P_{d_{A3}}$ [MW]
1	10.1147	13.9695	62.4044
2	17.3010	0.0	0.0
3	0.0	6.2105	0.0

As in the case of the IEEE 2-area system, a comparison between the BPNN and NR approaches to map the SB was also carried out. The mean square errors for the BPNN and the NR approximations are 2.6e-6 and 5.85e-6 respectively, demonstrating that the BPNN more effectively approximates the boundary than the NR polynomial.

4.5.2.2 Four Areas

The three test cases shown in Table 4.10 were used to test the proposed dispatch model; all operating points are located outside the security region. The total area load was assumed again to be proportionally distributed among the area buses based on their base loading val-

ues. Large curtailment value bids are assumed for the loads in each area: $C_{d_{A1}} = 800\,\$/MWh$, $C_{d_{A2}} = 100\,\$/MWh$, $C_{d_{A3}} = 300\,\$/MWh$, and $C_{d_{A4}} = 600\,\$/MWh$.

Table 4.10: 118-bus system 4-area loading scenarios.

Case	$P_{d_{A1}}$ [MW]	$P_{d_{A2}}$ [MW	$P_{d_{A3}}$ [MW]	$P_{d_{A4}}$ [MW]
1	790.0891	623.6631	1237.4465	1624.8792
2	807.7263	648.9401	1332.6901	1661.1514
3	798.8817	758.0656	1442.9201	1642.9618

The load changes obtained from solving the SBC-OPF model defined by Equations 4.10-4.20 for all three operating cases considered are shown in Table 4.11. The loads are curtailed according to their bids and their effect on system security. In this case, the most expensive loads in Area 1, as well as the cheaper loads in Areas 2 and 3, are not curtailed; only the loads in Area 4, which have the most impact on system security conditions, are shed the most.

Table 4.11: 118-bus system 4-area loading scenarios.

Case	$\triangle P_{d_{A1}}$ [MW]	$\triangle P_{d_{A2}}$ [MW]	$\triangle P_{d_{A3}}$ [MW]	$\triangle P_{d_{A4}}$ [MW]
1	0.0	0.0	0.0001	154.0212
2	0.0	0.0	0.0	190.2934
3	0.0	0.0	0.0	172.1038

4.6 Considerations

As long as the simulations were carried out, the following advantages and disadvantages were noticed. It is evident that the main advantage is having an explicit function, which represents the power system's security, in such a way that may be included as a security constraint into a SBC-OPF auction model, giving the system operator a clear indicator about the security of an operating point.

However, due to the fact that the BPNN neurons' activation function considered in the present work has exponential nature, numeric problems may arise during the SBC-OPF solution process, i.e. in some cases the exponential terms which form part of the security constraint may become too large yielding to the solver to diverge. Hence, care should be taken in order to monitor these exponential terms. In the present work, when numerical issues were presented a scaling in the training points reduced all exponentials and the resulting function

had well behavior. In addition, user-defined activation functions may be developed in order to avoid exponentials in the resulting function.

4.7 Conclusions

As a first step to present the proposed SBC-OPF, a typical SC-OPF was presented in this Chapter; this model includes the AC power flow equations as part of the optimization auction constraints. A technique that yields a better representation of the SB in form of an explicit function, which accounts for system dynamics was also presented; this technique represents an advance in terms of efficiently characterizing the SB with respect to previously proposed SC-OPF models.

Taking as reference this approach, the smooth-nonlinear differentiable function obtained from the BPNN was included as a security constraint into a SC-OPF auction model, resulting in the proposed SBC-OPF. This model was solved using two different types of solvers: the Newton-based approach and AMPL with the KNITRO solver. Numerical results of the proposed approach were presented by using two IEEE benchmark systems such as the 2-area system and the 118-bus system. For the first case when two loads were considered, some operating points were located outside the resulting SB assuming prespecified load curtailment cost values. The SBC-OPF relocates these points by shedding the load with the cheaper curtailment cost; the resulting points were located at the boundary of the security region. The proposed BPNN-SB representation was then replaced by the NR polynomial approximation. The resulting mean square errors showed that the BPNN approximation fits the boundary better than the NR polynomial approximation; differences in load curtailments were not significant, but the BPNN security constraint yields to more accurate results at similar computational costs.

The same simulation was carried out for the 2-area system considering three loads. Again, the proposed SBC-OPF relocates the "insecure" operating points into the security region by curtailing the load with the cheaper load shedding cost. Only for cases where there was no option, the load with the most expensive load curtailment cost was shed. Similarly to the first case, the polynomial approximation was employed showing that better results were obtained by using the BPNN approximation.

To prove the effectiveness of the proposed method with a more realistic system, the IEEE 188-bus benchmark system was used. For the case of three operating areas, three operating points were located outside the SB. The SBC-OPF curtailed the loads with cheaper shedding

costs as much as possible in order to return into the SB the "insecure" points. When four areas were considered, the loads were curtailed according to their bids and their effect on system security. It was shown how Area 4 had the most impact on system security conditions due to was shed the most.

Chapter 5

Conclusions and Contributions

5.1 Conclusions

This thesis proposes a new technique to obtain a differentiable function of power system variables from a BPNN approximation of the stability/security boundary. This function was introduced as a security constraint in a SC-OPF model for optimal dispatch in a competitive market environment, accounting for the load inelasticity in current auction and dispatch problems. The solution of the proposed SBC-OPF problem was shown to yield dispatch conditions that are within a feasible operating region from the stability/security viewpoint. The proposed model was tested using two IEEE benchmark systems, demonstrating its usefulness and feasibility in practical applications.

In order to achieve the aforementioned, the power system mathematical representation has been reviewed, showing that due to power system dynamics interact at widely-varying time constants, conversion equations are needed. Also, it was reviewed the main concepts of bifurcation theory, which allow to qualitatively describe the stability of solution points of the resulting power system model. Furthermore, based on bifurcation theory it was shown how the power system model expressed by a set of differential-algebraic equations can be analyzed as a set of ODEs.

It was introduced the concept of stability and security boundaries and it was established the SB determination procedure, which is based on a proposed critical load matrix. By using the techniques applied for this procedure, two types of SB were obtained for the IEEE 118-bus benchmark system: the loading directions-based SB and the dispatch directions-based SB, emphasizing their complex topology. Once these SB were obtained, two main approximation tools were considered: the BPNN and the NR.

For the BPNN case, the SB mapping process consists in obtaining the critical load matrix which constitutes the training and testing sets for the BPNN, training and testing the BPNN, and obtaining the explicit function representation from the BPNN. The BPNN considered in this work is composed of three layers: input, hidden, and output layers; this architecture was selected based on the criteria of having the simplest array of neurons, capable to map the SB with a reasonable precision. Hence, from the trained BPNN a smooth-nonlinear differentiable function was obtained, which may be represented either in the \lambda-parameter or P_{d}-parameter space. On the other hand, the SB may also be approximated by polynomial approximation by using NR.

The results of the proposed approach when used to map the SB and their comparison with respect to the results obtained by using the NR were presented in this work. Two test systems were considered, such as the IEEE 2-area and the IEEE 118-bus benchmark systems.

Two cases were presented for the IEEE 2-area benchmark system: two and three loads. In the former no significant differences were obtained due to the simplicity of the SB; however, better tolerances were obtained by using BPNN. In the later case, it was shown how due to the complexity and discontinuity of the SB better mapping results were obtained by using BPNN compared with the results obtained by using NR.

In order to test if the proposed approach is capable of handling more complex SBs and to compare its behavior against the NR-based mapping tool, the more realistic IEEE 118-bus benchmark system was considered, considering also the loading directions-based SB and the dispatch directions-based SB.

For the first case considering two loading areas, no significant differences were observed between the results obtained by using both mapping tools for the same reason as in the 2-area system. When three loading areas were considered, it was shown how the NR it was unable to successfully map the SB; there were unmapped areas and low precision was obtained compared with the better results obtained by using BPNN. When four areas were considered, it was evident the flexibility of the BPNN since it was capable of accurately mapping high-dimensional and complex surfaces.

For the second case where the dispatch directions were varied, two and three operating groups were considered. When two operating groups were considered, the NR was unable to map the SB even by using a 9th degree polynomial, because of the nonlinearity, discontinuities, and few available training points of the SB to be mapped. The proposed BPNN yielded the desired results by accurately mapping this more complex SB. When three operating groups were considered, several BPNN architectures were tested in order to obtain the simplest case because of the complexity of the SB. Again, it was shown how the NR

was unable to successfully map the SB whereas the BPNN showed high accuracy even when complex-shape security regions are presented.

Based on a model which includes the AC power flow equations as part of the optimization auction constraints, a technique that yields a better representation of the SB in form of an explicit function, which accounts for system dynamics was presented; this technique represents an advance in terms of efficiently characterizing the SB with respect to previously proposed SC-OPF models. As a result of analyzing this approach, the smooth-nonlinear differentiable function obtained from the BPNN was included as a security constraint into a SC-OPF auction model, resulting in the proposed SBC-OPF. Numerical results of the proposed approach were presented by using two IEEE benchmark systems such as the 2-area system and the 118-bus system. For the first case when two loads were considered, some operating points were located outside the resulting SB assuming prespecified load curtailment cost values. The SBC-OPF relocates these points by shedding the load with the cheaper curtailment cost; the resulting points were located at the boundary of the security region. The proposed BPNN-SB representation was then replaced by the NR polynomial approximation. The resulting mean square errors showed that the BPNN approximation fits the boundary better than the NR polynomial approximation; differences in load curtailments were not significant, but the BPNN security constraint yields to more accurate results at similar computational costs.

The same simulation was carried out for the 2-area system considering three loads. Again, the proposed SBC-OPF relocates the "insecure" operating points into the security region by curtailing the load with the cheaper load shedding cost. Only for cases where there was no option, the load with the most expensive load curtailment cost was shed. Similarly to the first case, the polynomial approximation was employed showing that better results were obtained by using the BPNN approximation.

To prove the effectiveness of the proposed method with a more realistic system, the IEEE 188-bus benchmark system was used. For the case of three operating areas, three operating points were located outside the SB. The SBC-OPF curtailed the loads with cheaper shedding costs as much as possible in order to return into the SB the "insecure" points. When four areas were considered, the loads were curtailed according to their bids and their effect on system security. It was shown how Area 4 had the most impact on system security conditions due to was shed the most.

Therefore, the SBC-OPF has proved to be a suitable tool to ensure that the resulting points are optimal from the economical and secure standpoint.

5.2 Contributions

The proposed approach represents a new and useful technique to deal with the issue of properly representing system congestion in OPF-based auction and dispatch mechanisms. Using the proposed SB representation obtained from a trained BPNN, system operators should have a full and more accurate idea of the shape and characteristics of the secure operating region, allowing them to properly dispatch generator and loads, as well as take preventive and corrective actions to avoid system instabilities.

The main contributions of the present work are listed below:

- A new methodology to obtain an explicit smooth-nonlinear-differentiable function reproducing the SB with adequate precision, in order to be included as a security constraint in a SC-OPF model in a straightforward way is presented and described in detail.

- The approach is based on the SB approximation, which is implemented with two different mapping tools: BPNN and NR. It has been shown that ANNs have good mapping characteristics, as well as a large degree of freedom that is basically model-independent, which make them easily modifiable in order to map complex multidimensional surfaces resulting from systems containing several generation and loading areas.

- The BPNN architecture used in this work was selected based on the criteria of having the simplest array of neurons, capable to map the security or stability boundary with a reasonable precision.

5.3 Future work

As it was mentioned in the previous Chapter, the development of a used-defined activation function for the BPNN neurons which avoids the use of exponentials it is an issue to be solved. This activation function must maintain the BPNN flexibility to map complex surfaces and must be suitable to allow the development of simple BPNN architectures.

Regarding the BPNN architectures, it must be considered the use of commercial software in order to obtain the better BPNN architecture. It is mentioned the commercial software due to it represents a faster and better alternative keeping in mind the main objective which is to reduce the mapping errors, fitting better the SB; the architecture considered in the present work was obtained by trial and error using the only consideration of simplicity which implies that an optimal architecture might not be considered.

The proposed SB representation cannot be applied to OPF-based dispatch and market auction models based on classical DC-OPF, which in practice is used in most energy dispatch and market clearing mechanisms. The author is currently working on developing practical DC-OPF dispatch model based on a linearization of the proposed BPNN-SB.

Analyze the impact of the electronically controlled devices (such as Flexible AC Transmission Systems) on the SB and to include the devices' state variables into the optimization model in order to achieve a secure and optimal control avoiding the induced bifurcations which result when these devices are embedded in the power system it represents another future work.

Appendix A

Smooth Nonlinear Differentiable Security Boundary Functions

The smooth nonlinear differentiable SB functions obtained from the NR and the BPNN, for the case studies considered in this work are presented in this Appendix. As mentioned in previous Chapters, for the case of the BPNN these functions were used as security constraints for the proposed SBC-OPF auction model.

A.1 IEEE 2-area Benchmark System

A.1.1 Two Areas

For the case when two loads are considered, as shown in Fig. 3.3, the resulting NR-based function obtained from the corresponding SB of Fig. 3.4 is

$$y = A_1x^9 + A_2x^8 + A_3x^7 + A_4x^6 + A_5x^5 + A_6x^4 + A_7x^3 + A_8x^2 + A_9x + A_{10} \qquad \text{(A.1)}$$

where

$$\begin{array}{cc} A_1 = -1754 & A_6 = 564.6 \\ A_2 = 5777 & A_7 = -68.74 \\ A_3 = -7870 & A_8 = 2.339 \\ A_4 = 5724 & A9 = 0.01492 \\ A_5 = -2385 & A_{10} = 0.3939 \end{array}$$

and

$$x = \alpha d_1$$
$$y = \alpha d_2$$

In addition, the resulting BPNN-based function is

$$\begin{aligned} y = 12.2084N_1 - 0.12464N_2 + 0.39917N_3 - 1.5423N_4 + 2.417N_5 + \\ +2.8707N_6 - 1.83N_7 + 1.1N_8 - 2.5109 \end{aligned} \tag{A.2}$$

where

$$\begin{aligned} & & n_A &= 2.9818x - 0.07202 \\ N_1 &= 2/(1+e^{(-2n_1)}) - 1 & n_1 &= -15.9261n_A + 39.7772 \\ N_2 &= 2/(1+e^{(-2n_2)}) - 1 & n_2 &= -9.7456n_A - 1.3514 \\ N_3 &= 2/(1+e^{(-2n_3)}) - 1 & n_3 &= -0.59004n_A + 1.2741 \\ N_4 &= 2/(1+e^{(-2n_4)}) - 1 & n_4 &= 12.2891n_A + 3.2302 \\ N_5 &= 2/(1+e^{(-2n_5)}) - 1 & n_5 &= -11.6928n_A - 3.9371 \\ N_6 &= 2/(1+e^{(-2n_6)}) - 1 & n_6 &= -11.2571n_A - 4.9281 \\ N_7 &= 2/(1+e^{(-2n_7)}) - 1 & n_7 &= 11.2001n_A + 8.0002 \\ N_8 &= 2/(1+e^{(-2n_8)}) - 1 & n_8 &= -11.2n_A - 11.2 \end{aligned}$$

and x and y are as defined above.

A.1.2 Three Areas

When three loads are considered, as shown in Fig. 3.5, the NR-based function obtained from the mapped SB shown in Fig. 3.6 is as follows:

$$z = -2.8867 * y^2 - 1.3345 * x^2 - 0.5183 * x * y - 0.4460 * y - 0.0779 * x + 2.0373$$

where

$$x = \alpha d_1$$
$$y = \alpha d_2$$
$$z = \alpha d_3$$

The resulting BPNN-based function is

$$z = 0.4909N_1 + 25.7972N_2 + 68.0697N_3 + 1.4051N_4 - 28.0054N_5 + \\ +42.828N_6 - 113.5545N_7 + 0.3171N_8 + 1.6534$$

where

$$\begin{aligned} N_1 &= 2/(1+e^{(-2n_1)}) - 1 & n_1 &= -1.2268x + 97.2039y - 67.4325 \\ N_2 &= 2/(1+e^{(-2n_2)}) - 1 & n_2 &= 0.4606x + 2.0556y - 0.4838 \\ N_3 &= 2/(1+e^{(-2n_3)}) - 1 & n_3 &= -3.5308x - 1.2824y + 3.1277 \\ N_4 &= 2/(1+e^{(-2n_4)}) - 1 & n_4 &= -7.6686x - 1.0385y + 5.9569 \\ N_5 &= 2/(1+e^{(-2n_5)}) - 1 & n_5 &= 0.5237x + 1.9386y - 0.5097 \\ N_6 &= 2/(1+e^{(-2n_6)}) - 1 & n_6 &= -3.4769x - 1.1874y + 2.5661 \\ N_7 &= 2/(1+e^{(-2n_7)}) - 1 & n_7 &= -3.3201x - 1.1537y + 2.749 \\ N_8 &= 2/(1+e^{(-2n_8)}) - 1 & n_8 &= 10.5585x - 245.0895y + 166.6335 \end{aligned}$$

and x, y, and z are defined as above.

A.2 IEEE 118-bus Benchmark System

A.2.1 Two Areas

Regarding the NR to map the SB shown in Fig. 3.7 for this system, the smooth nonlinear differentiable function is as follows:

$$y = A_1x^6 + A_2x^5 + A_3x^4 + A_4x^3 + A_5x^2 + A_6x + A_7 \tag{A.3}$$

where

$$\begin{aligned} A_1 &= 8.205^{-9} & A_5 &= 6.441^{6} \\ A_2 &= -0.0001324 & A_6 &= -6.929^{9} \\ A_3 &= 0.8904 & A_7 &= 3.105^{12} \\ A_4 &= -3193 & & \end{aligned}$$

and

$$x = \alpha d_1$$
$$y = \alpha d_2$$

For the case of the BPNN, defining x and y as above, the resulting function used as a

constraint in the proposed SBC-OPF auction model is

$$y = -0.0002N_1 + 0.0166N_2 - 0.0001N_3 - 0.0006N_4 - 0.0019N_5 + \\ +0.0002N_6 + 0.0006N_7 + 0.0011N_8 + 0.0057$$

where

$$\begin{aligned} N_1 &= 2/(1+e^{(-2n_1)}) - 1 \quad n_1 = 5166.9742x - 100.9904 \\ N_2 &= 2/(1+e^{(-2n_2)}) - 1 \quad n_2 = -241.0468x + 4.8036 \\ N_3 &= 2/(1+e^{(-2n_3)}) - 1 \quad n_3 = 1756.2883x - 26.1805 \\ N_4 &= 2/(1+e^{(-2n_4)}) - 1 \quad n_4 = 749.3498x - 9.1384 \\ N_5 &= 2/(1+e^{(-2n_5)}) - 1 \quad n_5 = 428.33x - 3.936 \\ N_6 &= 2/(1+e^{(-2n_6)}) - 1 \quad n_6 = -1282.3668x + 8.9246 \\ N_7 &= 2/(1+e^{(-2n_7)}) - 1 \quad n_7 = -899.4003x + 4.4339 \\ N_8 &= 2/(1+e^{(-2n_8)}) - 1 \quad n_8 = -567.6048x + 0.8939 \end{aligned}$$

A.2.2 Three Areas

For the SB shown in Fig. 3.8, the resulting smooth nonlinear differentiable function using the NR as a mapping tool is as follows:

$$z = -1.3345x^2 - 2.8867y^2 - 0.5183xy - 0.0779x - 0.4460y + 2.0373$$

where

$$\begin{aligned} x &= \alpha d_1 \\ y &= \alpha d_2 \\ z &= \alpha d_3 \end{aligned}$$

For the case of the BPNN, the resulting function is

$$z = -7.3805N_1 + 0.0047N_2 - 5.5378N_3 + 9.7261N_4 - 4.2577N_5 + \\ +0.0021N_6 + 0.0027N_7 + 7.7853N_8 - 15.0868$$

where

$$
\begin{aligned}
N_1 &= 2/(1+e^{(-2n_1)})-1 \quad & n_1 &= 347.2685x - 170.9192y - 13.4514 \\
N_2 &= 2/(1+e^{(-2n_2)})-1 \quad & n_2 &= -216.1512x - 272.4126y + 10.1801 \\
N_3 &= 2/(1+e^{(-2n_3)})-1 \quad & n_3 &= -249.4101x - 52.8251y + 6.8235 \\
N_4 &= 2/(1+e^{(-2n_4)})-1 \quad & n_4 &= -240.915x - 51.4847y + 6.654 \\
N_5 &= 2/(1+e^{(-2n_5)})-1 \quad & n_5 &= -228.3211x - 49.5281y + 6.4103 \\
N_6 &= 2/(1+e^{(-2n_6)})-1 \quad & n_6 &= 89.0137x - 135.3242y + 3.1167 \\
N_7 &= 2/(1+e^{(-2n_7)})-1 \quad & n_7 &= -142.54x - 59.252y + 2.3323 \\
N_8 &= 2/(1+e^{(-2n_8)})-1 \quad & n_8 &= 70.2355x - 313.4993y + 13.4296
\end{aligned}
$$

x, y, and z are defined as above.

A.2.3 Four Areas

For this case, the SB is only mapped by the BPNN because employing NR in multidimensional surfaces is not possible. As mentioned earlier, because of the BPNNs' flexibility as mapping tools, other possible alternatives capable of managing higher multidimensional surfaces go beyond the scope of this work. Hence, the resulting function is

$$
\begin{aligned}
z = &-0.007424N_1 + 0.0014775N_2 - 0.0032812N_3 + 0.00098494N_4 \\
&+0.0025951N_5 - 0.00072946N_6 + 0.006882N_7 - 0.0029058N_8 + 0.005462
\end{aligned}
$$

where

$$
\begin{aligned}
N_1 &= 2/(1+e^{(-2n_1)})-1 \quad & n_1 &= -104.7231w + 26.4597x - 34.951y + 2.1453 \\
N_2 &= 2/(1+e^{(-2n_2)})-1 \quad & n_2 &= -180.8856w + 62.8459x - 121.0512y + 4.8548 \\
N_3 &= 2/(1+e^{(-2n_3)})-1 \quad & n_3 &= -150.9193w - 29.5053x + 26.4502y + 2.1676 \\
N_4 &= 2/(1+e^{(-2n_4)})-1 \quad & n_4 &= -157.6627w + 17.2566x - 129.7312y + 2.5839 \\
N_5 &= 2/(1+e^{(-2n_5)})-1 \quad & n_5 &= 166.175w - 27.4839x + 61.7906y - 1.5158 \\
N_6 &= 2/(1+e^{(-2n_6)})-1 \quad & n_6 &= 35.8246w - 119.5784x + 147.2598y - 0.39664 \\
N_7 &= 2/(1+e^{(-2n_7)})-1 \quad & n_7 &= 58.549w - 150.2008x + 20.1553y + 5.6615 \\
N_8 &= 2/(1+e^{(-2n_8)})-1 \quad & n_8 &= -167.3856w - 27.0132x + 2.6647y + 1.0148
\end{aligned}
$$

and

$$w = \alpha d_1$$
$$x = \alpha d_2$$
$$y = \alpha d_3$$
$$z = \alpha d_4$$

Appendix B

IEEE 2-area Benchmark System Data

Table B.1: Transmission line parameters.

Nodes		$\boldsymbol{R}$(pu)	$\boldsymbol{X}$(pu)	$\boldsymbol{B}/2$(pu)	**Nodes**		$\boldsymbol{R}$(pu)	$\boldsymbol{X}$(pu)	$\boldsymbol{B}/2$(pu)
1	5	0	0.0167	0	3	11	0	0.0167	0
2	6	0	0.0167	0	4	10	0	0.0167	0
7	6	0.001	0.01	0.0175	9	8	0.011	0.11	0.1925
7	8	0.011	0.11	0.1925	9	8	0.011	0.11	0.1925
3	8	0.011	0.11	0.1925	9	10	0.001	0.01	0.0175
5	6	0.0025	0.025	0.0437	11	10	0.0025	0.025	0.0437

Table B.2: Load parameters.

Node	$\boldsymbol{P}$(Mw)	$\boldsymbol{Q}$(Mw)
7	967	100
9	1767	100

Table B.3: Generators parameters.

$\boldsymbol{X_d} = 1.8$	$\boldsymbol{X_q} = 1.7$	$\boldsymbol{X_l} = 0.2$	$\boldsymbol{X_d^{'}} = 0.3$	$\boldsymbol{X_q^{'}} = 0.55$
$\boldsymbol{X_d^{''}} = 0.25$	$\boldsymbol{X_q^{''}} = 0.25$	$\boldsymbol{R_a} = 0.0025$	$\boldsymbol{T_{d0}^{'}} = 8s$	$\boldsymbol{T_{q0}^{'}} = 0.4s$
$\boldsymbol{T_{d0}^{''}} = 0.03s$	$\boldsymbol{T_{q0}^{''}} = 0.05s$	$H = 6.5$	$D = 0$	

Table B.4: Exciter parameters.

Node	$\boldsymbol{K_A}$	$\boldsymbol{T_A}$(s)
1	200	0.05
2	200	0.05
3	200	0.05
4	200	0.05

Table B.7: Power generation bids for the 2-area system.

Gen.	C_s [$/MWh]	P_{smax} [MW]
1	70	900
2	70	1000
3	90	900
4	70	900

Table B.5: Turbine governor parameters.

Gen.	R (pu)	T_{max}(pu)	T_{min}(pu)	T_s(s)	T_c(s)	T_3(s)	T_4(s)	T_5(s)
1	0.04	1	0	0.1	0.5	0	1.25	5
2	0.04	1	0	0.1	0.5	0	1.25	5
3	0.04	1	0	0.1	0.5	0	1.25	5
4	0.04	1	0	0.1	0.5	0	1.25	5

Table B.6: Power system stabilizer parameters.

$v_{smax} = 0.2$	$K_w = 10$
$v_{smin} = -0.05$	$T_w = 10$
$T_1 = 0.05$	$T_2 = 0.01$
$T_3 = 0.05$	$T_4 = 0.01$

Appendix C

IEEE 118-bus Benchmark System Data

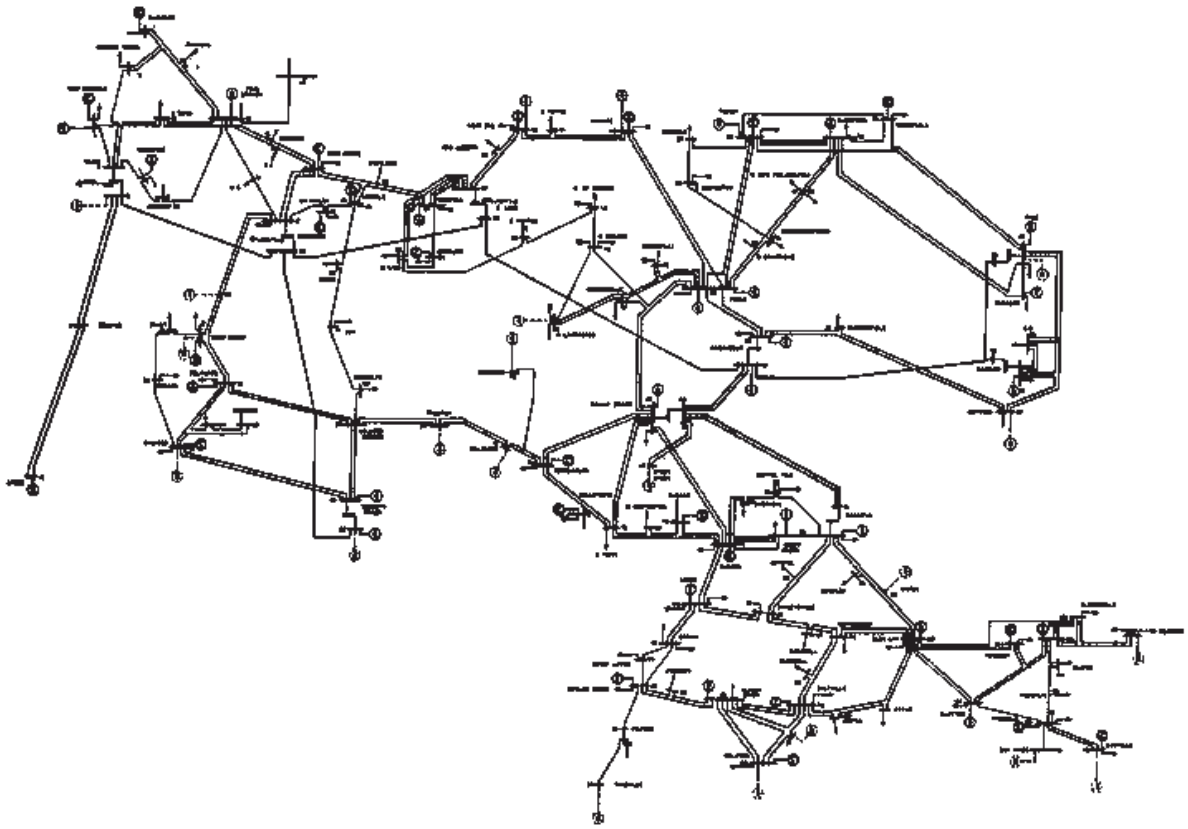

Figure C.1: IEEE 118-bus benchmark system.

Table C.1: Transmission line parameters.

Nodes		$\boldsymbol{R}$(pu)	$\boldsymbol{X}$(pu)	$\boldsymbol{B}/2$(pu)	**Nodes**		$\boldsymbol{R}$(pu)	$\boldsymbol{X}$(pu)	$\boldsymbol{B}/2$(pu)
1	2	0.0303	0.0999	0.0254	38	65	0.00901	0.0986	1.046
1	3	0.0129	0.0424	0.01082	64	65	0.00269	0.0302	0.38
4	5	0.00176	0.00798	0.0021	49	66	0.018	0.0919	0.0248
3	5	0.0241	0.108	0.0284	49	66	0.018	0.0919	0.0248
5	6	0.0119	0.054	0.01426	62	66	0.0482	0.218	0.0578
6	7	0.00459	0.0208	0.0055	62	67	0.0258	0.117	0.031
8	9	0.00244	0.0305	1.162	66	67	0.0224	0.1015	0.02682
9	10	0.00258	0.0322	1.23	65	68	0.00138	0.016	0.638
4	11	0.0209	0.0688	0.01748	47	69	0.0844	0.2778	0.07092
5	11	0.0203	0.0682	0.01738	49	69	0.0985	0.324	0.0828
11	12	0.00595	0.0196	0.00502	69	70	0.03	0.127	0.122
2	12	0.0187	0.0616	0.01572	24	70	0.00221	0.4115	0.10198
3	12	0.0484	0.16	0.0406	70	71	0.00882	0.0355	0.00878
7	12	0.00862	0.034	0.00874	24	72	0.0488	0.196	0.0488
11	13	0.02225	0.0731	0.01876	71	72	0.0446	0.18	0.04444
12	14	0.0215	0.0707	0.01816	71	73	0.00866	0.0454	0.01178
13	15	0.0744	0.2444	0.06268	70	74	0.0401	0.1323	0.03368
14	15	0.0595	0.195	0.0502	70	75	0.0428	0.141	0.036
12	16	0.0212	0.0834	0.0214	69	75	0.0405	0.122	0.124
15	17	0.0132	0.0437	0.0444	74	75	0.0123	0.0406	0.01034
16	17	0.0454	0.1801	0.0466	76	77	0.0444	0.148	0.0368
17	18	0.0123	0.0505	0.01298	69	77	0.0309	0.101	0.1038
18	19	0.01119	0.0493	0.01142	75	77	0.0601	0.1999	0.04978

19	20	0.0252	0.117	0.0298	77	78	0.00376	0.0124	0.01264
15	19	0.012	0.0394	0.0101	78	79	0.00546	0.0244	0.00648
20	21	0.0183	0.0849	0.0216	77	80	0.017	0.0485	0.0472
21	22	0.0209	0.097	0.0246	77	80	0.0294	0.105	0.0228
22	23	0.0342	0.159	0.0404	79	80	0.0156	0.0704	0.0187
23	24	0.0135	0.0492	0.0498	68	81	0.00175	0.0202	0.808
23	25	0.0156	0.08	0.0864	77	82	0.0298	0.0853	0.08174
25	27	0.0318	0.163	0.1764	82	83	0.0112	0.03665	0.03796
27	28	0.01913	0.0855	0.0216	83	84	0.0625	0.132	0.0258
28	29	0.0237	0.0943	0.0238	83	85	0.043	0.148	0.0348
8	30	0.00431	0.0504	0.514	84	85	0.0302	0.0641	0.01234
26	30	0.00799	0.086	0.908	85	86	0.035	0.123	0.0276
17	31	0.0474	0.1563	0.0399	86	87	0.02828	0.2074	0.0445
29	31	0.0108	0.0331	0.0083	85	88	0.02	0.102	0.0276
23	32	0.0317	0.1153	0.1173	85	89	0.0239	0.173	0.047
31	32	0.0298	0.0985	0.0251	88	89	0.0139	0.0712	0.01934
27	32	0.0229	0.0755	0.01926	89	90	0.0518	0.188	0.0528
15	33	0.038	0.1244	0.03194	89	90	0.0238	0.0997	0.106
19	34	0.0752	0.247	0.0632	90	91	0.0254	0.0836	0.0214
35	36	0.00224	0.0102	0.00268	89	92	0.0099	0.0505	0.0548
35	37	0.011	0.0497	0.01318	89	92	0.0393	0.1581	0.0414
33	37	0.0415	0.142	0.0366	91	92	0.0387	0.1272	0.03268
34	36	0.00871	0.0268	0.00568	92	93	0.0258	0.0848	0.0218
34	37	0.00256	0.0094	0.00984	92	94	0.0481	0.158	0.0406
37	39	0.0321	0.106	0.027	93	94	0.0223	0.0732	0.01876
37	40	0.0593	0.168	0.042	94	95	0.0132	0.0434	0.0111

30	38	0.00464	0.054	0.422	80	96	0.0356	0.182	0.0494
39	40	0.0184	0.0605	0.01552	82	96	0.0162	0.053	0.0544
40	41	0.0145	0.0487	0.01222	94	96	0.0269	0.0869	0.023
40	42	0.0555	0.183	0.0466	80	97	0.0183	0.0934	0.0254
41	42	0.041	0.135	0.0344	80	98	0.0238	0.108	0.0286
43	44	0.0608	0.2454	0.06068	80	99	0.0454	0.206	0.0546
34	43	0.0413	0.1681	0.04226	92	100	0.0648	0.295	0.0472
44	45	0.0224	0.0901	0.0224	94	100	0.0178	0.058	0.0604
45	46	0.04	0.1356	0.0332	95	96	0.0171	0.0547	0.01474
46	47	0.038	0.127	0.0316	96	97	0.0173	0.0885	0.024
46	48	0.0601	0.189	0.0472	98	100	0.0397	0.179	0.0476
47	49	0.0191	0.0625	0.01604	99	100	0.018	0.0813	0.0216
42	49	0.0715	0.323	0.086	100	101	0.0277	0.1262	0.0328
42	49	0.0715	0.323	0.086	92	102	0.0123	0.0559	0.01464
45	49	0.0684	0.186	0.0444	101	102	0.0246	0.112	0.0294
48	49	0.0179	0.0505	0.01258	100	103	0.016	0.0525	0.0536
49	50	0.0267	0.0752	0.01874	100	104	0.0451	0.204	0.0541
49	51	0.0486	0.137	0.0342	103	104	0.0466	0.1584	0.0407
51	52	0.0203	0.0588	0.01396	103	105	0.0535	0.1625	0.0408
52	53	0.0405	0.1635	0.04058	100	106	0.0605	0.229	0.062
53	54	0.0263	0.122	0.031	104	105	0.00994	0.0378	0.00986
49	54	0.073	0.289	0.0738	105	106	0.014	0.0547	0.01434
49	54	0.0869	0.291	0.073	105	107	0.053	0.183	0.0472
54	55	0.0169	0.0707	0.0202	105	108	0.0261	0.0703	0.01844
54	56	0.00275	0.00955	0.00732	106	107	0.053	0.183	0.0472
55	56	0.00488	0.0151	0.00374	108	109	0.0105	0.0288	0.0076

56	57	0.0343	0.0966	0.0242	103	110	0.03906	0.1813	0.0461
50	57	0.0474	0.134	0.0332	109	110	0.0278	0.0762	0.0202
56	58	0.0343	0.0966	0.0242	110	111	0.022	0.0755	0.02
51	58	0.0255	0.0719	0.01788	110	112	0.0247	0.064	0.062
54	59	0.0503	0.2293	0.0598	17	113	0.00913	0.0301	0.00768
56	59	0.0825	0.251	0.0569	32	113	0.0615	0.203	0.0518
56	59	0.0803	0.239	0.0536	32	114	0.0135	0.0612	0.01628
55	59	0.04739	0.2158	0.05646	27	115	0.0164	0.0741	0.01972
59	60	0.0317	0.145	0.0376	114	115	0.0023	0.0104	0.00276
59	61	0.0328	0.15	0.0388	68	116	0.00034	0.00405	0.164
60	61	0.00264	0.0135	0.01456	12	117	0.0329	0.14	0.0358
60	62	0.0123	0.0561	0.01468	75	118	0.0145	0.0481	0.01198
61	62	0.00824	0.0376	0.0098	76	118	0.0164	0.0544	0.01356
63	64	0.00172	0.02	0.216					

Table C.2: Transformer parameters.

Nodes		$\boldsymbol{R_s}$(pu)	$\boldsymbol{X_s}$(pu)	Tap T_v	Tap U_v	**Nodes**		$\boldsymbol{R_s}$(pu)	$\boldsymbol{X_s}$(pu)	Tap T_v	Tap U_v
8	5	0	0.0267	0.985	1.0	63	59	0	0.0386	0.96	1.0
26	25	0	0.0382	0.96	1.0	64	61	0	0.0268	0.985	1.0
30	17	0	0.0388	0.96	1.0	65	66	0	0.037	0.935	1.0
38	37	0	0.0375	0.935	1.0	68	69	0	0.037	0.935	1.0
						81	80	0	0.037	0.935	1.0

Table C.3: Load parameters.

Node	$\boldsymbol{P}$(Mw)	$\boldsymbol{Q}$(MVars)	**Node**	$\boldsymbol{P}$(Mw)	$\boldsymbol{Q}$(MVars)	**Node**	$\boldsymbol{P}$(Mw)	$\boldsymbol{Q}$(MVars)
1	51	27	41	37	10	80	130	26
2	20	9	42	37	23	82	54	27
3	39	10	43	18	7	83	20	10
4	30	12	44	16	8	84	11	7
6	52	22	45	53	22	85	24	15
7	19	2	46	28	10	86	21	10
11	70	23	47	34	0	88	48	10
12	47	10	48	20	11	90	78	42
13	34	16	49	87	30	92	65	10
14	14	1	50	17	4	93	12	7
15	90	30	51	17	8	94	30	16
16	25	10	52	18	5	95	42	31
17	11	3	53	23	11	96	38	15
18	60	34	54	113	32	97	15	9
19	45	25	55	63	22	98	34	8
20	18	3	56	84	18	100	37	18
21	14	8	57	12	3	101	22	15
22	10	5	58	12	3	102	5	3
23	7	3	59	277	113	103	23	16
27	62	13	60	78	3	104	38	25
28	17	7	62	77	14	105	31	26
29	24	4	66	39	18	106	43	16
31	43	27	67	28	7	107	28	12

32	59	23	70	66	20	108	2	1
33	23	9	74	68	27	109	8	3
34	59	26	75	47	11	110	39	30
35	33	9	76	68	36	112	25	13
36	31	17	77	61	28	114	8	3
39	27	11	78	71	26	115	22	7
40	20	23	79	39	32	117	20	8
						118	33	15

Table C.4: Shunt capacitors.

Node	***Q***(MVars)	**Node**	***Q***(MVars)
5	-40	74	12
34	14	79	20
37	-25	82	20
44	10	83	10
45	10	105	20
46	10	107	6
48	15	110	6

Table C.5: Generator parameters.

Node	***P*** (Mw)	Q (MVars)	Q_{max} (MVars)	Q_{min} (MVars)	**Node**	***P*** (Mw)	Q (MVars)	Q_{max} (MVars)	Q_{min} (MVars)
1	0	0	15	-5	65	391	0	200	-67
4	-9	0	300	-300	66	392	0	200	-67
6	0	0	50	-13	69	516.4	0	300	-300
8	-28	0	300	-300	70	0	0	32	-10
10	450	0	200	-147	72	-12	0	100	-100

12	85	0	120	-35	73	-6	0	100	-100
15	0	0	30	-10	74	0	0	9	-6
18	0	0	50	-16	76	0	0	23	-8
19	0	0	24	-8	77	0	0	70	-20
24	-13	0	300	-300	80	477	0	280	-165
25	220	0	140	-47	85	0	0	23	-8
26	314	0	1000	-1000	87	4	0	1000	-100
27	-9	0	300	-300	89	607	0	300	-210
31	7	0	300	-300	90	-85	0	300	-300
32	0	0	42	-14	91	-10	0	100	-100
34	0	0	24	-8	92	0	0	9	-3
36	0	0	24	-8	99	-42	0	100	-100
40	-46	0	300	-300	100	252	0	155	-50
42	-59	0	300	-300	103	40	0	40	-15
46	19	0	100	-100	104	0	0	23	-8
49	204	0	210	-85	105	0	0	23	-8
54	48	0	300	-300	107	-22	0	200	-200
55	0	0	23	-8	110	0	0	23	-8
56	0	0	15	-8	111	36	0	1000	-100
59	155	0	180	-60	112	-43	0	1000	-100
61	160	0	300	-100	113	-6	0	200	-100
62	0	0	20	-20	116	-184	0	1000	-1000

Table C.6: Power generation bids for the 118-bus system.

Gen.	C_s [$/MWh]	Gen.	C_s [$/MWh]	Gen.	C_s [$/MWh]
1	30	19	30	37	30
2	30	20	30	38	30
3	30	21	50	39	80
4	80	22	30	40	30
5	30	23	30	41	30
6	50	24	30	42	30
7	30	25	40	43	30
8	30	26	40	44	40
9	30	27	30	45	30
10	30	28	40	46	30
11	60	29	70	47	30
12	70	30	30	48	30
13	30	31	30	49	30
14	30	32	30	50	30
15	30	33	30	51	30
16	30	34	30	52	30
17	30	35	30	53	30
18	30	36	90	54	30

Next, the sequence of load nodes making up the loading groups are given:

- Two loading groups

Group 1: [1, 2, 3, 4, 6, 7, 11, 12, 13, 14, 15, 16, 17, 18, 19, 27, 31, 32, 34, 36, 40, 42, 46, 49, 54, 55, 56, 59, 62, 66, 70, 74, 76, 77, 80, 85, 90, 92, 100, 103, 104, 105, 107, 110, 112,]

Group 2: [20, 21, 22, 23, 28, 29, 33, 35, 39, 41, 43, 44, 45, 47, 48, 50, 51, 52, 53, 57, 58, 60, 67, 75, 78, 79, 82, 83, 84, 86, 88, 93, 94, 95, 96, 97, 98, 101, 102, 106, 108, 109, 114, 115, 117, 118]

- Three loading groups

Group 1: [1, 4, 6, 12, 15, 18, 19, 27, 31, 32, 34, 36, 40, 42, 46, 49, 54, 55, 56, 59, 62, 66, 70, 74, 76, 77, 80, 85, 90, 92, 103]

Group 2: [2, 3, 7, 11, 13, 14, 16, 17, 20, 21, 22, 23, 28, 29, 33, 35, 39, 41, 43, 44, 45, 48, 50, 51, 52, 100, 104, 105, 107, 110, 112]

Group 3: [47, 53, 57, 58, 60, 67, 75, 78, 79, 82, 83, 84, 86, 88, 93, 94, 95, 96, 97, 98, 101, 102, 106, 108, 109, 114, 115, 117, 118]

- Four Loading groups

Group 1: [1, 4, 6, 12, 15, 18, 19, 27, 31, 32, 34, 36, 40, 42, 46, 49, 54, 55, 56, 59, 62, 66]

Group 2: [2, 3, 7, 11, 13, 14, 16, 70, 74, 76, 77, 80, 85, 90, 92, 100, 103, 104, 105, 107, 110, 112]

Group 3: [17, 20, 21, 22, 23, 28, 29, 33, 35, 39, 41, 43, 44, 45, 48, 50, 51, 52, 53, 57, 58, 60]

Group 4: [47, 67, 75, 78, 79, 82, 83, 84, 86, 88, 93, 94, 95, 96, 97, 98, 101, 102, 106, 108, 109, 114, 115, 117, 118]

Furthermore, the sequence of generation nodes making up the generator groups are given:

- Two generator groups

Group 1: [1, 4, 6, 8, 10, 12, 15, 18, 19, 24, 25, 26, 27, 31, 32, 34, 36, 40, 42, 46, 49, 54, 55, 56, 59, 61]

Group 2: [62, 65, 66, 70, 72, 73, 74, 76, 77, 80, 85, 87, 89, 90, 91, 92, 99, 100, 103, 104, 105, 107, 110, 111, 112, 113, 116]

- Three generator groups

Group 1: [1, 8, 10, 24, 25, 26, 61, 65, 69, 72, 73, 87, 89, 91, 99, 111, 113, 116]

Group 2: [4, 6, 12, 15, 18, 19, 27, 31, 32, 34, 36, 40, 42, 46, 49, 54, 55, 56]

Group 3: [59, 62, 66, 70, 74, 76, 77, 80, 85, 90, 92, 100, 103, 104, 105, 107, 110, 112]

Appendix D

Loading/dispatch Directions

Table D.1: 21 directions for the case of two groups.

No.	d_1	d_2	No.	d_1	d_2	No.	d_1	d_2
1	0	1	8	0.35	0.65	15	0.7	0.3
2	0.05	0.95	9	0.4	0.6	16	0.75	0.25
3	0.1	0.9	10	0.45	0.55	17	0.8	0.2
4	0.15	0.85	11	0.5	0.5	18	0.85	0.15
5	0.2	0.8	12	0.55	0.45	19	0.9	0.1
6	0.25	0.75	13	0.6	0.4	20	0.95	0.05
7	0.3	0.7	14	0.65	0.35	21	1	0

Table D.2: 631 directions for the case of two groups.

No.	d_1	d_2	No.	d_1	d_2	No.	d_1	d_2
1	1	0	211	0.7	0.3	421	0.2667	0.7333
2	1	0	212	0.65	0.35	422	0.8167	0.1833
3	0.95	0.05	213	0.6	0.4	423	0.7667	0.2333
4	1	0	214	0.55	0.45	424	0.7167	0.2833
5	0.9	0.1	215	0.5	0.5	425	0.6667	0.3333
6	1	0	216	0.45	0.55	426	0.6167	0.3833
7	0.85	0.15	217	0.4	0.6	427	0.5667	0.4333
8	1	0	218	0.35	0.65	428	0.5167	0.4833

9	0.8	0.2	219	0.3	0.7	429	0.4667	0.5333
10	1	0	220	0.25	0.75	430	0.4167	0.5833
11	0.75	0.25	221	0.2	0.8	431	0.3667	0.6333
12	1	0	222	0.15	0.85	432	0.3167	0.6833
13	0.7	0.3	223	0.9333	0.0667	433	0.85	0.15
14	1	0	224	0.9333	0.0667	434	0.85	0.15
15	0.65	0.35	225	0.8833	0.1167	435	0.8	0.2
16	1	0	226	0.9333	0.0667	436	0.85	0.15
17	0.6	0.4	227	0.8333	0.1667	437	0.75	0.25
18	1	0	228	0.9333	0.0667	438	0.85	0.15
19	0.55	0.45	229	0.7833	0.2167	439	0.7	0.3
20	1	0	230	0.9333	0.0667	440	0.85	0.15
21	0.5	0.5	231	0.7333	0.2667	441	0.65	0.35
22	1	0	232	0.9333	0.0667	442	0.85	0.15
23	0.45	0.55	233	0.6833	0.3167	443	0.6	0.4
24	1	0	234	0.9333	0.0667	444	0.85	0.15
25	0.4	0.6	235	0.6333	0.3667	445	0.55	0.45
26	1	0	236	0.9333	0.0667	446	0.85	0.15
27	0.35	0.65	237	0.5833	0.4167	447	0.5	0.5
28	1	0	238	0.9333	0.0667	448	0.85	0.15
29	0.3	0.7	239	0.5333	0.4667	449	0.45	0.55
30	1	0	240	0.9333	0.0667	450	0.85	0.15
31	0.25	0.75	241	0.4833	0.5167	451	0.4	0.6
32	1	0	242	0.9333	0.0667	452	0.85	0.15
33	0.2	0.8	243	0.4333	0.5667	453	0.35	0.65
34	1	0	244	0.9333	0.0667	454	0.85	0.15
35	0.15	0.85	245	0.3833	0.6167	455	0.3	0.7
36	1	0	246	0.9333	0.0667	456	0.8	0.2
37	0.1	0.9	247	0.3333	0.6667	457	0.75	0.25
38	1	0	248	0.9333	0.0667	458	0.7	0.3
39	0.05	0.95	249	0.2833	0.7167	459	0.65	0.35
40	1	0	250	0.9333	0.0667	460	0.6	0.4
41	0	1	251	0.2333	0.7667	461	0.55	0.45

42	0.9833	0.0167	252	0.9333	0.0667	462	0.5	0.5
43	0.95	0.05	253	0.1833	0.8167	463	0.45	0.55
44	0.9	0.1	254	0.9333	0.0667	464	0.4	0.6
45	0.85	0.15	255	0.1333	0.8667	465	0.35	0.65
46	0.8	0.2	256	0.8833	0.1167	466	0.8333	0.1667
47	0.75	0.25	257	0.8333	0.1667	467	0.8333	0.1667
48	0.7	0.3	258	0.7833	0.2167	468	0.7833	0.2167
49	0.65	0.35	259	0.7333	0.2667	469	0.8333	0.1667
50	0.6	0.4	260	0.6833	0.3167	470	0.7333	0.2667
51	0.55	0.45	261	0.6333	0.3667	471	0.8333	0.1667
52	0.5	0.5	262	0.5833	0.4167	472	0.6833	0.3167
53	0.45	0.55	263	0.5333	0.4667	473	0.8333	0.1667
54	0.4	0.6	264	0.4833	0.5167	474	0.6333	0.3667
55	0.35	0.65	265	0.4333	0.5667	475	0.8333	0.1667
56	0.3	0.7	266	0.3833	0.6167	476	0.5833	0.4167
57	0.25	0.75	267	0.3333	0.6667	477	0.8333	0.1667
58	0.2	0.8	268	0.2833	0.7167	478	0.5333	0.4667
59	0.15	0.85	269	0.2333	0.7667	479	0.8333	0.1667
60	0.1	0.9	270	0.1833	0.8167	480	0.4833	0.5167
61	0.05	0.95	271	0.9167	0.0833	481	0.8333	0.1667
62	0.9833	0.0167	272	0.9167	0.0833	482	0.4333	0.5667
63	0.9333	0.0667	273	0.8667	0.1333	483	0.8333	0.1667
64	0.9833	0.0167	274	0.9167	0.0833	484	0.3833	0.6167
65	0.8833	0.1167	275	0.8167	0.1833	485	0.8333	0.1667
66	0.9833	0.0167	276	0.9167	0.0833	486	0.3333	0.6667
67	0.8333	0.1667	277	0.7667	0.2333	487	0.7833	0.2167
68	0.9833	0.0167	278	0.9167	0.0833	488	0.7333	0.2667
69	0.7833	0.2167	279	0.7167	0.2833	489	0.6833	0.3167
70	0.9833	0.0167	280	0.9167	0.0833	490	0.6333	0.3667
71	0.7333	0.2667	281	0.6667	0.3333	491	0.5833	0.4167
72	0.9833	0.0167	282	0.9167	0.0833	492	0.5333	0.4667
73	0.6833	0.3167	283	0.6167	0.3833	493	0.4833	0.5167
74	0.9833	0.0167	284	0.9167	0.0833	494	0.4333	0.5667

75	0.6333	0.3667	285	0.5667	0.4333	495	0.3833	0.6167
76	0.9833	0.0167	286	0.9167	0.0833	496	0.8167	0.1833
77	0.5833	0.4167	287	0.5167	0.4833	497	0.8167	0.1833
78	0.9833	0.0167	288	0.9167	0.0833	498	0.7667	0.2333
79	0.5333	0.4667	289	0.4667	0.5333	499	0.8167	0.1833
80	0.9833	0.0167	290	0.9167	0.0833	500	0.7167	0.2833
81	0.4833	0.5167	291	0.4167	0.5833	501	0.8167	0.1833
82	0.9833	0.0167	292	0.9167	0.0833	502	0.6667	0.3333
83	0.4333	0.5667	293	0.3667	0.6333	503	0.8167	0.1833
84	0.9833	0.0167	294	0.9167	0.0833	504	0.6167	0.3833
85	0.3833	0.6167	295	0.3167	0.6833	505	0.8167	0.1833
86	0.9833	0.0167	296	0.9167	0.0833	506	0.5667	0.4333
87	0.3333	0.6667	297	0.2667	0.7333	507	0.8167	0.1833
88	0.9833	0.0167	298	0.9167	0.0833	508	0.5167	0.4833
89	0.2833	0.7167	299	0.2167	0.7833	509	0.8167	0.1833
90	0.9833	0.0167	300	0.9167	0.0833	510	0.4667	0.5333
91	0.2333	0.7667	301	0.1667	0.8333	511	0.8167	0.1833
92	0.9833	0.0167	302	0.8667	0.1333	512	0.4167	0.5833
93	0.1833	0.8167	303	0.8167	0.1833	513	0.8167	0.1833
94	0.9833	0.0167	304	0.7667	0.2333	514	0.3667	0.6333
95	0.1333	0.8667	305	0.7167	0.2833	515	0.7667	0.2333
96	0.9833	0.0167	306	0.6667	0.3333	516	0.7167	0.2833
97	0.0833	0.9167	307	0.6167	0.3833	517	0.6667	0.3333
98	0.9833	0.0167	308	0.5667	0.4333	518	0.6167	0.3833
99	0.0333	0.9667	309	0.5167	0.4833	519	0.5667	0.4333
100	0.9333	0.0667	310	0.4667	0.5333	520	0.5167	0.4833
101	0.8833	0.1167	311	0.4167	0.5833	521	0.4667	0.5333
102	0.8333	0.1667	312	0.3667	0.6333	522	0.4167	0.5833
103	0.7833	0.2167	313	0.3167	0.6833	523	0.8	0.2
104	0.7333	0.2667	314	0.2667	0.7333	524	0.8	0.2
105	0.6833	0.3167	315	0.2167	0.7833	525	0.75	0.25
106	0.6333	0.3667	316	0.9	0.1	526	0.8	0.2
107	0.5833	0.4167	317	0.9	0.1	527	0.7	0.3

108	0.5333	0.4667	318	0.85	0.15	528	0.8	0.2
109	0.4833	0.5167	319	0.9	0.1	529	0.65	0.35
110	0.4333	0.5667	320	0.8	0.2	530	0.8	0.2
111	0.3833	0.6167	321	0.9	0.1	531	0.6	0.4
112	0.3333	0.6667	322	0.75	0.25	532	0.8	0.2
113	0.2833	0.7167	323	0.9	0.1	533	0.55	0.45
114	0.2333	0.7667	324	0.7	0.3	534	0.8	0.2
115	0.1833	0.8167	325	0.9	0.1	535	0.5	0.5
116	0.1333	0.8667	326	0.65	0.35	536	0.8	0.2
117	0.0833	0.9167	327	0.9	0.1	537	0.45	0.55
118	0.9667	0.0333	328	0.6	0.4	538	0.8	0.2
119	0.9667	0.0333	329	0.9	0.1	539	0.4	0.6
120	0.9167	0.0833	330	0.55	0.45	540	0.75	0.25
121	0.9667	0.0333	331	0.9	0.1	541	0.7	0.3
122	0.8667	0.1333	332	0.5	0.5	542	0.65	0.35
123	0.9667	0.0333	333	0.9	0.1	543	0.6	0.4
124	0.8167	0.1833	334	0.45	0.55	544	0.55	0.45
125	0.9667	0.0333	335	0.9	0.1	545	0.5	0.5
126	0.7667	0.2333	336	0.4	0.6	546	0.45	0.55
127	0.9667	0.0333	337	0.9	0.1	547	0.7833	0.2167
128	0.7167	0.2833	338	0.35	0.65	548	0.7833	0.2167
129	0.9667	0.0333	339	0.9	0.1	549	0.7333	0.2667
130	0.6667	0.3333	340	0.3	0.7	550	0.7833	0.2167
131	0.9667	0.0333	341	0.9	0.1	551	0.6833	0.3167
132	0.6167	0.3833	342	0.25	0.75	552	0.7833	0.2167
133	0.9667	0.0333	343	0.9	0.1	553	0.6333	0.3667
134	0.5667	0.4333	344	0.2	0.8	554	0.7833	0.2167
135	0.9667	0.0333	345	0.85	0.15	555	0.5833	0.4167
136	0.5167	0.4833	346	0.8	0.2	556	0.7833	0.2167
137	0.9667	0.0333	347	0.75	0.25	557	0.5333	0.4667
138	0.4667	0.5333	348	0.7	0.3	558	0.7833	0.2167
139	0.9667	0.0333	349	0.65	0.35	559	0.4833	0.5167
140	0.4167	0.5833	350	0.6	0.4	560	0.7833	0.2167

141	0.9667	0.0333	351	0.55	0.45	561	0.4333	0.5667
142	0.3667	0.6333	352	0.5	0.5	562	0.7333	0.2667
143	0.9667	0.0333	353	0.45	0.55	563	0.6833	0.3167
144	0.3167	0.6833	354	0.4	0.6	564	0.6333	0.3667
145	0.9667	0.0333	355	0.35	0.65	565	0.5833	0.4167
146	0.2667	0.7333	356	0.3	0.7	566	0.5333	0.4667
147	0.9667	0.0333	357	0.25	0.75	567	0.4833	0.5167
148	0.2167	0.7833	358	0.8833	0.1167	568	0.7667	0.2333
149	0.9667	0.0333	359	0.8833	0.1167	569	0.7667	0.2333
150	0.1667	0.8333	360	0.8333	0.1667	570	0.7167	0.2833
151	0.9667	0.0333	361	0.8833	0.1167	571	0.7667	0.2333
152	0.1167	0.8833	362	0.7833	0.2167	572	0.6667	0.3333
153	0.9667	0.0333	363	0.8833	0.1167	573	0.7667	0.2333
154	0.0667	0.9333	364	0.7333	0.2667	574	0.6167	0.3833
155	0.9167	0.0833	365	0.8833	0.1167	575	0.7667	0.2333
156	0.8667	0.1333	366	0.6833	0.3167	576	0.5667	0.4333
157	0.8167	0.1833	367	0.8833	0.1167	577	0.7667	0.2333
158	0.7667	0.2333	368	0.6333	0.3667	578	0.5167	0.4833
159	0.7167	0.2833	369	0.8833	0.1167	579	0.7667	0.2333
160	0.6667	0.3333	370	0.5833	0.4167	580	0.4667	0.5333
161	0.6167	0.3833	371	0.8833	0.1167	581	0.7167	0.2833
162	0.5667	0.4333	372	0.5333	0.4667	582	0.6667	0.3333
163	0.5167	0.4833	373	0.8833	0.1167	583	0.6167	0.3833
164	0.4667	0.5333	374	0.4833	0.5167	584	0.5667	0.4333
165	0.4167	0.5833	375	0.8833	0.1167	585	0.5167	0.4833
166	0.3667	0.6333	376	0.4333	0.5667	586	0.75	0.25
167	0.3167	0.6833	377	0.8833	0.1167	587	0.75	0.25
168	0.2667	0.7333	378	0.3833	0.6167	588	0.7	0.3
169	0.2167	0.7833	379	0.8833	0.1167	589	0.75	0.25
170	0.1667	0.8333	380	0.3333	0.6667	590	0.65	0.35
171	0.1167	0.8833	381	0.8833	0.1167	591	0.75	0.25
172	0.95	0.05	382	0.2833	0.7167	592	0.6	0.4
173	0.95	0.05	383	0.8833	0.1167	593	0.75	0.25

174	0.9	0.1	384	0.2333	0.7667	594	0.55	0.45
175	0.95	0.05	385	0.8333	0.1667	595	0.75	0.25
176	0.85	0.15	386	0.7833	0.2167	596	0.5	0.5
177	0.95	0.05	387	0.7333	0.2667	597	0.7	0.3
178	0.8	0.2	388	0.6833	0.3167	598	0.65	0.35
179	0.95	0.05	389	0.6333	0.3667	599	0.6	0.4
180	0.75	0.25	390	0.5833	0.4167	600	0.55	0.45
181	0.95	0.05	391	0.5333	0.4667	601	0.7333	0.2667
182	0.7	0.3	392	0.4833	0.5167	602	0.7333	0.2667
183	0.95	0.05	393	0.4333	0.5667	603	0.6833	0.3167
184	0.65	0.35	394	0.3833	0.6167	604	0.7333	0.2667
185	0.95	0.05	395	0.3333	0.6667	605	0.6333	0.3667
186	0.6	0.4	396	0.2833	0.7167	606	0.7333	0.2667
187	0.95	0.05	397	0.8667	0.1333	607	0.5833	0.4167
188	0.55	0.45	398	0.8667	0.1333	608	0.7333	0.2667
189	0.95	0.05	399	0.8167	0.1833	609	0.5333	0.4667
190	0.5	0.5	400	0.8667	0.1333	610	0.6833	0.3167
191	0.95	0.05	401	0.7667	0.2333	611	0.6333	0.3667
192	0.45	0.55	402	0.8667	0.1333	612	0.5833	0.4167
193	0.95	0.05	403	0.7167	0.2833	613	0.7167	0.2833
194	0.4	0.6	404	0.8667	0.1333	614	0.7167	0.2833
195	0.95	0.05	405	0.6667	0.3333	615	0.6667	0.3333
196	0.35	0.65	406	0.8667	0.1333	616	0.7167	0.2833
197	0.95	0.05	407	0.6167	0.3833	617	0.6167	0.3833
198	0.3	0.7	408	0.8667	0.1333	618	0.7167	0.2833
199	0.95	0.05	409	0.5667	0.4333	619	0.5667	0.4333
200	0.25	0.75	410	0.8667	0.1333	620	0.6667	0.3333
201	0.95	0.05	411	0.5167	0.4833	621	0.6167	0.3833
202	0.2	0.8	412	0.8667	0.1333	622	0.7	0.3
203	0.95	0.05	413	0.4667	0.5333	623	0.7	0.3
204	0.15	0.85	414	0.8667	0.1333	624	0.65	0.35
205	0.95	0.05	415	0.4167	0.5833	625	0.7	0.3
206	0.1	0.9	416	0.8667	0.1333	626	0.6	0.4

207	0.9	0.1	417	0.3667	0.6333	627	0.65	0.35
208	0.85	0.15	418	0.8667	0.1333	628	0.6833	0.3167
209	0.8	0.2	419	0.3167	0.6833	629	0.6833	0.3167
210	0.75	0.25	420	0.8667	0.1333	630	0.6333	0.3667
						631	0.6667	0.3333

Table D.3: 631 directions for the case of three groups.

No.	d_1	d_2	d_3	No.	d_1	d_2	d_3	No.	d_1	d_2	d_3
1	1	0	0	211	0.05	0.65	0.3	421	0.1333	0.1333	0.7333
2	0.95	0.05	0	212	0.05	0.6	0.35	422	0.1333	0.6833	0.1833
3	0.95	0	0.05	213	0.05	0.55	0.4	423	0.1333	0.6333	0.2333
4	0.9	0.1	0	214	0.05	0.5	0.45	424	0.1333	0.5833	0.2833
5	0.9	0	0.1	215	0.05	0.45	0.5	425	0.1333	0.5333	0.3333
6	0.85	0.15	0	216	0.05	0.4	0.55	426	0.1333	0.4833	0.3833
7	0.85	0	0.15	217	0.05	0.35	0.6	427	0.1333	0.4333	0.4333
8	0.8	0.2	0	218	0.05	0.3	0.65	428	0.1333	0.3833	0.4833
9	0.8	0	0.2	219	0.05	0.25	0.7	429	0.1333	0.3333	0.5333
10	0.75	0.25	0	220	0.05	0.2	0.75	430	0.1333	0.2833	0.5833
11	0.75	0	0.25	221	0.05	0.15	0.8	431	0.1333	0.2333	0.6333
12	0.7	0.3	0	222	0.05	0.1	0.85	432	0.1333	0.1833	0.6833
13	0.7	0	0.3	223	0.8667	0.0667	0.0667	433	0.7	0.15	0.15
14	0.65	0.35	0	224	0.8167	0.1167	0.0667	434	0.65	0.2	0.15
15	0.65	0	0.35	225	0.8167	0.0667	0.1167	435	0.65	0.15	0.2
16	0.6	0.4	0	226	0.7667	0.1667	0.0667	436	0.6	0.25	0.15
17	0.6	0	0.4	227	0.7667	0.0667	0.1667	437	0.6	0.15	0.25
18	0.55	0.45	0	228	0.7167	0.2167	0.0667	438	0.55	0.3	0.15
19	0.55	0	0.45	229	0.7167	0.0667	0.2167	439	0.55	0.15	0.3
20	0.5	0.5	0	230	0.6667	0.2667	0.0667	440	0.5	0.35	0.15
21	0.5	0	0.5	231	0.6667	0.0667	0.2667	441	0.5	0.15	0.35
22	0.45	0.55	0	232	0.6167	0.3167	0.0667	442	0.45	0.4	0.15
23	0.45	0	0.55	233	0.6167	0.0667	0.3167	443	0.45	0.15	0.4

24	0.4	0.6	0	234	0.5667	0.3667	0.0667	444	0.4	0.45	0.15
25	0.4	0	0.6	235	0.5667	0.0667	0.3667	445	0.4	0.15	0.45
26	0.35	0.65	0	236	0.5167	0.4167	0.0667	446	0.35	0.5	0.15
27	0.35	0	0.65	237	0.5167	0.0667	0.4167	447	0.35	0.15	0.5
28	0.3	0.7	0	238	0.4667	0.4667	0.0667	448	0.3	0.55	0.15
29	0.3	0	0.7	239	0.4667	0.0667	0.4667	449	0.3	0.15	0.55
30	0.25	0.75	0	240	0.4167	0.5167	0.0667	450	0.25	0.6	0.15
31	0.25	0	0.75	241	0.4167	0.0667	0.5167	451	0.25	0.15	0.6
32	0.2	0.8	0	242	0.3667	0.5667	0.0667	452	0.2	0.65	0.15
33	0.2	0	0.8	243	0.3667	0.0667	0.5667	453	0.2	0.15	0.65
34	0.15	0.85	0	244	0.3167	0.6167	0.0667	454	0.15	0.7	0.15
35	0.15	0	0.85	245	0.3167	0.0667	0.6167	455	0.15	0.15	0.7
36	0.1	0.9	0	246	0.2667	0.6667	0.0667	456	0.15	0.65	0.2
37	0.1	0	0.9	247	0.2667	0.0667	0.6667	457	0.15	0.6	0.25
38	0.05	0.95	0	248	0.2167	0.7167	0.0667	458	0.15	0.55	0.3
39	0.05	0	0.95	249	0.2167	0.0667	0.7167	459	0.15	0.5	0.35
40	0	1	0	250	0.1667	0.7667	0.0667	460	0.15	0.45	0.4
41	0	0	1	251	0.1667	0.0667	0.7667	461	0.15	0.4	0.45
42	0.9667	0.0167	0.0167	252	0.1167	0.8167	0.0667	462	0.15	0.35	0.5
43	0	0.95	0.05	253	0.1167	0.0667	0.8167	463	0.15	0.3	0.55
44	0	0.9	0.1	254	0.0667	0.8667	0.0667	464	0.15	0.25	0.6
45	0	0.85	0.15	255	0.0667	0.0667	0.8667	465	0.15	0.2	0.65
46	0	0.8	0.2	256	0.0667	0.8167	0.1167	466	0.6667	0.1667	0.1667
47	0	0.75	0.25	257	0.0667	0.7667	0.1667	467	0.6167	0.2167	0.1667
48	0	0.7	0.3	258	0.0667	0.7167	0.2167	468	0.6167	0.1667	0.2167
49	0	0.65	0.35	259	0.0667	0.6667	0.2667	469	0.5667	0.2667	0.1667
50	0	0.6	0.4	260	0.0667	0.6167	0.3167	470	0.5667	0.1667	0.2667
51	0	0.55	0.45	261	0.0667	0.5667	0.3667	471	0.5167	0.3167	0.1667
52	0	0.5	0.5	262	0.0667	0.5167	0.4167	472	0.5167	0.1667	0.3167
53	0	0.45	0.55	263	0.0667	0.4667	0.4667	473	0.4667	0.3667	0.1667
54	0	0.4	0.6	264	0.0667	0.4167	0.5167	474	0.4667	0.1667	0.3667
55	0	0.35	0.65	265	0.0667	0.3667	0.5667	475	0.4167	0.4167	0.1667
56	0	0.3	0.7	266	0.0667	0.3167	0.6167	476	0.4167	0.1667	0.4167

57	0	0.25	0.75	267	0.0667	0.2667	0.6667	477	0.3667	0.4667	0.1667
58	0	0.2	0.8	268	0.0667	0.2167	0.7167	478	0.3667	0.1667	0.4667
59	0	0.15	0.85	269	0.0667	0.1667	0.7667	479	0.3167	0.5167	0.1667
60	0	0.1	0.9	270	0.0667	0.1167	0.8167	480	0.3167	0.1667	0.5167
61	0	0.05	0.95	271	0.8333	0.0833	0.0833	481	0.2667	0.5667	0.1667
62	0.9167	0.0667	0.0167	272	0.7833	0.1333	0.0833	482	0.2667	0.1667	0.5667
63	0.9167	0.0167	0.0667	273	0.7833	0.0833	0.1333	483	0.2167	0.6167	0.1667
64	0.8667	0.1167	0.0167	274	0.7333	0.1833	0.0833	484	0.2167	0.1667	0.6167
65	0.8667	0.0167	0.1167	275	0.7333	0.0833	0.1833	485	0.1667	0.6667	0.1667
66	0.8167	0.1667	0.0167	276	0.6833	0.2333	0.0833	486	0.1667	0.1667	0.6667
67	0.8167	0.0167	0.1667	277	0.6833	0.0833	0.2333	487	0.1667	0.6167	0.2167
68	0.7667	0.2167	0.0167	278	0.6333	0.2833	0.0833	488	0.1667	0.5667	0.2667
69	0.7667	0.0167	0.2167	279	0.6333	0.0833	0.2833	489	0.1667	0.5167	0.3167
70	0.7167	0.2667	0.0167	280	0.5833	0.3333	0.0833	490	0.1667	0.4667	0.3667
71	0.7167	0.0167	0.2667	281	0.5833	0.0833	0.3333	491	0.1667	0.4167	0.4167
72	0.6667	0.3167	0.0167	282	0.5333	0.3833	0.0833	492	0.1667	0.3667	0.4667
73	0.6667	0.0167	0.3167	283	0.5333	0.0833	0.3833	493	0.1667	0.3167	0.5167
74	0.6167	0.3667	0.0167	284	0.4833	0.4333	0.0833	494	0.1667	0.2667	0.5667
75	0.6167	0.0167	0.3667	285	0.4833	0.0833	0.4333	495	0.1667	0.2167	0.6167
76	0.5667	0.4167	0.0167	286	0.4333	0.4833	0.0833	496	0.6333	0.1833	0.1833
77	0.5667	0.0167	0.4167	287	0.4333	0.0833	0.4833	497	0.5833	0.2333	0.1833
78	0.5167	0.4667	0.0167	288	0.3833	0.5333	0.0833	498	0.5833	0.1833	0.2333
79	0.5167	0.0167	0.4667	289	0.3833	0.0833	0.5333	499	0.5333	0.2833	0.1833
80	0.4667	0.5167	0.0167	290	0.3333	0.5833	0.0833	500	0.5333	0.1833	0.2833
81	0.4667	0.0167	0.5167	291	0.3333	0.0833	0.5833	501	0.4833	0.3333	0.1833
82	0.4167	0.5667	0.0167	292	0.2833	0.6333	0.0833	502	0.4833	0.1833	0.3333
83	0.4167	0.0167	0.5667	293	0.2833	0.0833	0.6333	503	0.4333	0.3833	0.1833
84	0.3667	0.6167	0.0167	294	0.2333	0.6833	0.0833	504	0.4333	0.1833	0.3833
85	0.3667	0.0167	0.6167	295	0.2333	0.0833	0.6833	505	0.3833	0.4333	0.1833
86	0.3167	0.6667	0.0167	296	0.1833	0.7333	0.0833	506	0.3833	0.1833	0.4333
87	0.3167	0.0167	0.6667	297	0.1833	0.0833	0.7333	507	0.3333	0.4833	0.1833
88	0.2667	0.7167	0.0167	298	0.1333	0.7833	0.0833	508	0.3333	0.1833	0.4833
89	0.2667	0.0167	0.7167	299	0.1333	0.0833	0.7833	509	0.2833	0.5333	0.1833

90	0.2167	0.7667	0.0167	300	0.0833	0.8333	0.0833	510	0.2833	0.1833	0.5333
91	0.2167	0.0167	0.7667	301	0.0833	0.0833	0.8333	511	0.2333	0.5833	0.1833
92	0.1667	0.8167	0.0167	302	0.0833	0.7833	0.1333	512	0.2333	0.1833	0.5833
93	0.1667	0.0167	0.8167	303	0.0833	0.7333	0.1833	513	0.1833	0.6333	0.1833
94	0.1167	0.8667	0.0167	304	0.0833	0.6833	0.2333	514	0.1833	0.1833	0.6333
95	0.1167	0.0167	0.8667	305	0.0833	0.6333	0.2833	515	0.1833	0.5833	0.2333
96	0.0667	0.9167	0.0167	306	0.0833	0.5833	0.3333	516	0.1833	0.5333	0.2833
97	0.0667	0.0167	0.9167	307	0.0833	0.5333	0.3833	517	0.1833	0.4833	0.3333
98	0.0167	0.9667	0.0167	308	0.0833	0.4833	0.4333	518	0.1833	0.4333	0.3833
99	0.0167	0.0167	0.9667	309	0.0833	0.4333	0.4833	519	0.1833	0.3833	0.4333
100	0.0167	0.9167	0.0667	310	0.0833	0.3833	0.5333	520	0.1833	0.3333	0.4833
101	0.0167	0.8667	0.1167	311	0.0833	0.3333	0.5833	521	0.1833	0.2833	0.5333
102	0.0167	0.8167	0.1667	312	0.0833	0.2833	0.6333	522	0.1833	0.2333	0.5833
103	0.0167	0.7667	0.2167	313	0.0833	0.2333	0.6833	523	0.6	0.2	0.2
104	0.0167	0.7167	0.2667	314	0.0833	0.1833	0.7333	524	0.55	0.25	0.2
105	0.0167	0.6667	0.3167	315	0.0833	0.1333	0.7833	525	0.55	0.2	0.25
106	0.0167	0.6167	0.3667	316	0.8	0.1	0.1	526	0.5	0.3	0.2
107	0.0167	0.5667	0.4167	317	0.75	0.15	0.1	527	0.5	0.2	0.3
108	0.0167	0.5167	0.4667	318	0.75	0.1	0.15	528	0.45	0.35	0.2
109	0.0167	0.4667	0.5167	319	0.7	0.2	0.1	529	0.45	0.2	0.35
110	0.0167	0.4167	0.5667	320	0.7	0.1	0.2	530	0.4	0.4	0.2
111	0.0167	0.3667	0.6167	321	0.65	0.25	0.1	531	0.4	0.2	0.4
112	0.0167	0.3167	0.6667	322	0.65	0.1	0.25	532	0.35	0.45	0.2
113	0.0167	0.2667	0.7167	323	0.6	0.3	0.1	533	0.35	0.2	0.45
114	0.0167	0.2167	0.7667	324	0.6	0.1	0.3	534	0.3	0.5	0.2
115	0.0167	0.1667	0.8167	325	0.55	0.35	0.1	535	0.3	0.2	0.5
116	0.0167	0.1167	0.8667	326	0.55	0.1	0.35	536	0.25	0.55	0.2
117	0.0167	0.0667	0.9167	327	0.5	0.4	0.1	537	0.25	0.2	0.55
118	0.9333	0.0333	0.0333	328	0.5	0.1	0.4	538	0.2	0.6	0.2
119	0.8833	0.0833	0.0333	329	0.45	0.45	0.1	539	0.2	0.2	0.6
120	0.8833	0.0333	0.0833	330	0.45	0.1	0.45	540	0.2	0.55	0.25
121	0.8333	0.1333	0.0333	331	0.4	0.5	0.1	541	0.2	0.5	0.3
122	0.8333	0.0333	0.1333	332	0.4	0.1	0.5	542	0.2	0.45	0.35

123	0.7833	0.1833	0.0333	333	0.35	0.55	0.1	543	0.2	0.4	0.4
124	0.7833	0.0333	0.1833	334	0.35	0.1	0.55	544	0.2	0.35	0.45
125	0.7333	0.2333	0.0333	335	0.3	0.6	0.1	545	0.2	0.3	0.5
126	0.7333	0.0333	0.2333	336	0.3	0.1	0.6	546	0.2	0.25	0.55
127	0.6833	0.2833	0.0333	337	0.25	0.65	0.1	547	0.5667	0.2167	0.2167
128	0.6833	0.0333	0.2833	338	0.25	0.1	0.65	548	0.5167	0.2667	0.2167
129	0.6333	0.3333	0.0333	339	0.2	0.7	0.1	549	0.5167	0.2167	0.2667
130	0.6333	0.0333	0.3333	340	0.2	0.1	0.7	550	0.4667	0.3167	0.2167
131	0.5833	0.3833	0.0333	341	0.15	0.75	0.1	551	0.4667	0.2167	0.3167
132	0.5833	0.0333	0.3833	342	0.15	0.1	0.75	552	0.4167	0.3667	0.2167
133	0.5333	0.4333	0.0333	343	0.1	0.8	0.1	553	0.4167	0.2167	0.3667
134	0.5333	0.0333	0.4333	344	0.1	0.1	0.8	554	0.3667	0.4167	0.2167
135	0.4833	0.4833	0.0333	345	0.1	0.75	0.15	555	0.3667	0.2167	0.4167
136	0.4833	0.0333	0.4833	346	0.1	0.7	0.2	556	0.3167	0.4667	0.2167
137	0.4333	0.5333	0.0333	347	0.1	0.65	0.25	557	0.3167	0.2167	0.4667
138	0.4333	0.0333	0.5333	348	0.1	0.6	0.3	558	0.2667	0.5167	0.2167
139	0.3833	0.5833	0.0333	349	0.1	0.55	0.35	559	0.2667	0.2167	0.5167
140	0.3833	0.0333	0.5833	350	0.1	0.5	0.4	560	0.2167	0.5667	0.2167
141	0.3333	0.6333	0.0333	351	0.1	0.45	0.45	561	0.2167	0.2167	0.5667
142	0.3333	0.0333	0.6333	352	0.1	0.4	0.5	562	0.2167	0.5167	0.2667
143	0.2833	0.6833	0.0333	353	0.1	0.35	0.55	563	0.2167	0.4667	0.3167
144	0.2833	0.0333	0.6833	354	0.1	0.3	0.6	564	0.2167	0.4167	0.3667
145	0.2333	0.7333	0.0333	355	0.1	0.25	0.65	565	0.2167	0.3667	0.4167
146	0.2333	0.0333	0.7333	356	0.1	0.2	0.7	566	0.2167	0.3167	0.4667
147	0.1833	0.7833	0.0333	357	0.1	0.15	0.75	567	0.2167	0.2667	0.5167
148	0.1833	0.0333	0.7833	358	0.7667	0.1167	0.1167	568	0.5333	0.2333	0.2333
149	0.1333	0.8333	0.0333	359	0.7167	0.1667	0.1167	569	0.4833	0.2833	0.2333
150	0.1333	0.0333	0.8333	360	0.7167	0.1167	0.1667	570	0.4833	0.2333	0.2833
151	0.0833	0.8833	0.0333	361	0.6667	0.2167	0.1167	571	0.4333	0.3333	0.2333
152	0.0833	0.0333	0.8833	362	0.6667	0.1167	0.2167	572	0.4333	0.2333	0.3333
153	0.0333	0.9333	0.0333	363	0.6167	0.2667	0.1167	573	0.3833	0.3833	0.2333
154	0.0333	0.0333	0.9333	364	0.6167	0.1167	0.2667	574	0.3833	0.2333	0.3833
155	0.0333	0.8833	0.0833	365	0.5667	0.3167	0.1167	575	0.3333	0.4333	0.2333

156	0.0333	0.8333	0.1333	366	0.5667	0.1167	0.3167	576	0.3333	0.2333	0.4333
157	0.0333	0.7833	0.1833	367	0.5167	0.3667	0.1167	577	0.2833	0.4833	0.2333
158	0.0333	0.7333	0.2333	368	0.5167	0.1167	0.3667	578	0.2833	0.2333	0.4833
159	0.0333	0.6833	0.2833	369	0.4667	0.4167	0.1167	579	0.2333	0.5333	0.2333
160	0.0333	0.6333	0.3333	370	0.4667	0.1167	0.4167	580	0.2333	0.2333	0.5333
161	0.0333	0.5833	0.3833	371	0.4167	0.4667	0.1167	581	0.2333	0.4833	0.2833
162	0.0333	0.5333	0.4333	372	0.4167	0.1167	0.4667	582	0.2333	0.4333	0.3333
163	0.0333	0.4833	0.4833	373	0.3667	0.5167	0.1167	583	0.2333	0.3833	0.3833
164	0.0333	0.4333	0.5333	374	0.3667	0.1167	0.5167	584	0.2333	0.3333	0.4333
165	0.0333	0.3833	0.5833	375	0.3167	0.5667	0.1167	585	0.2333	0.2833	0.4833
166	0.0333	0.3333	0.6333	376	0.3167	0.1167	0.5667	586	0.5	0.25	0.25
167	0.0333	0.2833	0.6833	377	0.2667	0.6167	0.1167	587	0.45	0.3	0.25
168	0.0333	0.2333	0.7333	378	0.2667	0.1167	0.6167	588	0.45	0.25	0.3
169	0.0333	0.1833	0.7833	379	0.2167	0.6667	0.1167	589	0.4	0.35	0.25
170	0.0333	0.1333	0.8333	380	0.2167	0.1167	0.6667	590	0.4	0.25	0.35
171	0.0333	0.0833	0.8833	381	0.1667	0.7167	0.1167	591	0.35	0.4	0.25
172	0.9	0.05	0.05	382	0.1667	0.1167	0.7167	592	0.35	0.25	0.4
173	0.85	0.1	0.05	383	0.1167	0.7667	0.1167	593	0.3	0.45	0.25
174	0.85	0.05	0.1	384	0.1167	0.1167	0.7667	594	0.3	0.25	0.45
175	0.8	0.15	0.05	385	0.1167	0.7167	0.1667	595	0.25	0.5	0.25
176	0.8	0.05	0.15	386	0.1167	0.6667	0.2167	596	0.25	0.25	0.5
177	0.75	0.2	0.05	387	0.1167	0.6167	0.2667	597	0.25	0.45	0.3
178	0.75	0.05	0.2	388	0.1167	0.5667	0.3167	598	0.25	0.4	0.35
179	0.7	0.25	0.05	389	0.1167	0.5167	0.3667	599	0.25	0.35	0.4
180	0.7	0.05	0.25	390	0.1167	0.4667	0.4167	600	0.25	0.3	0.45
181	0.65	0.3	0.05	391	0.1167	0.4167	0.4667	601	0.4667	0.2667	0.2667
182	0.65	0.05	0.3	392	0.1167	0.3667	0.5167	602	0.4167	0.3167	0.2667
183	0.6	0.35	0.05	393	0.1167	0.3167	0.5667	603	0.4167	0.2667	0.3167
184	0.6	0.05	0.35	394	0.1167	0.2667	0.6167	604	0.3667	0.3667	0.2667
185	0.55	0.4	0.05	395	0.1167	0.2167	0.6667	605	0.3667	0.2667	0.3667
186	0.55	0.05	0.4	396	0.1167	0.1667	0.7167	606	0.3167	0.4167	0.2667
187	0.5	0.45	0.05	397	0.7333	0.1333	0.1333	607	0.3167	0.2667	0.4167
188	0.5	0.05	0.45	398	0.6833	0.1833	0.1333	608	0.2667	0.4667	0.2667

189	0.45	0.5	0.05	399	0.6833	0.1333	0.1833	609	0.2667	0.2667	0.4667
190	0.45	0.05	0.5	400	0.6333	0.2333	0.1333	610	0.2667	0.4167	0.3167
191	0.4	0.55	0.05	401	0.6333	0.1333	0.2333	611	0.2667	0.3667	0.3667
192	0.4	0.05	0.55	402	0.5833	0.2833	0.1333	612	0.2667	0.3167	0.4167
193	0.35	0.6	0.05	403	0.5833	0.1333	0.2833	613	0.4333	0.2833	0.2833
194	0.35	0.05	0.6	404	0.5333	0.3333	0.1333	614	0.3833	0.3333	0.2833
195	0.3	0.65	0.05	405	0.5333	0.1333	0.3333	615	0.3833	0.2833	0.3333
196	0.3	0.05	0.65	406	0.4833	0.3833	0.1333	616	0.3333	0.3833	0.2833
197	0.25	0.7	0.05	407	0.4833	0.1333	0.3833	617	0.3333	0.2833	0.3833
198	0.25	0.05	0.7	408	0.4333	0.4333	0.1333	618	0.2833	0.4333	0.2833
199	0.2	0.75	0.05	409	0.4333	0.1333	0.4333	619	0.2833	0.2833	0.4333
200	0.2	0.05	0.75	410	0.3833	0.4833	0.1333	620	0.2833	0.3833	0.3333
201	0.15	0.8	0.05	411	0.3833	0.1333	0.4833	621	0.2833	0.3333	0.3833
202	0.15	0.05	0.8	412	0.3333	0.5333	0.1333	622	0.4	0.3	0.3
203	0.1	0.85	0.05	413	0.3333	0.1333	0.5333	623	0.35	0.35	0.3
204	0.1	0.05	0.85	414	0.2833	0.5833	0.1333	624	0.35	0.3	0.35
205	0.05	0.9	0.05	415	0.2833	0.1333	0.5833	625	0.3	0.4	0.3
206	0.05	0.05	0.9	416	0.2333	0.6333	0.1333	626	0.3	0.3	0.4
207	0.05	0.85	0.1	417	0.2333	0.1333	0.6333	627	0.3	0.35	0.35
208	0.05	0.8	0.15	418	0.1833	0.6833	0.1333	628	0.3667	0.3167	0.3167
209	0.05	0.75	0.2	419	0.1833	0.1333	0.6833	629	0.3167	0.3667	0.3167
210	0.05	0.7	0.25	420	0.1333	0.7333	0.1333	630	0.3167	0.3167	0.3667
								631	0.3333	0.3333	0.3333

Table D.4: 631 directions for the case of four groups.

No.	d_1	d_2	d_3	d_4	No.	d_1	d_2	d_3	d_4
1	0.5	0	0	0.5	316	0.4	0.1	0.1	0.4
2	0.475	0.05	0	0.475	317	0.375	0.15	0.1	0.375
3	0.475	0	0.05	0.475	318	0.375	0.1	0.15	0.375
4	0.45	0.1	0	0.45	319	0.35	0.2	0.1	0.35
5	0.45	0	0.1	0.45	320	0.35	0.1	0.2	0.35

6	0.425	0.15	0	0.425	321	0.325	0.25	0.1	0.325
7	0.425	0	0.15	0.425	322	0.325	0.1	0.25	0.325
8	0.4	0.2	0	0.4	323	0.3	0.3	0.1	0.3
9	0.4	0	0.2	0.4	324	0.3	0.1	0.3	0.3
10	0.375	0.25	0	0.375	325	0.275	0.35	0.1	0.275
11	0.375	0	0.25	0.375	326	0.275	0.1	0.35	0.275
12	0.35	0.3	0	0.35	327	0.25	0.4	0.1	0.25
13	0.35	0	0.3	0.35	328	0.25	0.1	0.4	0.25
14	0.325	0.35	0	0.325	329	0.225	0.45	0.1	0.225
15	0.325	0	0.35	0.325	330	0.225	0.1	0.45	0.225
16	0.3	0.4	0	0.3	331	0.2	0.5	0.1	0.2
17	0.3	0	0.4	0.3	332	0.2	0.1	0.5	0.2
18	0.275	0.45	0	0.275	333	0.175	0.55	0.1	0.175
19	0.275	0	0.45	0.275	334	0.175	0.1	0.55	0.175
20	0.25	0.5	0	0.25	335	0.15	0.6	0.1	0.15
21	0.25	0	0.5	0.25	336	0.15	0.1	0.6	0.15
22	0.225	0.55	0	0.225	337	0.125	0.65	0.1	0.125
23	0.225	0	0.55	0.225	338	0.125	0.1	0.65	0.125
24	0.2	0.6	0	0.2	339	0.1	0.7	0.1	0.1
25	0.2	0	0.6	0.2	340	0.1	0.1	0.7	0.1
26	0.175	0.65	0	0.175	341	0.075	0.75	0.1	0.075
27	0.175	0	0.65	0.175	342	0.075	0.1	0.75	0.075
28	0.15	0.7	0	0.15	343	0.05	0.8	0.1	0.05
29	0.15	0	0.7	0.15	344	0.05	0.1	0.8	0.05
30	0.125	0.75	0	0.125	345	0.05	0.75	0.15	0.05
31	0.125	0	0.75	0.125	346	0.05	0.7	0.2	0.05
32	0.1	0.8	0	0.1	347	0.05	0.65	0.25	0.05
33	0.1	0	0.8	0.1	348	0.05	0.6	0.3	0.05
34	0.075	0.85	0	0.075	349	0.05	0.55	0.35	0.05
35	0.075	0	0.85	0.075	350	0.05	0.5	0.4	0.05
36	0.05	0.9	0	0.05	351	0.05	0.45	0.45	0.05
37	0.05	0	0.9	0.05	352	0.05	0.4	0.5	0.05
38	0.025	0.95	0	0.025	353	0.05	0.35	0.55	0.05

39	0.025	0	0.95	0.025	354	0.05	0.3	0.6	0.05
40	0	1	0	0	355	0.05	0.25	0.65	0.05
41	0	0	1	0	356	0.05	0.2	0.7	0.05
42	0.4833	0.0167	0.0167	0.4833	357	0.05	0.15	0.75	0.05
43	0	0.95	0.05	0	358	0.3833	0.1167	0.1167	0.3833
44	0	0.9	0.1	0	359	0.3583	0.1667	0.1167	0.3583
45	0	0.85	0.15	0	360	0.3583	0.1167	0.1667	0.3583
46	0	0.8	0.2	0	361	0.3333	0.2167	0.1167	0.3333
47	0	0.75	0.25	0	362	0.3333	0.1167	0.2167	0.3333
48	0	0.7	0.3	0	363	0.3083	0.2667	0.1167	0.3083
49	0	0.65	0.35	0	364	0.3083	0.1167	0.2667	0.3083
50	0	0.6	0.4	0	365	0.2833	0.3167	0.1167	0.2833
51	0	0.55	0.45	0	366	0.2833	0.1167	0.3167	0.2833
52	0	0.5	0.5	0	367	0.2583	0.3667	0.1167	0.2583
53	0	0.45	0.55	0	368	0.2583	0.1167	0.3667	0.2583
54	0	0.4	0.6	0	369	0.2333	0.4167	0.1167	0.2333
55	0	0.35	0.65	0	370	0.2333	0.1167	0.4167	0.2333
56	0	0.3	0.7	0	371	0.2083	0.4667	0.1167	0.2083
57	0	0.25	0.75	0	372	0.2083	0.1167	0.4667	0.2083
58	0	0.2	0.8	0	373	0.1833	0.5167	0.1167	0.1833
59	0	0.15	0.85	0	374	0.1833	0.1167	0.5167	0.1833
60	0	0.1	0.9	0	375	0.1583	0.5667	0.1167	0.1583
61	0	0.05	0.95	0	376	0.1583	0.1167	0.5667	0.1583
62	0.4583	0.0667	0.0167	0.4583	377	0.1333	0.6167	0.1167	0.1333
63	0.4583	0.0167	0.0667	0.4583	378	0.1333	0.1167	0.6167	0.1333
64	0.4333	0.1167	0.0167	0.4333	379	0.1083	0.6667	0.1167	0.1083
65	0.4333	0.0167	0.1167	0.4333	380	0.1083	0.1167	0.6667	0.1083
66	0.4083	0.1667	0.0167	0.4083	381	0.0833	0.7167	0.1167	0.0833
67	0.4083	0.0167	0.1667	0.4083	382	0.0833	0.1167	0.7167	0.0833
68	0.3833	0.2167	0.0167	0.3833	383	0.0583	0.7667	0.1167	0.0583
69	0.3833	0.0167	0.2167	0.3833	384	0.0583	0.1167	0.7667	0.0583
70	0.3583	0.2667	0.0167	0.3583	385	0.0583	0.7167	0.1667	0.0583
71	0.3583	0.0167	0.2667	0.3583	386	0.0583	0.6667	0.2167	0.0583

72	0.3333	0.3167	0.0167	0.3333	387	0.0583	0.6167	0.2667	0.0583
73	0.3333	0.0167	0.3167	0.3333	388	0.0583	0.5667	0.3167	0.0583
74	0.3083	0.3667	0.0167	0.3083	389	0.0583	0.5167	0.3667	0.0583
75	0.3083	0.0167	0.3667	0.3083	390	0.0583	0.4667	0.4167	0.0583
76	0.2833	0.4167	0.0167	0.2833	391	0.0583	0.4167	0.4667	0.0583
77	0.2833	0.0167	0.4167	0.2833	392	0.0583	0.3667	0.5167	0.0583
78	0.2583	0.4667	0.0167	0.2583	393	0.0583	0.3167	0.5667	0.0583
79	0.2583	0.0167	0.4667	0.2583	394	0.0583	0.2667	0.6167	0.0583
80	0.2333	0.5167	0.0167	0.2333	395	0.0583	0.2167	0.6667	0.0583
81	0.2333	0.0167	0.5167	0.2333	396	0.0583	0.1667	0.7167	0.0583
82	0.2083	0.5667	0.0167	0.2083	397	0.3667	0.1333	0.1333	0.3667
83	0.2083	0.0167	0.5667	0.2083	398	0.3417	0.1833	0.1333	0.3417
84	0.1833	0.6167	0.0167	0.1833	399	0.3417	0.1333	0.1833	0.3417
85	0.1833	0.0167	0.6167	0.1833	400	0.3167	0.2333	0.1333	0.3167
86	0.1583	0.6667	0.0167	0.1583	401	0.3167	0.1333	0.2333	0.3167
87	0.1583	0.0167	0.6667	0.1583	402	0.2917	0.2833	0.1333	0.2917
88	0.1333	0.7167	0.0167	0.1333	403	0.2917	0.1333	0.2833	0.2917
89	0.1333	0.0167	0.7167	0.1333	404	0.2667	0.3333	0.1333	0.2667
90	0.1083	0.7667	0.0167	0.1083	405	0.2667	0.1333	0.3333	0.2667
91	0.1083	0.0167	0.7667	0.1083	406	0.2417	0.3833	0.1333	0.2417
92	0.0833	0.8167	0.0167	0.0833	407	0.2417	0.1333	0.3833	0.2417
93	0.0833	0.0167	0.8167	0.0833	408	0.2167	0.4333	0.1333	0.2167
94	0.0583	0.8667	0.0167	0.0583	409	0.2167	0.1333	0.4333	0.2167
95	0.0583	0.0167	0.8667	0.0583	410	0.1917	0.4833	0.1333	0.1917
96	0.0333	0.9167	0.0167	0.0333	411	0.1917	0.1333	0.4833	0.1917
97	0.0333	0.0167	0.9167	0.0333	412	0.1667	0.5333	0.1333	0.1667
98	0.0083	0.9667	0.0167	0.0083	413	0.1667	0.1333	0.5333	0.1667
99	0.0083	0.0167	0.9667	0.0083	414	0.1417	0.5833	0.1333	0.1417
100	0.0083	0.9167	0.0667	0.0083	415	0.1417	0.1333	0.5833	0.1417
101	0.0083	0.8667	0.1167	0.0083	416	0.1167	0.6333	0.1333	0.1167
102	0.0083	0.8167	0.1667	0.0083	417	0.1167	0.1333	0.6333	0.1167
103	0.0083	0.7667	0.2167	0.0083	418	0.0917	0.6833	0.1333	0.0917
104	0.0083	0.7167	0.2667	0.0083	419	0.0917	0.1333	0.6833	0.0917

105	0.0083	0.6667	0.3167	0.0083	420	0.0667	0.7333	0.1333	0.0667
106	0.0083	0.6167	0.3667	0.0083	421	0.0667	0.1333	0.7333	0.0667
107	0.0083	0.5667	0.4167	0.0083	422	0.0667	0.6833	0.1833	0.0667
108	0.0083	0.5167	0.4667	0.0083	423	0.0667	0.6333	0.2333	0.0667
109	0.0083	0.4667	0.5167	0.0083	424	0.0667	0.5833	0.2833	0.0667
110	0.0083	0.4167	0.5667	0.0083	425	0.0667	0.5333	0.3333	0.0667
111	0.0083	0.3667	0.6167	0.0083	426	0.0667	0.4833	0.3833	0.0667
112	0.0083	0.3167	0.6667	0.0083	427	0.0667	0.4333	0.4333	0.0667
113	0.0083	0.2667	0.7167	0.0083	428	0.0667	0.3833	0.4833	0.0667
114	0.0083	0.2167	0.7667	0.0083	429	0.0667	0.3333	0.5333	0.0667
115	0.0083	0.1667	0.8167	0.0083	430	0.0667	0.2833	0.5833	0.0667
116	0.0083	0.1167	0.8667	0.0083	431	0.0667	0.2333	0.6333	0.0667
117	0.0083	0.0667	0.9167	0.0083	432	0.0667	0.1833	0.6833	0.0667
118	0.4667	0.0333	0.0333	0.4667	433	0.35	0.15	0.15	0.35
119	0.4417	0.0833	0.0333	0.4417	434	0.325	0.2	0.15	0.325
120	0.4417	0.0333	0.0833	0.4417	435	0.325	0.15	0.2	0.325
121	0.4167	0.1333	0.0333	0.4167	436	0.3	0.25	0.15	0.3
122	0.4167	0.0333	0.1333	0.4167	437	0.3	0.15	0.25	0.3
123	0.3917	0.1833	0.0333	0.3917	438	0.275	0.3	0.15	0.275
124	0.3917	0.0333	0.1833	0.3917	439	0.275	0.15	0.3	0.275
125	0.3667	0.2333	0.0333	0.3667	440	0.25	0.35	0.15	0.25
126	0.3667	0.0333	0.2333	0.3667	441	0.25	0.15	0.35	0.25
127	0.3417	0.2833	0.0333	0.3417	442	0.225	0.4	0.15	0.225
128	0.3417	0.0333	0.2833	0.3417	443	0.225	0.15	0.4	0.225
129	0.3167	0.3333	0.0333	0.3167	444	0.2	0.45	0.15	0.2
130	0.3167	0.0333	0.3333	0.3167	445	0.2	0.15	0.45	0.2
131	0.2917	0.3833	0.0333	0.2917	446	0.175	0.5	0.15	0.175
132	0.2917	0.0333	0.3833	0.2917	447	0.175	0.15	0.5	0.175
133	0.2667	0.4333	0.0333	0.2667	448	0.15	0.55	0.15	0.15
134	0.2667	0.0333	0.4333	0.2667	449	0.15	0.15	0.55	0.15
135	0.2417	0.4833	0.0333	0.2417	450	0.125	0.6	0.15	0.125
136	0.2417	0.0333	0.4833	0.2417	451	0.125	0.15	0.6	0.125
137	0.2167	0.5333	0.0333	0.2167	452	0.1	0.65	0.15	0.1

138	0.2167	0.0333	0.5333	0.2167	453	0.1	0.15	0.65	0.1
139	0.1917	0.5833	0.0333	0.1917	454	0.075	0.7	0.15	0.075
140	0.1917	0.0333	0.5833	0.1917	455	0.075	0.15	0.7	0.075
141	0.1667	0.6333	0.0333	0.1667	456	0.075	0.65	0.2	0.075
142	0.1667	0.0333	0.6333	0.1667	457	0.075	0.6	0.25	0.075
143	0.1417	0.6833	0.0333	0.1417	458	0.075	0.55	0.3	0.075
144	0.1417	0.0333	0.6833	0.1417	459	0.075	0.5	0.35	0.075
145	0.1167	0.7333	0.0333	0.1167	460	0.075	0.45	0.4	0.075
146	0.1167	0.0333	0.7333	0.1167	461	0.075	0.4	0.45	0.075
147	0.0917	0.7833	0.0333	0.0917	462	0.075	0.35	0.5	0.075
148	0.0917	0.0333	0.7833	0.0917	463	0.075	0.3	0.55	0.075
149	0.0667	0.8333	0.0333	0.0667	464	0.075	0.25	0.6	0.075
150	0.0667	0.0333	0.8333	0.0667	465	0.075	0.2	0.65	0.075
151	0.0417	0.8833	0.0333	0.0417	466	0.3333	0.1667	0.1667	0.3333
152	0.0417	0.0333	0.8833	0.0417	467	0.3083	0.2167	0.1667	0.3083
153	0.0167	0.9333	0.0333	0.0167	468	0.3083	0.1667	0.2167	0.3083
154	0.0167	0.0333	0.9333	0.0167	469	0.2833	0.2667	0.1667	0.2833
155	0.0167	0.8833	0.0833	0.0167	470	0.2833	0.1667	0.2667	0.2833
156	0.0167	0.8333	0.1333	0.0167	471	0.2583	0.3167	0.1667	0.2583
157	0.0167	0.7833	0.1833	0.0167	472	0.2583	0.1667	0.3167	0.2583
158	0.0167	0.7333	0.2333	0.0167	473	0.2333	0.3667	0.1667	0.2333
159	0.0167	0.6833	0.2833	0.0167	474	0.2333	0.1667	0.3667	0.2333
160	0.0167	0.6333	0.3333	0.0167	475	0.2083	0.4167	0.1667	0.2083
161	0.0167	0.5833	0.3833	0.0167	476	0.2083	0.1667	0.4167	0.2083
162	0.0167	0.5333	0.4333	0.0167	477	0.1833	0.4667	0.1667	0.1833
163	0.0167	0.4833	0.4833	0.0167	478	0.1833	0.1667	0.4667	0.1833
164	0.0167	0.4333	0.5333	0.0167	479	0.1583	0.5167	0.1667	0.1583
165	0.0167	0.3833	0.5833	0.0167	480	0.1583	0.1667	0.5167	0.1583
166	0.0167	0.3333	0.6333	0.0167	481	0.1333	0.5667	0.1667	0.1333
167	0.0167	0.2833	0.6833	0.0167	482	0.1333	0.1667	0.5667	0.1333
168	0.0167	0.2333	0.7333	0.0167	483	0.1083	0.6167	0.1667	0.1083
169	0.0167	0.1833	0.7833	0.0167	484	0.1083	0.1667	0.6167	0.1083
170	0.0167	0.1333	0.8333	0.0167	485	0.0833	0.6667	0.1667	0.0833

171	0.0167	0.0833	0.8833	0.0167	486	0.0833	0.1667	0.6667	0.0833
172	0.45	0.05	0.05	0.45	487	0.0833	0.6167	0.2167	0.0833
173	0.425	0.1	0.05	0.425	488	0.0833	0.5667	0.2667	0.0833
174	0.425	0.05	0.1	0.425	489	0.0833	0.5167	0.3167	0.0833
175	0.4	0.15	0.05	0.4	490	0.0833	0.4667	0.3667	0.0833
176	0.4	0.05	0.15	0.4	491	0.0833	0.4167	0.4167	0.0833
177	0.375	0.2	0.05	0.375	492	0.0833	0.3667	0.4667	0.0833
178	0.375	0.05	0.2	0.375	493	0.0833	0.3167	0.5167	0.0833
179	0.35	0.25	0.05	0.35	494	0.0833	0.2667	0.5667	0.0833
180	0.35	0.05	0.25	0.35	495	0.0833	0.2167	0.6167	0.0833
181	0.325	0.3	0.05	0.325	496	0.3167	0.1833	0.1833	0.3167
182	0.325	0.05	0.3	0.325	497	0.2917	0.2333	0.1833	0.2917
183	0.3	0.35	0.05	0.3	498	0.2917	0.1833	0.2333	0.2917
184	0.3	0.05	0.35	0.3	499	0.2667	0.2833	0.1833	0.2667
185	0.275	0.4	0.05	0.275	500	0.2667	0.1833	0.2833	0.2667
186	0.275	0.05	0.4	0.275	501	0.2417	0.3333	0.1833	0.2417
187	0.25	0.45	0.05	0.25	502	0.2417	0.1833	0.3333	0.2417
188	0.25	0.05	0.45	0.25	503	0.2167	0.3833	0.1833	0.2167
189	0.225	0.5	0.05	0.225	504	0.2167	0.1833	0.3833	0.2167
190	0.225	0.05	0.5	0.225	505	0.1917	0.4333	0.1833	0.1917
191	0.2	0.55	0.05	0.2	506	0.1917	0.1833	0.4333	0.1917
192	0.2	0.05	0.55	0.2	507	0.1667	0.4833	0.1833	0.1667
193	0.175	0.6	0.05	0.175	508	0.1667	0.1833	0.4833	0.1667
194	0.175	0.05	0.6	0.175	509	0.1417	0.5333	0.1833	0.1417
195	0.15	0.65	0.05	0.15	510	0.1417	0.1833	0.5333	0.1417
196	0.15	0.05	0.65	0.15	511	0.1167	0.5833	0.1833	0.1167
197	0.125	0.7	0.05	0.125	512	0.1167	0.1833	0.5833	0.1167
198	0.125	0.05	0.7	0.125	513	0.0917	0.6333	0.1833	0.0917
199	0.1	0.75	0.05	0.1	514	0.0917	0.1833	0.6333	0.0917
200	0.1	0.05	0.75	0.1	515	0.0917	0.5833	0.2333	0.0917
201	0.075	0.8	0.05	0.075	516	0.0917	0.5333	0.2833	0.0917
202	0.075	0.05	0.8	0.075	517	0.0917	0.4833	0.3333	0.0917
203	0.05	0.85	0.05	0.05	518	0.0917	0.4333	0.3833	0.0917

204	0.05	0.05	0.85	0.05	519	0.0917	0.3833	0.4333	0.0917
205	0.025	0.9	0.05	0.025	520	0.0917	0.3333	0.4833	0.0917
206	0.025	0.05	0.9	0.025	521	0.0917	0.2833	0.5333	0.0917
207	0.025	0.85	0.1	0.025	522	0.0917	0.2333	0.5833	0.0917
208	0.025	0.8	0.15	0.025	523	0.3	0.2	0.2	0.3
209	0.025	0.75	0.2	0.025	524	0.275	0.25	0.2	0.275
210	0.025	0.7	0.25	0.025	525	0.275	0.2	0.25	0.275
211	0.025	0.65	0.3	0.025	526	0.25	0.3	0.2	0.25
212	0.025	0.6	0.35	0.025	527	0.25	0.2	0.3	0.25
213	0.025	0.55	0.4	0.025	528	0.225	0.35	0.2	0.225
214	0.025	0.5	0.45	0.025	529	0.225	0.2	0.35	0.225
215	0.025	0.45	0.5	0.025	530	0.2	0.4	0.2	0.2
216	0.025	0.4	0.55	0.025	531	0.2	0.2	0.4	0.2
217	0.025	0.35	0.6	0.025	532	0.175	0.45	0.2	0.175
218	0.025	0.3	0.65	0.025	533	0.175	0.2	0.45	0.175
219	0.025	0.25	0.7	0.025	534	0.15	0.5	0.2	0.15
220	0.025	0.2	0.75	0.025	535	0.15	0.2	0.5	0.15
221	0.025	0.15	0.8	0.025	536	0.125	0.55	0.2	0.125
222	0.025	0.1	0.85	0.025	537	0.125	0.2	0.55	0.125
223	0.4333	0.0667	0.0667	0.4333	538	0.1	0.6	0.2	0.1
224	0.4083	0.1167	0.0667	0.4083	539	0.1	0.2	0.6	0.1
225	0.4083	0.0667	0.1167	0.4083	540	0.1	0.55	0.25	0.1
226	0.3833	0.1667	0.0667	0.3833	541	0.1	0.5	0.3	0.1
227	0.3833	0.0667	0.1667	0.3833	542	0.1	0.45	0.35	0.1
228	0.3583	0.2167	0.0667	0.3583	543	0.1	0.4	0.4	0.1
229	0.3583	0.0667	0.2167	0.3583	544	0.1	0.35	0.45	0.1
230	0.3333	0.2667	0.0667	0.3333	545	0.1	0.3	0.5	0.1
231	0.3333	0.0667	0.2667	0.3333	546	0.1	0.25	0.55	0.1
232	0.3083	0.3167	0.0667	0.3083	547	0.2833	0.2167	0.2167	0.2833
233	0.3083	0.0667	0.3167	0.3083	548	0.2583	0.2667	0.2167	0.2583
234	0.2833	0.3667	0.0667	0.2833	549	0.2583	0.2167	0.2667	0.2583
235	0.2833	0.0667	0.3667	0.2833	550	0.2333	0.3167	0.2167	0.2333
236	0.2583	0.4167	0.0667	0.2583	551	0.2333	0.2167	0.3167	0.2333

237	0.2583	0.0667	0.4167	0.2583	552	0.2083	0.3667	0.2167	0.2083
238	0.2333	0.4667	0.0667	0.2333	553	0.2083	0.2167	0.3667	0.2083
239	0.2333	0.0667	0.4667	0.2333	554	0.1833	0.4167	0.2167	0.1833
240	0.2083	0.5167	0.0667	0.2083	555	0.1833	0.2167	0.4167	0.1833
241	0.2083	0.0667	0.5167	0.2083	556	0.1583	0.4667	0.2167	0.1583
242	0.1833	0.5667	0.0667	0.1833	557	0.1583	0.2167	0.4667	0.1583
243	0.1833	0.0667	0.5667	0.1833	558	0.1333	0.5167	0.2167	0.1333
244	0.1583	0.6167	0.0667	0.1583	559	0.1333	0.2167	0.5167	0.1333
245	0.1583	0.0667	0.6167	0.1583	560	0.1083	0.5667	0.2167	0.1083
246	0.1333	0.6667	0.0667	0.1333	561	0.1083	0.2167	0.5667	0.1083
247	0.1333	0.0667	0.6667	0.1333	562	0.1083	0.5167	0.2667	0.1083
248	0.1083	0.7167	0.0667	0.1083	563	0.1083	0.4667	0.3167	0.1083
249	0.1083	0.0667	0.7167	0.1083	564	0.1083	0.4167	0.3667	0.1083
250	0.0833	0.7667	0.0667	0.0833	565	0.1083	0.3667	0.4167	0.1083
251	0.0833	0.0667	0.7667	0.0833	566	0.1083	0.3167	0.4667	0.1083
252	0.0583	0.8167	0.0667	0.0583	567	0.1083	0.2667	0.5167	0.1083
253	0.0583	0.0667	0.8167	0.0583	568	0.2667	0.2333	0.2333	0.2667
254	0.0333	0.8667	0.0667	0.0333	569	0.2417	0.2833	0.2333	0.2417
255	0.0333	0.0667	0.8667	0.0333	570	0.2417	0.2333	0.2833	0.2417
256	0.0333	0.8167	0.1167	0.0333	571	0.2167	0.3333	0.2333	0.2167
257	0.0333	0.7667	0.1667	0.0333	572	0.2167	0.2333	0.3333	0.2167
258	0.0333	0.7167	0.2167	0.0333	573	0.1917	0.3833	0.2333	0.1917
259	0.0333	0.6667	0.2667	0.0333	574	0.1917	0.2333	0.3833	0.1917
260	0.0333	0.6167	0.3167	0.0333	575	0.1667	0.4333	0.2333	0.1667
261	0.0333	0.5667	0.3667	0.0333	576	0.1667	0.2333	0.4333	0.1667
262	0.0333	0.5167	0.4167	0.0333	577	0.1417	0.4833	0.2333	0.1417
263	0.0333	0.4667	0.4667	0.0333	578	0.1417	0.2333	0.4833	0.1417
264	0.0333	0.4167	0.5167	0.0333	579	0.1167	0.5333	0.2333	0.1167
265	0.0333	0.3667	0.5667	0.0333	580	0.1167	0.2333	0.5333	0.1167
266	0.0333	0.3167	0.6167	0.0333	581	0.1167	0.4833	0.2833	0.1167
267	0.0333	0.2667	0.6667	0.0333	582	0.1167	0.4333	0.3333	0.1167
268	0.0333	0.2167	0.7167	0.0333	583	0.1167	0.3833	0.3833	0.1167
269	0.0333	0.1667	0.7667	0.0333	584	0.1167	0.3333	0.4333	0.1167

270	0.0333	0.1167	0.8167	0.0333	585	0.1167	0.2833	0.4833	0.1167
271	0.4167	0.0833	0.0833	0.4167	586	0.25	0.25	0.25	0.25
272	0.3917	0.1333	0.0833	0.3917	587	0.225	0.3	0.25	0.225
273	0.3917	0.0833	0.1333	0.3917	588	0.225	0.25	0.3	0.225
274	0.3667	0.1833	0.0833	0.3667	589	0.2	0.35	0.25	0.2
275	0.3667	0.0833	0.1833	0.3667	590	0.2	0.25	0.35	0.2
276	0.3417	0.2333	0.0833	0.3417	591	0.175	0.4	0.25	0.175
277	0.3417	0.0833	0.2333	0.3417	592	0.175	0.25	0.4	0.175
278	0.3167	0.2833	0.0833	0.3167	593	0.15	0.45	0.25	0.15
279	0.3167	0.0833	0.2833	0.3167	594	0.15	0.25	0.45	0.15
280	0.2917	0.3333	0.0833	0.2917	595	0.125	0.5	0.25	0.125
281	0.2917	0.0833	0.3333	0.2917	596	0.125	0.25	0.5	0.125
282	0.2667	0.3833	0.0833	0.2667	597	0.125	0.45	0.3	0.125
283	0.2667	0.0833	0.3833	0.2667	598	0.125	0.4	0.35	0.125
284	0.2417	0.4333	0.0833	0.2417	599	0.125	0.35	0.4	0.125
285	0.2417	0.0833	0.4333	0.2417	600	0.125	0.3	0.45	0.125
286	0.2167	0.4833	0.0833	0.2167	601	0.2333	0.2667	0.2667	0.2333
287	0.2167	0.0833	0.4833	0.2167	602	0.2083	0.3167	0.2667	0.2083
288	0.1917	0.5333	0.0833	0.1917	603	0.2083	0.2667	0.3167	0.2083
289	0.1917	0.0833	0.5333	0.1917	604	0.1833	0.3667	0.2667	0.1833
290	0.1667	0.5833	0.0833	0.1667	605	0.1833	0.2667	0.3667	0.1833
291	0.1667	0.0833	0.5833	0.1667	606	0.1583	0.4167	0.2667	0.1583
292	0.1417	0.6333	0.0833	0.1417	607	0.1583	0.2667	0.4167	0.1583
293	0.1417	0.0833	0.6333	0.1417	608	0.1333	0.4667	0.2667	0.1333
294	0.1167	0.6833	0.0833	0.1167	609	0.1333	0.2667	0.4667	0.1333
295	0.1167	0.0833	0.6833	0.1167	610	0.1333	0.4167	0.3167	0.1333
296	0.0917	0.7333	0.0833	0.0917	611	0.1333	0.3667	0.3667	0.1333
297	0.0917	0.0833	0.7333	0.0917	612	0.1333	0.3167	0.4167	0.1333
298	0.0667	0.7833	0.0833	0.0667	613	0.2167	0.2833	0.2833	0.2167
299	0.0667	0.0833	0.7833	0.0667	614	0.1917	0.3333	0.2833	0.1917
300	0.0417	0.8333	0.0833	0.0417	615	0.1917	0.2833	0.3333	0.1917
301	0.0417	0.0833	0.8333	0.0417	616	0.1667	0.3833	0.2833	0.1667
302	0.0417	0.7833	0.1333	0.0417	617	0.1667	0.2833	0.3833	0.1667

303	0.0417	0.7333	0.1833	0.0417	618	0.1417	0.4333	0.2833	0.1417
304	0.0417	0.6833	0.2333	0.0417	619	0.1417	0.2833	0.4333	0.1417
305	0.0417	0.6333	0.2833	0.0417	620	0.1417	0.3833	0.3333	0.1417
306	0.0417	0.5833	0.3333	0.0417	621	0.1417	0.3333	0.3833	0.1417
307	0.0417	0.5333	0.3833	0.0417	622	0.2	0.3	0.3	0.2
308	0.0417	0.4833	0.4333	0.0417	623	0.175	0.35	0.3	0.175
309	0.0417	0.4333	0.4833	0.0417	624	0.175	0.3	0.35	0.175
310	0.0417	0.3833	0.5333	0.0417	625	0.15	0.4	0.3	0.15
311	0.0417	0.3333	0.5833	0.0417	626	0.15	0.3	0.4	0.15
312	0.0417	0.2833	0.6333	0.0417	627	0.15	0.35	0.35	0.15
313	0.0417	0.2333	0.6833	0.0417	628	0.1833	0.3167	0.3167	0.1833
314	0.0417	0.1833	0.7333	0.0417	629	0.1583	0.3667	0.3167	0.1583
315	0.0417	0.1333	0.7833	0.0417	630	0.1583	0.3167	0.3667	0.1583
					631	0.1667	0.3333	0.3333	0.1667

Bibliography

[Aggoune et al., 1991] M. Aggoune, M. A. El-Sharkawi, D. C. Park, M. J. Damborg, and R. J. Marks II, "Preliminary results on using artificial neural networks for security assessment," *IEEE Trans. on Power Systems*, vol. 6, no. 2, pp. 252-258, May 1991.

[Ajjarapu and Cristy, 1992] V. Ajjarapu and C. Cristy, "The continuation power flow: a tool for steady state voltage stability analysis," *IEEE Trans. on Power Systems*, vol. 7, no. 1, pp. 416-423, February 1992.

[Avalos, 2008] R. J. Avalos, "Analysis and application of optimization techniques to power system security and electricity markets," Ph.D. dissertation, Dept. of Elect. and Computer Eng., University of Waterloo, Waterloo, ON, Canada, 2008.

[Avalos et al., 2008] R. J. Avalos, C. A. Cañizares, and M. F. Anjos, "A practical voltage-stability-constrained optimal power flow," in *Proc. IEEE-PES General Meeting*, July 2008.

[Avalos et al., 2009] R. J. Avalos, C. A. Cañizares, F. Milano, and A. Conejo, "Equivalency of continuation and optimization methods to determine Saddle-node and Limit-induced bifurcations in power systems," *IEEE Trans. on Circuits and Systems I*, vol. 56, no. 1, pp. 210-223, January 2009.

[Banakar and Galiana, 1981] M.H. Banakar and F.D. Galiana, "Power system security corridors concept and computation," *IEEE Trans. on PAS*, vol. 100, pp. 4524-4532, 1981.

[Bompard et al., 2000] E. Bompard, E. Carpaneto, G. Chicco, and G. Gross, "The role of load demand elasticity in congestion management and pricing," in *Proc. IEEE-PES SM*, pp. 2229-2234, July 2000.

[Bruno et al., 2002] S. Bruno, E. D. Tuglie, and M. La Scala, "Transient security dispatch for the concurrent optimization of plural postulated contingencies," *IEEE Trans. on Power Systems*, vol. 17, no. 3, pp. 707-714, August 2002.

[Cañizares, 1995] C. A. Cañizares, "Conditions for saddle-node bifurcations in AC/DC power systems," *International Journal of Electrical Power and Energy Systems*, vol. 17, no. 1, pp. 61–68, January 1995.

[Cañizares and Alvarado, 1993] C. A. Cañizares and F. L. Alvarado, "Point of collapse and continuation methods for large AC/DC systems," *IEEE Trans. on Power Systems*, vol. 8, no. 1, pp. 1-8, February, 1993.

[Cañizares and Kodsi, 2006] C. A. Cañizares and S. K. M. Kodsi, "Power system security in market clearing and dispatch mechanisms," in *Proc. IEEE-PES General Meeting*, 6 pp., June 2006.

[Cañizares et al., 2001] C. A. Cañizares, W. Rosehart, A. Berizzi, and C. Bovo, "Comparison of voltage security constrained optimal power flow techniques," in *Proc. IEEE-PES Summer Meeting*, Vancouver, BC, Canada, pp. 1680-1685, July 2001.

[Chassiakos and Masri, 1996] A. G. Chassiakos and S. F. Masri, "Modelling unknown structural systems through the use of neural networks," in *Proc. Earthquake Engineering and Structural Dynamics*, vol. 25, pp. 117-128, 1996.

[DeMaio et al., 1976] J.A. DeMaio, and R. Fischl, "Fast identification of the steady-state security regions for power system security enhancement," *IEEE Winter Power Meeting*, vol.95, no.3, p. 758, 1976.

[Demoth et al., 2008] H. Demoth, M. Beale, and M. Hagan, *Neural network toolbox 6*, The Mathworks Inc., 2008.

[Dobson and Chiang, 1989] I. Dobson and H. D. Chiang, "Towards a theory of voltage collapse in electric power systems," *Systems & Control Letters*, vol. 13, pp. 253–262, 1989.

[Dobson and Lu, 1992] I. Dobson and L. Lu, "Voltage collapse precipitated by the immediate change in stability when generator reactive power limits are encountered," *IEEE Trans. Circuits Syst. I*, vol. 39, no. 9, pp. 762–766, September 1992.

[Eduards et al., 1996] A. R. Eduards, K. W. Chan, R. W. Dunn, and A. R. Daniels, "Transient stability screening using artificial neural networks within a dynamic security assessment," *IEE Proc. on Generation, Transmission and Distribution*, vol. 143, no. 2, pp. 129-134, March 1996.

[Fischl et al., 1976] R. Fischl, G.C. Ejebe, and J.A. DeMaio, "Identification of power system steady-state security regions under load uncertainty," *IEEE Summer Power Meeting*, vol.95, no.6, p. 1767, 1976.

[Fluek, 1996] A. J. Fluek, "Advances in numerical analysis of nonlinear dynamical systems and the application to transfer capability of power systems," PhD Thesis, Cornell University, August, 1996.

[Fourer et al., 2003] R. Fourer, D. M. Gay, and B. W. Kernighan, *AMPL: a modeling language for mathematical programming*, 2nd ed. Thomson, 2003.

[Fuerte-Esquivel et al., 1998] C. R. Fuerte-Esquivel, E. Acha, S. G. Tan, and J. J. Rico, "Efficient object oriented power systems software for the analysis of large scale networks containing FACTS-controlled branches," *IEEE Trans. Power Systems*, vol. 12, no. 2, pp. 464-472, May 1998.

[Gan et al., 2000] D. Gan, R. J. Thomas, and R. D. Zimmerman, "Stability-constrained optimal power flow," *IEEE Trans. on Power Systems*, vol. 15, no. 2, pp. 535-540, May 2000.

[Ghasemi and Maria, 2008] H. Ghasemi and A. Maria, "Benefits of employing an on-line security limit derivation tool in electricity markets," in *Proc. IEEE-PES General Meeting*, 6pp., July 2008.

[Glendinning, 1994] P. Glendinning, *Stability, instability and chaos: an introduction to the theory of nonlinear differential equations, Cambridge University Press*, 1994.

[Gomez-Exposito et al., 2009] A. Gomez-Exposito, A. J. Conejo, and C. A. Cañizares, *Electric energy systems: analysis and operation*, CRC Press, 2009.

[Gu and Cañizares, 2007] X. Gu, and C. A. Cañizares, "Fast prediction of loadability margins using neural networks to approximate security boundaries of power systems," *IET Generation, Transmission and Distribution*, vol. 1, no. 3, pp. 466-475, May 2007.

[Haykin, 1999] S. Haykin, *Neural networks: a comprehensive foundation*. Prentice Hall, Second Edition, 1999.

[Hill and Mareels, 1990] D. J. Hill and I. M. Y. Mareels, "Stability theory for differential/algebraic systems with application to power systems," *IEEE Trans. Circuits Systems*, vol. 37, no. 11, pp. 1416–1423, November 1990.

[Hines et al., 2008] P. Hines, J. Apt, and S. Talukdar, "Trends in the history of large blackouts in the United States," in *Proc. IEEE-PES General Meeting*, 8 pp., July 2008.

[Hirodontis et al., 2009] S. Hirodontis, H. Li, P. A. Crossley, "Load shedding in a distribution network," *International Conference on Sustainable Power Generation and Supply*, pp. 1-6, 2009.

[Hnyilicza et al., 1975] E. Hnyilicza, S.T.Y. Lee, and F.C. Schweppe, "Steady-state security regions: set-theoretic approach," in *Proc. of Power Industry and Computer Applications Conference*, pp. 347-355, June, 1975.

[Hornik et al., 1989] K. Hornik, M. Stinchcombe, and H. White, "Multilayered feedforward networks are universal approximators," *Neural Networks*, vol. 2, no. 5, 1989, pp. 359-366.

[IEEE/PES Tech. Rep., 2002] "Voltage stability assessment: concepts, practices and tools," IEEE/PES Power System Stability Subcommittee, Tech. Rep. SP101PSS, August 2002.

[IEEE Committee Report, 1981] IEEE Committee Report, "Excitation system models for power system stability studies," *IEEE Trans. on Power Apparatus and Systems*, vol. PAS-100, no. 2, pp. 494-509, February 1981.

[Illic and Zaborszky, 2000] M. Ilic and J. Zaborszky, *Dynamics and control of large electric power systems*, John Wiley & Sons Inc., 2000.

[Jayasekara and Annakkage, 2006] B. Jayasekara and U. Annakkage, "Derivation of an accurate polynomial representation of the transient stability boundary," *IEEE Trans. on Power Systems*, vol. 21, no. 4, pp. 1856-1863, November 2006.

[Jarjis and Galiana, 1981] J. Jarjis and F. D. Galiana, "Quantitative analysis of steady state stability in power networks," *IEEE Trans. on Power App. Syst.*, vol. PAS-100, no. 1, pp. 318-326, January 1981.

[Kaye and Wu, 1982] R. Kaye and F. Wu, "Dynamic security regions of power systems," *IEEE Trans. on Circuits and Systems*, vol. 29, no. 9, pp. 612–623, 1982.

[KNITRO] KNITRO. [Online]. Available: http://www.ziena.com.

[Kodsi and Cañizares, 2007] S. K. M. Kodsi and C. A. Cañizares, "Application of a stability constrained optimal power flow to tuning of oscillation controls in competitive electricity markets," *IEEE Trans. on Power Systems*, vol. 22, no. 4, pp. 1944-1954, November 2007.

[Kundur, 1994] P. Kundur, *Power system stability and control*. McGraw-Hill, 1994.

[Kundur et al., 2004] P. Kundur, et. al., "Definition and classification of power system stability," *IEEE Trans. on Power Systems*, vol. 19, no. 2, pp. 1387-1401, May 2004.

[Lof et al., 1992] P. A. Lof, T. Smed, G. Andersson, and D. J. Hill, "Fast calculation of a voltage stability index," *IEEE Trans. on Power Systems*, vol. 7, no. 1, pp. 54-64, February 1992.

[Luzardo-Flores, 1997] J. A. Luzardo-Flores, "Neural networks for approximation and control of continuous time nonlinear systems," Ph.D. dissertation, Graduate Faculty of Engineering Mathematics, California State University, Long Beach, California, USA, 1997.

[Makarov et al., 2010] Y. V. Makarov, S. Lu, X. Guo, J. F. Gronquist, P. Du, T. B. Nguyen, and J. W. Burns, "Wide area security region," Final Report, Pacific Northwest National Laboratory, March 2010.

[McCalley et al., 1997] J. D. McCalley, S. Wang, R. T. Treinen, and A. D. Papalexopoulos, "Security boundary visualization for power systems operation," *IEEE Trans. on Power Systems*, vol. 12, no. 2, pp. 940-947, May 1997.

[Milano, 2005] F. Milano, "An open source power system analysis toolbox," *IEEE Trans. on Power Systems*, vol. 20, no. 3, p. 1199-1206, August 2005.

[Miranda et al., 1995] V. Miranda, J. N. Fidalgo, J. A. Pecas Lopes, and L. B. Almeida, "Real time preventive actions for transient stability enhancement with a hybrid neural network – optimization approach," *IEEE Trans. on Power Systems*, vol. 10, no. 2, pp. 1029-1035, May 1995.

[Nayfeh and Balachandran, 2004] A. H. Nayfeh, and B. Balachandran, *Applied nonlinear dynamics: analytical, computational, and experimental methods*, John Wiley and Sons Inc., 2004.

[Nguyen, 1995] T. T. Nguyen, "Neural network load flow," *IEE Proc. Generation, Transmission and Distribution*, vol. 142, no. 1, pp. 51-58, January 1995.

[Pizano-Martinez et al., 2007] A. Pizano-Martinez, C. R. Fuerte-Esquivel, H. Ambriz-Perez, and E. Acha, "Modeling of VSC-based HVDC systems for a Newton-Raphson OPF algorithm," *IEEE Trans. Power Systems*, vol. 22, no. 4, pp. 1794-1803, November 2007.

[Ritcher and Decarlo, 1983] S. L. Richter, R. A. Decarlo, "Continuation methods: theory and applications", *IEEE Trans. on Circuits and Systems*, vol. CAS-30, no. 6, pp. 347-352, June 1983.

[Rosehart et al., 1999] W. Rosehart, C. Cañizares, and V. Quintana, "Optimal Power Flow Incorporating Voltage Collapse Constraints," in *Proc. IEEE-PES Summer Meeting*, pp. 820-825, July 1999.

[Sahari et al., 2003] S. Sahari, A. F. Abdin, and T. K. Rahaman, "Development of artificial neural network for voltage stability monitoring," in *Proc. National Power Engineering Conferenc*e, pp. 37-42, December 2003.

[Sauer and Pai, 1988] P. W. Sauer and M. A. Pai, *Power system dynamics and stability.* Prentice Hall, 1988.

[Sauer and Pai, 1990] P. W. Sauer and M. A. Pai, "Power system steady-state stability and the load flow Jacobian," *IEEE Trans. on Power Systems*, PWRS-5, pp. 1374-1383, November 1990.

[Seydel, 2010] R. Seydel, *Practical bifurcation and stability analysis*, 3rd ed. Springer-Verlag, 2010.

[Sun et al., 1984] D. I. Sun, B. Ashley, B. Brewer, A. Hughes, and W. F. Tinney, "Optimal power flow by Newton approach," *IEEE Trans. On Power App. and Syst.*, vol. PAS-103, no. 10, pp. 2864-2880, October 1984.

[U. S., Canada, Power System Outage Task Force, 2004] "Final report on the August 14, 2003 blackout in the United States and Canada: causes and recommendations," U. S. – Canada Power System Outage Task Force, April 2004.

[UWPFLOW] UWPFLOW, April 2006. [Online]. Available: http://thunderbox.uwaterloo.ca/~claudio/software/pflow.htm

[Van Cutsem, 1991] T. Van Cutsem, "A method to compute reactive power margins with respect to voltage collapse," *IEEE Trans. on Power Systems*, vol. 6, no. 1, pp. 145–155, February 1991.

[Van Cutsem and Vournas, 2008] T.Van Cutsem and C. Vournas, *Voltage stability of electric power systems*, Springer, 2008.

[Venkatasubramanian et al., 1995] V. Venkatasubramanian, H. Schättler, and J. Zaborszky, "Dynamics of large constrained nonlinear systems - a taxonomy theory," in *Proc. of the IEEE*, vol. 83, no. 11, pp. 1530–1560, November 1995.

[Venkatasubramanian et al., 1995-1] V. Venkatasubramanian, H. Schättler, and J. Zaborszky, "Local bifurcations and feasibility regions in differential-algebraic systems," *IEEE Trans. on Automatic Control*, vol. 40, no. 12, pp. 1992-2013, December 1995.

[Vu and Liu, 1992] K. T. Vu and C. Liu, "Shrinking stability regions and voltage collapse in power systems," *IEEE Trans. on Circuits and Systems I: Fundamental Theory and Applications*, vol. 39, no. 4, pp. 271-289, April 1992.

[Washington] Power systems test case archive, Electrical Engineering, University of Washington. [Online]. Available: http://www.ee.washington.edu/research/pstca/

[Wu and Kumagai, 1982] F. Wu and S. Kumagai, "Steady-state security regions of power systems," *IEEE Trans. on Circuits and Systems*, vol. 29, no. 11, pp. 703–711, 1982

[Zhu, 2001] T. Zhu, "Voltage stability analysis in the new deregulated environment," PhD Thesis, Texas A&M University, Texas, December, 2001.